JEDEC STANDARD

Measurement and Reporting of Alpha Particle and Terrestrial Cosmic Ray-Induced Soft Errors in Semiconductor Devices

JESD89A

(Revision of JESD89, August 2001)

OCTOBER 2006
(Reaffirmed: JANUARY 2012)

JEDEC SOLID STATE TECHNOLOGY ASSOCIATION

Downloaded by xu yajun (xuyj@beice-sh.com) on Jun 29, 2018, 12:46 am PDT
联系方式：xuyj@beice-sh.com 13917165676
BC LABORATORY beice 北测（上海）电子科技有限公司

NOTICE

JEDEC standards and publications contain material that has been prepared, reviewed, and approved through the JEDEC Board of Directors level and subsequently reviewed and approved by the JEDEC legal counsel.

JEDEC standards and publications are designed to serve the public interest through eliminating misunderstandings between manufacturers and purchasers, facilitating interchangeability and improvement of products, and assisting the purchaser in selecting and obtaining with minimum delay the proper product for use by those other than JEDEC members, whether the standard is to be used either domestically or internationally.

JEDEC standards and publications are adopted without regard to whether or not their adoption may involve patents or articles, materials, or processes. By such action JEDEC does not assume any liability to any patent owner, nor does it assume any obligation whatever to parties adopting the JEDEC standards or publications.

The information included in JEDEC standards and publications represents a sound approach to product specification and application, principally from the solid state device manufacturer viewpoint. Within the JEDEC organization there are procedures whereby a JEDEC standard or publication may be further processed and ultimately become an ANSI standard.

No claims to be in conformance with this standard may be made unless all requirements stated in the standard are met.

Inquiries, comments, and suggestions relative to the content of this JEDEC standard or publication should be addressed to JEDEC at the address below, or refer to www.jedec.org under Standards and Documents for alternative contact information.

Published by
©JEDEC Solid State Technology Association 2012
3103 North 10th Street
Suite 240 South
Arlington, VA 22201-2107

This document may be downloaded free of charge; however JEDEC retains the copyright on this material. By downloading this file the individual agrees not to charge for or resell the resulting material.

PRICE: Contact JEDEC

Printed in the U.S.A.
All rights reserved

Downloaded by xu yajun (xuyj@beice-sh.com) on Jun 29, 2018, 12:46 am PDT
联系方式：xuyj@beice-sh.com 13917165676

PLEASE!

DON'T VIOLATE
THE
LAW!

This document is copyrighted by JEDEC and may not be
reproduced without permission.

For information, contact:

JEDEC Solid State Technology Association
3103 North 10th Street
Suite 240 South
Arlington, VA 22201-2107

or refer to www.jedec.org under Standards-Documents/Copyright Information.

Downloaded by xu yajun (xuyj@beice-sh.com) on Jun 29, 2018, 12:46 am PDT
联系方式：xuyj@beice-sh.com 13917165676

BC LABORATORY
beice
北测（上海）电子科技有限公司
Downloaded by xu yajun (xuyj@beice-sh.com) on Jun 29, 2018 12:46 am PDT
联系方式：xuyj@beice-sh.com 13917165676

MEASUREMENT AND REPORTING OF ALPHA PARTICLE AND TERRESTRIAL COSMIC RAY INDUCED SOFT ERRORS IN SEMICONDUCTOR DEVICES

CONTENTS

Page
Foreword ... iii
Introduction ... iii

1 Scope ... 1

2 Terms and definitions ... 1

3 Test equipment and software requirements ... 5
3.1 Test equipment ... 5
3.2 Test plan ... 6
3.3 Test conditions ... 8
3.4 Setup procedure ... 10
3.5 General testing specifications ... 11
3.6 Data collection ... 11
3.7 Considerations for testing non-memory components ... 11

4 Real-time (unaccelerated and high-altitude) test procedures ... 15
4.1 Background ... 15
4.2 Test facilities and equipment ... 16
4.3 Testing procedures ... 18
4.4 Differences in real-time ser tests and actual end-user observed fail rates ... 20
4.5 Final report ... 20

5 Accelerated alpha particle test procedure ... 22
5.1 Background ... 22
5.2 Alpha particle environment ... 23
5.3 Packaging for alpha particle testing ... 23
5.4 Alpha particle sources ... 24
5.5 Basic test methodology ... 26
5.6 Test procedure and results ... 27
5.7 Interferences ... 30
5.8 Final report ... 32

6 Accelerated terrestrial cosmic ray test procedures ... 33
6.1 Background ... 33
6.2 Test facilities ... 34
6.3 Basic test methodology ... 34
6.4 Basic test procedure ... 34
6.5 Beam parameters ... 35
6.6 Fundamental quantities: seu cross-section and seu rate ... 36
6.7 Interferences ... 42
6.8 Final report ... 43

Downloaded by xu yajun (xuyj@beice-sh.com) on Jun 29, 2018, 12:46 am PDT
联系方式：xuyj@beice-sh.com 13917165676

MEASUREMENT AND REPORTING OF ALPHA PARTICLE AND TERRESTRIAL COSMIC RAY INDUCED SOFT ERRORS IN SEMICONDUCTOR DEVICES

CONTENTS (cont'd)

Page

7 Accelerated thermal neutron test procedures 44
7.1 Background 44
7.2 The terrestrial thermal neutron environment 46
7.3 Packaging for thermal neutron testing 46
7.4 Thermal neutron sources 47
7.5 Basic test methodology 49
7.6 Test procedure and results 49
7.7 Interferences 52
7.8 Final report 53

Annexes

A (normative) Determination of terrestrial neutron flux 55
B (normative) Counting statistics 70
C (normative) Real-time testing statistics 71
D (informative) The alpha particle environment 75
E (informative) Neutron and proton test facilities 79
F Bibliographic References 82
G Differences Between JESD89A and JESD89 84

Downloaded by xu yajun (xuyj@beice-sh.com) on Jun 29, 2018, 12:46 am PDT
联系方式：xuyj@beice-sh.com 13917165676

Foreword

This specification defines the standard requirements and procedures for terrestrial soft error rate (SER) testing of integrated circuits and reporting of results. Both real-time (unaccelerated) and accelerated testing procedures are described. At terrestrial, Earth-based altitudes, the predominant sources of radiation include both cosmic-ray radiation, dominated by high- and low-energy neutron-induced reactions, and alpha-particle radiation from radioisotopic impurities in the package and chip materials. An overall assessment of a device's SER is complete, ***only*** when an unaccelerated test is done under actual use conditions, ***or*** accelerated SER data for the alpha-particle component, the high-energy cosmic-radiation component, and if necessary, the thermal neutron component (see **7** for details) has been obtained and extrapolated to the use conditions.

Annexes D and E are informative; Annexes A, B, and C are normative.

Introduction

Soft errors are nondestructive functional errors induced by energetic ion strikes. Soft errors are a subset of single event effects (SEE), and include single-event upsets (SEU), multiple-bit upsets (MBU), single-event functional interrupts (SEFI), single-event transients (SET) that, if latched, become SEU, and single-event latchup (SEL) where the formation of parasitic bipolar action in CMOS wells induce a low-impedance path between power and ground, producing a high current condition (SEL can also cause latent and hard errors).

In general, soft errors may be induced by alpha particles emitted from radioactive impurities in materials nearby the sensitive volume, such as packaging, solder bumps, etc., and by highly ionizing secondary particles produced from the reaction of both thermal and high-energy neutrons with component materials.

There are two fundamental methods to determine a product's SER. One is to test a large number of actual production devices for a long enough period of time (weeks or months) until enough soft errors have been accumulated to give a reasonably confident estimate of the SER. This is generally referred to as a real-time or unaccelerated SER testing. Real-time testing has the advantage of being a direct measurement of the actual product SER requiring no intense radiation sources, extrapolations to use conditions, etc. (provided the test is performed in a building location similar to the actual use environment - see A.5). However, real-time testing does require an expensive system capable of monitoring hundreds or thousands of devices in parallel, for long periods of time.

The other method commonly employed to allow more rapid SER estimations and to clarify the source of errors is accelerated-SER (ASER) testing. In ASER testing, devices are exposed to a specific radiation source whose intensity is much higher than the ambient levels of radiation the device would normally encounter. ASER allows useful data to be obtained in a fraction of the time required by unaccelerated real-time testing. Only a few units are needed and complete evaluations can often be done in a few hours or days instead of weeks or months. The disadvantages of ASER are that the results must be extrapolated to use conditions and that several different radiation sources ***must*** be used to ensure that the estimation accounts for soft errors induced by both alpha particle and cosmic-ray-neutron events.

Downloaded by xu yajun (xuyj@beice-sh.com) on Jun 29, 2018, 12:46 am PDT
联系方式：xuyj@beice-sh.com 13917165676

beice
北测（上海）电子科技有限公司

Downloaded by xu yajun (xuyj@beice-sh.com) on Jun 29, 2018, 12:46 am PDT
联系方式：xuyj@beice-sh.com 13917165676

MEASUREMENT AND REPORTING OF ALPHA PARTICLE AND TERRESTRIAL COSMIC RAY INDUCED SOFT ERRORS IN SEMICONDUCTOR DEVICES

(From JEDEC Board ballot JCB-06-63, formulated under the cognizance of the JC-13.4 Subcommittee on Radiation Hardness: Assurance and Characterization.)

1 Scope

This standard specification covers soft errors due to alpha particles and low and high-energy atmospheric neutrons. 3 covers test methods and issues common to all test types, 4 covers real-time or unaccelerated measurements, 5 covers accelerated soft error rate test procedures related to alpha particles, 6 covers accelerated soft error rate test procedures related to high-energy neutron reactions (>1 MeV), and 7 covers test procedures for thermal neutron reactions with ^{10}B.

This specification defines the standard requirements and procedures for terrestrial soft error rate (including real-time and accelerated) testing of integrated circuits and a standardized methodology for reporting the results of the tests.

The procedures apply to components including memory and logic.

Warning: These tests may involve hazardous materials, operations, and equipment. It is the responsibility of the user of this test method in consultation with radiation safety personnel to establish the appropriate safety and health practices and to determine the applicability of regulatory limitations prior to use.

2 Terms and definitions

ATE: Automatic test equipment

component: A packaged die or integrated circuit.

NOTE This may be either a test vehicle or an actual product.

collected charge: The charge collected by a particular device node during the passage of a particle.

NOTE The collected charge is dependent on the geometry and doping of the node, the particle mass, energy, and trajectory, and the density and type of material in the volume being penetrated by the incident radiation.

critical charge: The minimum amount of collected charge that will cause a device node to change state.

device, electronic: synonymous with component or microcircuit

Downloaded by xu yajun (xuyj@beice-sh.com) on Jun 29, 2018, 12:46 am PDT
联系方式：xuyj@beice-sh.com 13917165676

2 Terms and definitions (cont'd)

differential flux: The time rate of fluence per unit energy, the rate of the quantity of radiation, particle fluence, per unit area incident on a surface per unit energy.

NOTE 1 Differential flux is usually expressed in particles per unit area per unit energy per unit time, e.g., n/(cm² MeV hr).

NOTE 2 The term differential flux in this standard is synonymous with spectral flux density used in other publications.

DUT: Device under test.

ECC: Error correction code, sometimes called error detection and correction (EDAC).

FITs: Failures in time; the number of failures per 10^9 device-hours.

fluence (of particle radiation incident on a surface): The total amount of particle radiant energy incident on a surface in a given period of time, divided by the area of the surface. NOTE This fluence is usually expressed in particles per unit area (e.g., N/cm2).

flux: The time rate of flow of particle radiant energy incident on a surface, divided by the area of that surface.

NOTE 1 Flux is usually expressed in particles per unit area, per unit time (e.g., N/cm2h).

NOTE 2 The term "flux" is used in this standard whereas other standards might use the term "flux density" for the same meaning.

hard error: An irreversible change in operation that is typically associated with permanent damage to one or more elements of a device or circuit (e.g., gate oxide rupture, destructive latch-up events).NOTE The error is "hard" because the data is lost and the component or device no longer functions properly, even after power reset and re-initialization.

multiple-bit upset (MBU): A multiple-cell upset in which two or more error bits occur in the same word.

NOTE An MBU cannot be corrected by a simple single-bit ECC.

multiple-cell upset (MCU): A single event that induces several bits in an IC to fail at one time.

NOTE The error bits are usually, but not always, adjacent.

process: A combination of people, procedures, methods, machines, materials, measurement equipment, and/or environment for specific work activities to produce a given product or service.

NOTE For the purposes of this standard the process is specifically the manufacturing steps and methodologies used to fabricate an IC.

Downloaded by xu yajun (xuyj@beice-sh.com) on Jun 29, 2018, 12:46 am PDT
联系方式：xuyj@beice-sh.com 13917165676

2 Terms and definitions (cont'd)

product: A component or service sold to satisfy a particular customer application.

NOTE For the purposes of this standard a product is a complete integrated circuit sold to satisfy a particular customer application.

radiation: Energy emitted in the form of electromagnetic waves or moving nuclear particles.

NOTE For purposes of this standard the primary radiation of concern is ionizing and includes protons, electrons, alpha particles, and nuclear reaction products.

real-time soft error rate (RTSER): Soft error rate measurement technique under a naturally occurring alpha particle and neutron environment using a large number of devices to obtain a statistically significant error count. This is in contrast to an accelerated SER test where an intense radiation source is used on a single, or small number of devices. RTSER error counts can be increased by using a higher neutron flux at higher altitudes, but for the purposes of this specification, the term accelerated is reserved for intense radiation sources that do not occur in natural terrestrial environments. System SER (SSER) is another term that is often used and is considered synonymous with RTSER.

sensitive volume: A region, or multiple regions, containing nodes whose states can be changed by incident radiation.

NOTE The sensitive volume is determined by the angle of the incident radiation, the mass and energy of the incident particles, and the density and type of material in the volume being penetrated by the incident radiation.

single-event effect (SEE): Any measurable or observable change in state or performance of a microelectronic device, component, subsystem, or system (digital or analog) resulting from a single energetic particle strike.

NOTE Single-event effects include single-event upset (SEU), multiple-bit upset (MBU), multiple-cell upset (MCU), single-event functional interrupt (SEFI), single-event latch-up (SEL), single-event hard error (SHE) and single-event transient (SET), single-event burnout (SEB), and single-event gate rupture (SEGR).

single-event functional interrupt (SEFI): A soft error that causes the component to reset, lock-up, or otherwise malfunction in a detectable way, but does not require power cycling of the device (off and back on) to restore operability, unlike single-event latch-up (SEL), or result in permanent damage as in single-event burnout (SEB).

NOTE A SEFI is often associated with an upset in a control bit or register.

Downloaded by xu yajun (xuyj@beice-sh.com) on Jun 29, 2018, 12:46 am PDT
联系方式：xuyj@beice-sh.com 13917165676

2 Terms and definitions (cont'd)

single-event latch-up (SEL): An abnormal high-current state in a device caused by the passage of a single energetic particle through sensitive regions of the device structure and resulting in the loss of device functionality.

NOTE 1 SEL may cause permanent damage to the device. If the device is not permanently damaged, power cycling of the device (off and back on) is necessary to restore normal operation.

NOTE 2 An example of SEL in a CMOS device is when the passage of a single particle induces the creation of parasitic bipolar (p-n-p-n) shorting of power to ground.

single event transient (SET): A momentary voltage excursion (voltage spike) at a node in an integrated circuit caused by a single energetic particle strike.

single-event upset (SEU): A soft error caused by the transient signal induced by a single energetic particle strike.

single-event upset (SEU) cross-section: the number of events per unit fluence. For device SEU cross-section, the dimensions are area per device. For bit SEU cross-section, the dimensions are area per bit.

single-event upset (SEU) rate: the rate at which single event upsets occur.

soft error, device: An erroneous output signal from a latch or memory cell that can be corrected by performing one or more normal functions of the device containing the latch or memory cell.

NOTE 1 As commonly used, the term refers to an error caused by radiation or electromagnetic pulses and not to an error associated with a physical defect introduced during the manufacturing process.

NOTE 2 Soft errors can be generated from SEU, SEFI, MBU, MCU, and or SET. The term SER has been adopted by the commercial industry while the more specific terms SEU, SEFI, etc.. are typically used by the avionics, space and military electronics communities.

NOTE 3 The term "soft error" was first introduced (for DRAMs and ICs) by May and Woods of Intel in their April 1978 paper at the IRPS and the term "single event upset" was introduced by Guenzer, Wolicki and Allas of NRL in their 1979 NSREC paper (SEU of DRAMs by neutrons and protons).

soft error rate (SER): The rate at which soft errors occur.

storage element: A circuit or device that can be programmed to hold (or store) different states. For example, a DRAM cell, that can store charge (or not) on a capacitor. An SRAM cell or a flip-flop is another example.

test vehicle: Acircuit or IC designed for the purpose of evaluating one or many device characteristics. For the purposes of this document, the characterization would be the soft error sensitivity of a particular process technology. But the test vehicle can incorporate other structures used to characterize different parameters, such as yield, speed, voltage margin, etc.

NOTE This test vehicle is not typically a product but is a dedicated component or section of an IC chip designed to be used to extrapolate to the SER of a product.

Downloaded by xu yajun (xuyj@beice-sh.com) on Jun 29, 2018, 12:46 am PDT
联系方式：xuyj@beice-sh.com 13917165676

3 Test equipment and software requirements

3.1 Test equipment

3.1.1 ATE hardware

The automatic test equipment (ATE) hardware used for testing may be conventional electronic test gear or custom-built equipment. The ATE must be able to tolerate stray radiation and potentially poor quality power. So the use of uninterruptible battery-backed power supplies is recommended.

The ATE hardware must be capable of exercising the DUT over the range of operating conditions such as power supply voltage, access cycle speed and temperature that are specified in the test plan. Proper operation of the ATE under all of these operating conditions must be rigorously confirmed prior to the beginning of testing with a radiation source. The use of cabling to connect the DUT and test equipment, power supply accuracy at the DUT, and the exposure of the ATE to scattered radiation during testing should all be considered.

For accelerated testing with a high-intensity radiation source, the ATE is generally designed to hold a small number of DUTs at a time while they are irradiated. The ATE for field-testing, also known as real-time testing, is designed to hold a large number of DUTs while they are being irradiated, typically by the unaccelerated environmental exposure.

The ATE for use at a neutron or proton beam facility must be capable of remote operation since the operators will be shielded in the control room during an exposure. Cabling between the control room and beam station may be provided by the beam facility or be the responsibility of the experimenter. If the ATE is constructed as a holder and a separate electronics package to exercise the DUT, the cabling between them must be carefully designed and constructed to minimize the potential for errors during operation. Test cables should be short enough to allow sufficient test speeds without electrical noise problems.

Careful coordination with the beam facility prior to arrival can save a great deal of setup time. In general, the physical dimensions, accessibility and power availability at the test facility should be carefully checked before making a trip. The ATE must be rugged enough to withstand shipping to the test site and to be reassembled in a reasonable time.

In addition to the above, the following features are desirable,

1) The ability to adjust and monitor the temperature of the DUT.
2) Monitoring power supply current compliance to check for latchup.
3) Operation at, or near, the rated DUT clock speed if test performed in dynamic mode.
4) The ability to record particle fluence for each test if electronic data access from a detection system is provided by the test facility (this enables each test run to store the fluence with the data file).

Downloaded by xu yajun (xuyj@beice-sh.com) on Jun 29, 2018, 12:46 am PDT
联系方式：xuyj@beice-sh.com 13917165676

3.1 Test equipment (cont'd)

3.1.2 ATE software

The ATE software creates the proper conditions for the test, and identifies, records and corrects errors as they are detected. Operation of the device with good fault coverage is required. When designing the test system, the experimenter should understand the portions of the die, signal path, and latching circuits of the device being tested in order to arrive at a quantitative result. The fraction of time the device is in an SEE susceptible mode and what fractions of the DUT's susceptible elements are not tested should be known. Complex devices do not always permit easy testing access.

The ATE software should be capable of

1) Controlling device initialization and rudimentary functional checks.
2) Device operation in dynamic or static operation, as required by the test plan.
3) Resetting the DUT during irradiation or real-time testing.
4) Error detection and logging, including the time that the error was detected. It is important during error detection that new errors are not omitted or that corrections are made for system dead time.

In addition to the characteristics listed above, the following features are also desirable

1) Bit error mapping and data processing, storage and retrieval for display.
2) Applicability to a variety of device types.
3) High-speed operation and a high duty factor.
4) Real-time DUT data display capability providing a higher test throughput and allowing for more precise control of testing.
5) The ability to do preliminary data analysis while the test is in progress. This feature is desirable for modification / optimization of test procedures in light of the data being collected.
6) Reliable audit path for data collection to allow correlation of experimental notes and collected data from the ATE.
7) Recording the particle fluence, either automatically acquired from the test facility or manually entered.

3.2 Test plan

A test plan shall be developed to support each test. This test plan will serve as a guide for the procedures and decisions to be made during the irradiation period. In most cases the test plan cannot be followed exclusively, as adjustments must be made during the course of testing based on equipment performance, observations and other factors.

BC LABORATORY beice 北测（上海）电子科技有限公司
Downloaded by xu yajun (xuyj@beice-sh.com) on Jun 29, 2018, 12:46 am PDT
联系方式：xuyj@beice-sh.com 13917165676

3.2 Test plan (cont'd)

For all soft error testing it is necessary to accurately measure the following:

1) Particle fluence at the DUT, either by estimation using Annex A in the case of real time SER (RTSER) testing or measurement in the case accelerated SER testing.
2) Number of storage elements that are subject to upset,
3) Number of upsets that occur in each storage element.

Measurement of the particle fluence depends on the test setup and is a matter of good laboratory practice and metrology. The number of storage elements, and the number of upsets in them caused by irradiation is easy to assess for a memory component, but may be much harder to determine for other types of components such as microprocessors or FPGAs. Whereas each storage element is generally visible in a memory, other types of components may have large numbers of inaccessible elements, particularly when they are being tested without knowledge of the proprietary internal structure. For this reason, the comparison of soft error rates for non-memory devices following even slightly different testing procedures is generally not meaningful.

A minimal test plan includes:

1) Description of the radiation flux to be used for testing, including calibration in the case of accelerated SER, or geographic description of the test location in the case of RTSER (see A for details).
2) For each DUT, the number of samples, supply voltages and required error counts.
3) Specification of the data to be collected for each exposure.
4) Test procedures for each phase of testing.

Minimum accelerated beam or alpha particle source test procedure:

1) Setup and checkout the ATE operation
2) Dosimetry calibration for beam testing or alpha particle source calibration information (see 5.4.2).
3) Check against reference DUT from previous testing for beam testing.
4) Initial test run for DUT to confirm exposure rate.
5) Data collection for each DUT, at planned supply voltages.
6) Final test using the same conditions as step 4 to verify consistency of results.
7) Final dosimetry and setup checks using the reference DUT for beam testing.

Steps 4 through 6 are repeated for each DUT type to be tested.

Minimum real-time test procedure:

1) Setup and check ATE operation
2) Data acquisition phase, typically lasting several weeks or months, depending on the sample size and DUT sensitivity.
3) Final setup checks.

After testing is completed a final report is written describing the DUT error rate for each of the test conditions. The requirements for what data and parameters to include in the final report are described at the end of 4, 5, 6, and 7.

Downloaded by xu yajun (xuyj@beice-sh.com) on Jun 29, 2018, 12:46 am PDT
联系方式：xuyj@beice-sh.com 13917165676

3.3 Test conditions

Test conditions for soft error testing are often limited by the capabilities of the portable ATE used to cycle the DUT.

3.3.1 Test pattern

The basic data pattern for all memory circuits is a logical checkerboard, alternating by address and bit. If detailed layout information for the DUT is available, a physical checkerboard is also useful. A determination of the best test pattern is left to the discretion of the experimenter, but must be documented in the final report.

The use of physical data patterns, i.e., patterns that are related to the actual layout of the DUT, rather than logical addressing is recommended where possible. These patterns may provide insight into the ionizing radiation sensitivity of the DUT. Because layout information is generally proprietary only DUT manufacturers would generally be expected to be able to meet this recommendation.

Some devices, particularly dynamic RAMs (DRAMs) and logic elements often have a "preferred" soft error failure, either 0 → 1 or 1 → 0. The selected test pattern must consider this possibility in its design. For testing when there is no *a priori* knowledge of the device the test pattern should balance the number of 0's and 1's. If the relative failure rates are known, perhaps from previous test experience, the test pattern may be adjusted to improve statistics of the less likely transition. The use of an unbalanced test pattern must be described fully in the final report and data analysis.

3.3.2 Supply voltage

The test plan defines the required supply voltage for the test. Since the soft error rate may be very sensitive to the supply voltage it is critically important that this parameter be accurately measured and controlled. Note that characterization of SER dependency on applied supply voltage is required by many customers. Some parts have internally regulated supply voltages that may interact with the measurement. These internally regulated supplies may automatically change their settings depending on operating mode, making the SER measurement dependent on the specific test method.

The DUT supply voltage needs to be carefully adjusted to match the values called for in the test plan. The soft error performance of many devices is very sensitive to the supply voltage so careful adjustment is required to assure consistent results. Some DUTs have internal voltage regulators and will be insensitive to supply voltage variations.

3.3.3 Static vs. dynamic testing

Depending on the objectives of the test program, static or dynamic operation of the DUT may be specified. For static tests the DUT is initialized to a known state, and then the DUT is irradiated. Following the irradiation, the state of the DUT is read out and compared with the initialized value to determine the number of upset events.

Downloaded by xu yajun (xuyj@beice-sh.com) on Jun 29, 2018, 12:46 am PDT
联系方式：xuyj@beice-sh.com 13917165676

3.3.3 Static vs. dynamic testing (cont'd)

In dynamic testing the DUT is also initialized prior to irradiation to a known state. Once irradiation begins, the DUT is continuously accessed, at a rate specified in the test plan, counting upset events as they are detected. Once the irradiation stops, sufficient time to read all of the DUT is allowed to assure that all upsets induced by the radiation have been tabulated. Generally, the DUT state is rewritten with a new pattern as it is being accessed, to correct upset events and to exercise more internal data states.

The pattern of accesses for dynamic testing has to be planned to eliminate "dead-time" between a read of a location and a subsequent write to that location. Any upset that occurs between a read from a location and the next write will not be detected since it is overwritten. Failure to account for this dead time will result in an erroneously low estimate of SER. The final report must include details of the dead-time calculation.

Use of a "write array" followed by "read array" update is not recommended. Soft errors that occur between the last read of a location and its next write cannot be detected and result in excessive dead time. For the case where continuous updating of the array is used, this method would result in 50% of the test time being unused and the SER value being too low by a factor of 2.

Dynamic testing of memory is often carried out through the device's normal access method. Non-memory components may use test access modes, such as JTAG boundary scan, for access to internal logic.

One example of a dynamic test cycle uses 2 cycles per address. The first cycle reads the value stored at the address, comparing it with the expected value and noting any errors. The second cycle writes a value to the same address to correct any errors. The second access writes the complement of the expected value so that every bit in the DUT changes state with each complete pass through the memory. This cycle has a very short dead time of approximately 1 memory cycle for each complete scan through the DUT.

Both types of testing are illustrated in the flow diagram in Figure 3.1. For these flows, a logical "checkerboard" pattern of alternating 0 and 1 value is assumed, along with a complementary rewrite operation for the dynamic test.

When testing non-memory components, such as microprocessors, the choice of static or dynamic testing may have a very large effect on the measured results, particularly at clock rates over 200 MHz. The

Downloaded by xu yajun (xuyj@beice-sh.com) on Jun 29, 2018, 12:46 am PDT
联系方式：xuyj@beice-sh.com 13917165676

3.3.3 Static vs. dynamic testing (cont'd)

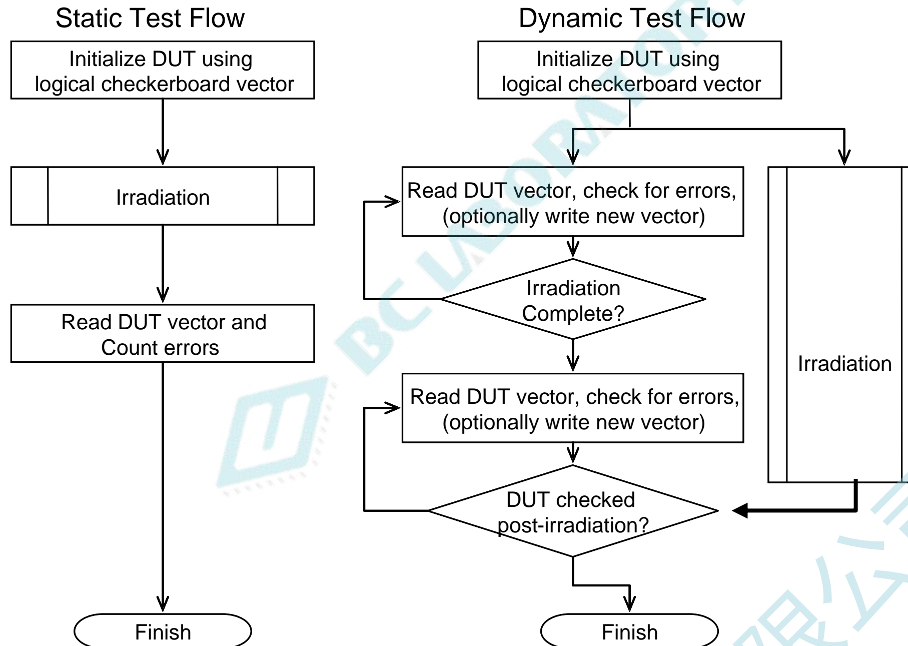

Figure 3.1 — Flow diagram comparing static and dynamic testing.

dynamic case will have a higher soft error rate due to the effects of errors in combinational logic being clocked into sequential logic elements and from race conditions created by particle strikes on the clock network.

3.4 Setup procedure

3.4.1 DUT packaging and handling

Special care must be taken in handling the DUTs used for real-time SER tests. All parts must be handled with the precautions for parts susceptible to damage from electrostatic discharge. The use of ground planes and straps is highly recommended whenever possible. In order for real-time SER results to be valid, standard production packaging (or a close replication) should be used whenever possible. While this might not be as important for neutron SER, the package can act as a source as well as shield for alpha SER. At the very least, the same molding compound and bump material (where appropriate) should be used.

3.4.2 Test equipment location

The test equipment should be set up close to the DUT holder to avoid noise issues related to long cabling. In the case of beam testing, this consideration must be balanced against test equipment upset from being too close to the scattered beam. Also ensure that cables are not physically blocking any areas accessed during the replacement of DUTs.

Downloaded by xu yajun (xuyj@beice-sh.com) on Jun 29, 2018, 12:46 am PDT
联系方式：xuyj@beice-sh.com 13917165676

3.4.3 Test setup checkout

An ATE checkout should be performed with the equipment that will be used to perform the test, including all cables connected, as they will be during the irradiation. After any major changes such as replacing the DUT, or modifying the cabling arrangement, a short dry-run test should be run to verify proper operation of the devices and the test system. It is important to test the entire system, with all the DUTs in place for some time in order to ensure ATE integrity.

For accelerated testing, particularly neutron and proton beam testing, the ATE setup should be checked without irradiation to confirm that the error rate is less than 1% of the expected value. A very low error rate may be seen at some facilities due to residual radiation even when the beam is nominally “off.” If these errors are suspected of being due to electrical noise issues rather than residual radiation, the test must be halted and the source of noise eliminated.

3.5 General testing specifications

Keep testing the DUTs until the desired number of errors has been observed or until the appropriate test duration is reached (determined by the required confidence intervals in B.1).

A minimal test will include the following operations:

1) Load DUTs.
2) Verify correct test program execution and that all DUTs are nominal.
3) Monitor error location and time of detection.

3.6 Data collection

For each run, record all data required for the final report (see last section of 4, 5, 6, or 7). For tests using a radiation beam, the distance from a reference point must be noted to account for solid angle effects if appropriate. Record any problems or unusual behavior.

If possible, record failure signatures. The impact of upsets on different circuits will result in observable differences at an IC’s output. For example, a hit on an address decode circuit may cause data to be written to the wrong address, causing two addresses to show up as fails – the address where the data was supposed to be written and the incorrect address where the data was actually written. Verify that the part is being properly operated, e.g., the appropriate address space is being covered for memory DUTs.

3.7 Considerations for testing non-memory components

Testing for non-memory components is a complex topic that cannot be completely described herein. This section addresses some specific issues to be considered for testing of various non-memory components such as random logic, microprocessors, and FPGAs.

A carefully written test plan and report are essential for meaningful non-memory testing. It is particularly important to consider the number of storage elements that are exposed during irradiation and the observability of errors in those elements. Errors in sequential logic, control structures and even FPGA configuration logic is often not observed during operation because it is masked by the operational state of the device or choice of test vectors. A minor change in the test conditions may have a large effect on the rate of observed errors.

Downloaded by xu yajun (xuyj@beice-sh.com) on Jun 29, 2018, 12:46 am PDT
联系方式：xuyj@beice-sh.com 13917165676

3.7.1 Random logic circuits

Testing procedures of the following types of logic circuits and devices are specified:

1) Sequential Logic (includes dynamic combinatorial logic)
2) Register Files
3) Static Combinatorial Logic

The SER testing procedure critically depends on the type of logic device under investigation. Testing of types 1 and 2 are somewhat similar to SRAM testing, since both types of cells are memory/storage cells with feedback devices at the state nodes. SER testing of type 3 is much more involved due to the transient nature of the propagating glitches and the dependency on the circuit's logic configuration and state at the time a transient reaches a sequential cell or output.

<u>Sequential Logic:</u> In this section, the procedure to measure the *nominal* SER of sequential logic is described. (Note: The *nominal* SER refers to conditions where logic sequentials hold data statically, without clocks being exercised.) Clock upsets of nodes located in the sequential logic are not covered in this specification. Note that the actual SER of sequential logic in a product can be vastly different from nominal values and depends critically on the circuit context in which the sequential has been placed. The actual SER of sequential logic in a data path depends on the logic depth of the stage and on the clock frequency. The nominal SER of sequential logic can be tested using a shift register or array type architecture.

A sequential logic testing procedure typically involves the following steps:

1) The clock signal (or clock signals, if a race proof scheme is implemented) is running at a low speed (typically kHz to a few MHz range) and the data are shifted in.
2) The clock(s) is (are) stopped and the devices are irradiated.
3) Irradiation is stopped.
4) Clocks are turned on and data are shifted out and logged.

Due to the asymmetric nature of sequential nodes, critical charges and therefore failure rates of different sequential nodes are state dependent. At a minimum, data patterns must include a logical checkerboard pattern and its complement or both solid ones and solid zeros to cover all potential transitions and states. Patterns are written into the shift register before exposure and then irradiated for a given exposure time. After exposure data are shifted out and checked for any upsets. This procedure allows identification of the sequential logic cells that were upset during exposure.

For tests where the clock is running during irradiation, use of a test structure with a non-overlapping clocking scheme, where the master and slave stages of a flip-flop are clocked separately, is recommended to avoid minimum-delay problems. If master/slave flip-flops are used in a shift register topology together with a non-overlapping clock scheme, the state information of one stage (master or slave) is lost because the shifting process overwrites the state of one of the stages after both clocks have been stopped. Testing is recommended at slow clock speeds, i.e., at clock speeds where the cycle time is orders of magnitude longer than the internal device delays.[1, 2]

Downloaded by xu yajun (xuyj@beice-sh.com) on Jun 29, 2018, 12:46 am PDT
联系方式：xuyj@beice-sh.com 13917165676

3.7.1 Random logic circuits (cont'd)

The DUT can be designed to have significant SEU contributions from one node only by increasing the critical charge Qcrit of other nodes sufficiently. This allows for a separation of 1→ 0 and 0 → 1 transitions. Furthermore, by implementing various sequential flavors with different diffusion area sizes of the most critical node, the diffusion area scaling can be characterized [3].

The functionality of the sequential logic circuit must be tested prior to the radiation exposure for all patterns over the planned voltage range.

The nominal SER of sequential logic can also be assessed by exploiting scan chains implemented in products for testing purposes. The testing procedure in this case is very similar to the one above since scan chains are usually implemented in the form of shift registers.

Multiport Register Files: The SER of register files may be assessed using a memory array structure where all register file cells can be individually written and read. Testing guidelines are the same as for memory components. One important difference is, however, that for multiport devices the write and read logic also needs to be tested for its susceptibility to upsets.

Static Combinatorial Logic: The soft error rate of static combinatorial logic is defined here as the rate of latched glitches induced by upsets of combinatorial nodes. A glitch by itself is not considered a soft error and a static combinatorial gate by itself does not have a well-defined soft error rate. Its SER contribution depends on the circuitry it feeds into. The glitch induced by radiation can be attenuated or even blocked by consecutive stages. The arrival time at the latching element determines if the glitch is latched and therefore whether the event is relevant.

Static combinational SER has to be tested in its natural circuit environment. Static combinational SER can be tested using a shift register architecture as described in [4]. This architecture comprises shift registers of various lengths and with different logic depths to quantify the impact of clock speed and electrical masking on the failure rate. Because attenuation (electrical masking) depends on the gate delay relative to the pulse width, it is highly recommended that the static combinational test structures comprise paths with different logic depths and different logic-cell sizes (i.e., gate speeds).

To maximize the signal due to upsets occurring in combinatorial nodes in a test circuit, the SER contribution of sequential elements needs to be minimized. This can be achieved by using a minimum number of hardened sequential elements.

Because the content of the receiving latch impacts the sensitivity to the minimum magnitude and width of the glitch to be latched, data patterns must include a logical checkerboard pattern and its complement as well as solid 1 and solid 0 patterns [5].

Recommended variable evaluations include:

1) Voltage: nominal +/- tolerance; Expanded range of test voltages is highly recommended.
2) Different cycle times; please note that the SER of static combinational logic increases linearly with clock speed.

Downloaded by xu yajun (xuyj@beice-sh.com) on Jun 29, 2018, 12:46 am PDT
联系方式：xuyj@beice-sh.com 13917165676

3.7.2 Field programmable gate arrays

When testing FPGAs for soft error effects, one should design the test strategy to detect:

1) SEU in the configuration memory
2) SEFI in the logic blocks
3) SEFI in the IO blocks
4) SEFI in the configuration circuitry
5) SEU in flip-flops embedded in logic blocks
6) SEU in RAM blocks

The final report should clearly show results for all failure mechanisms separately.

One approach for measuring SEFI and SEU in configuration memory uses a test strategy based on the continuous monitoring of the outputs of a combinatorial circuit implemented in the FPGA under test. As soon as a permanent mismatch of the output values is observed, the test is stopped and the configuration memory read back and stored in a file. Additionally, the FPGA configuration memory is periodically read back, even if the output values are correct. The test strategy enables identification of the non-critical and the critical SEU in the configuration memory, that is, those SEU in the configuration memory that do not create an error in the output, and those that create an error in the output.

For SEU in embedded logic blocks and RAM blocks, a similar approach to other stand-alone components may be used.

3.7.3 Microprocessors

The SER of microprocessors comprises failure contributions from the components described above. The microprocessor SER can be assessed either by properly adding up the contributions of those components tested individually, or by directly measuring the SER on the microprocessor itself [3.6]. In the latter case the microprocessor needs to be tested in either a real system or on a high speed ATE. In both cases the failure rate of a microprocessor is application dependent.

Testing in a real system involves running diagnostic software on the system that logs detected upsets. Note that this constitutes only one potential contribution of the overall microprocessor SER. Changes in unobserved states, also known as silent data corruption, can be observed for only by transforming silent errors into detected errors. Another complication arises from the fact that a system might crash and no data might be available on what caused the crash. Great care needs to be taken to ensure that the system is stable and that other intermittent errors are not mistaken as radiation-induced soft errors. In the case of accelerated testing of microprocessors in systems, it is important that only the DUT be irradiated and other peripheral chips are not accidentally irradiated.

Running the microprocessor on a high speed ATE while exposing it to radiation has the advantage that more of the relevant errors can be detected and less ambiguity exists. In this case the SER is typically assessed for specific patterns that might yield SER values very different from actual systems deployed in the field.

Downloaded by xu yajun (xuyj@beice-sh.com) on Jun 29, 2018, 12:46 am PDT
联系方式：xuyj@beice-sh.com 13917165676

4 Real-time (unaccelerated and high-altitude) SER procedures

4.1 Background

4.1.1 Introduction

The most direct way to measure SER in a device is simply to observe it under standard operating conditions under normal ambient background radiation. The inherent problem with this approach is that the effective failure rate is so low that a single device would take decades to generate a statistically significant number of soft errors. In order to circumvent this limitation, real-time (unaccelerated) SER (RTSER) testing utilizes a very large number of devices in parallel to reduce the required test time. Testing can also be done at elevated altitudes where the higher neutron flux will generate a higher error rate. The system can either be a set of custom designed boards populated with a large number of the devices to be tested or a large server or other complex system (or array of servers/systems) containing a high part count.

Since RTSER testing typically involves a large number of devices and relatively long test times (weeks or months), a good test plan is crucial. It is extremely helpful to have some accelerated SER data (alpha particle and neutron) to get an estimate of the average failure rate. This estimate can then be used with the chi-squared statistics in C.2 to optimize the sample size and test duration so that the measured real-time SER will be valid to the desired confidence interval.

The procedures for non-accelerated RTSER and accelerated testing are similar. For real-time testing, the neutron flux is generally assumed to be a nominal value, based on the location of the ATE (see annex A). Alternatively, a measurement of the actual flux during the test may be made. This is a difficult measurement and beyond the scope of this specification. The alpha particle flux from the DUT packaging materials is assumed to be representative of the actual packaging. Separating the alpha and neutron contributions is complicated, requiring accelerated beam testing or system tests conducted at multiple locations. If RTSER results are to be used for SER estimates at other locations, this separation of effects is required. The minimum test procedures are listed separately below.

4.1.2 Guideline

The test method described below defines the requirements and procedures for RTSER testing without an ionizing source, i.e., only the natural ambient background radiation due to terrestrial cosmic rays and alpha particles from packaging and chip materials. Accelerated or ASER testing with alpha particles, high-energy neutrons/protons, and thermal neutrons are discussed in 5, 6 and 7, respectively.

4.1.3 Limits of test method

This test method can be used to test large arrays of SRAM or DRAM memory, and can be adapted for use with other types of components, such as microprocessors. The RTSER test algorithm and hardware must have allowances for separating actual radiation induced soft errors from errors induced by system noise. Since the RTSER test method does not discriminate between alpha particle and neutron induced soft errors, doing real-time tests on the same components in different environments, such as in a cave for shielding the terrestrial neutron flux, at high altitudes for enhancing terrestrial neutron flux, and thermal neutron shielding for shielding thermal neutrons (see 7) allow the alpha particle SER contribution (which will be constant) to be separated from the terrestrial high-energy and thermal neutron-induced SER.

Downloaded by xu yajun (xuyj@beice-sh.com) on Jun 29, 2018, 12:46 am PDT
联系方式：xuyj@beice-sh.com 13917165676

4.1.4 Goal of test method

The primary goal of RTSER testing is to obtain a well-defined estimate of the total soft failure rate for products/components using a uniform test methodology.

4.2 Test facilities and equipment

4.2.1 Basic test requirement

The basic RTSER test requirement is to monitor each DUT's output vector and continually verify that the measured output matches the expected output vector. A vector could simply be a pattern of data stored within the memory array of a DUT, or a stream of data generated as an operation or sequence of operations performed by the DUT on an input vector. The latter would be relevant for logic devices such as microprocessors. If the vector from the DUT does not match the expected vector, then a soft error may have occurred. The system consists of the input stimulus generator and response recorder that is designed to accommodate the specified device. Testing requires some sequence of writing data to the DUT, reading the data back, comparing the output data to the written data, and tabulating the number of detected errors.

4.2.2 DUT board hardware

RTSER testing requires a DUT board capable of supporting a large number of DUTs. Several DUT boards may be used in a single system. The boards are controlled by a computer driven system that monitors and communicates with the DUTs during the test interval.

4.2.3 Test hardware

The test cables should be short enough and designed with the proper shielding to allow sufficient test speeds without electrical noise problems. If this is not possible, then on-board controllers should be used to allow high-speed operation of the DUTs and low speed communication off-board. The ATE should be capable of being configured to do both static and dynamic testing.

The following features are also desirable:

1) the ability to adjust and monitor the temperature of the DUTs or at least the ambient in which the DUT boards are located;
2) the ability to monitor power supply current of individual DUTs to check for latchup (preferably the ability to individually remove power from latched-up DUTs should also be provided);
3) if BPSG is used in the device process, the ability to shield the DUT enclosure from background thermal neutrons to determine their contribution to the SER (see 7);
4) operation at the rated core cycle for the DUT. If this is not possible due to power consumption issues, the deviation should be noted in the final report.

Downloaded by xu yajun (xuyj@beice-sh.com) on Jun 29, 2018, 12:46 am PDT
联系方式：xuyj@beice-sh.com 13917165676

4.2.4 Test software

The basic requirements for a RTSER DUT test system are as follows:

1) Create test conditions for the DUT. A suite of test patterns should be selected that represents the intended operation of the DUT. In general, the test program for memories or arrays of latches should include patterns of ones, zeros and more complex variations, such as internal checkerboards, alternating rows and alternating columns to determine if the component has any preferred data states that are more robust or can be affected by nearest neighbors.

2) Identify and record any errors based on the selected test conditions. If an error does not go away when the component is rewritten or power cycled (powered down and then powered up), then it is a hard or intermittent fail. Hard fail events should be noted in the final report with an explanation of the source (e.g., a latent defect in the DUT, an early life fail, a power supply malfunction, etc.).

3) Provide adequate fault coverage and failure bit mapping. This is effective in distinguishing multiple independent failures from a cluster of nearest neighbor upsets from a single multi-cell upset caused by a single energetic particle (MCU). If a redundancy latch is hit and brings a defective row or column back into a repaired memory array, the signature of the error pattern should be distinguishable from a normal SEU or MCU. Likewise, if latchup occurs in a memory array, the signature of that event (typically inducing a large number of contiguous failing bits) should be uniquely distinguishable.

4) Initialization of control devices and rudimentary functional checks. Any upset of the control devices or power supplies should be distinguished from upsets of the DUT.

5) Select operation mode (dynamic or static operation) and provide resetting capability. For example, static testing of memory would be to write a test pattern once and store it for an extended period before reading the pattern back out. Dynamic testing of memory would involve writing once and then reading continuously or interleaving write and read operations at a specified operating frequency.

6) Provide error detection and logging. Typical error correction codes can correct a single bit and detect double bit errors but are ineffective at detecting multi-bit errors with a bit count greater than 2. Bit-by-bit comparison of the read pattern with the original write pattern is required to determine the details of particle hits.

7) Data analysis and logging while the test is in process. This is required to help separate independent events due to multiple particle hits from single events that upset multiple cells. (Note: This is less of a concern for real-time SER than accelerated SER due to the lower flux levels, but should not be ignored.)

8) Ability to distinguish and report different soft error types (e.g., single memory cell upset, multiple cell upsets, latchup, functional interrupts from hits on the address or control registers, etc.). See 2 for definition of types of soft errors.

Downloaded by xu yajun (xuyj@beice-sh.com) on Jun 29, 2018, 12:46 am PDT
联系方式：xuyj@beice-sh.com 13917165676

4.3 Testing procedures

4.3.1 Pretest preparations

4.3.1.1 Sample selection

Component variability for RTSER is generally small for components produced with the same masks and fabrication steps. The system user must be sure that components tested are equivalent to actual baseline production components, because manufacturers may make process/design changes affecting SER without changing the component's designation.

In general a minimum requirement to establish a product's RTSER is to run the test with roughly equal numbers of nominal devices from at least three different baseline lots. If a product is tested that has on-board error-correction codes/circuits (ECC), tests should to be run under two conditions, both with ECC enabled and with ECC disabled if possible. The presence of ECC and its on/off status during each data collection run must be included in the final report. (Note: In general, ECC is effective at masking single-bit cell upsets. But it will be ineffective with non-cell related events such as neutron-induced latchup or other single-event functional interrupts).

4.3.1.2 DUT preparation and orientation

The DUT package used for the RTSER test must be identical to the package used for production components. This is critical for the alpha component of RTSER. If a finned heat sink is required, this can have an impact on the neutron flux reaching the DUT. Since there is some angular dependence for high-energy neutrons (more neutrons have normal incidence to the Earth's surface), the DUTs should be mounted in an orientation similar to the end use where the tester does not dictate otherwise. If this is not known, then the DUTs should be mounted horizontally to expose them to the maximum flux where the tester does not dictate otherwise. Care must be taken in considering the path of atmospheric neutrons in the real-time SER setup and the effects of building shielding. For example, vertical stacking of DRAM DIMMs that are each oriented in a horizontal position would cause a neutron to traverse many DRAMs before reaching the final device. The possibility of generating secondary particles as well as the attenuation of flux could lead to anomalous results. Therefore, the layout of the DUTs in real-time SER testing should avoid this. If this is not possible, an attempt should be made to note any differences in SER FIT between the top and bottom devices. Ideally, where other constraints do not exist, the testing location should also be done on the top floor or roof to avoid building shielding effects. Finally, the use of heatsinks, the orientation of the DUTs and stacking of DUTs should be noted in the final report.

4.3.1.3 Load DUT

Place the desired population of DUTs in their sockets on each DUT board and run the test program to verify proper operation of all the DUTs. Make necessary adjustments to system and DUTs to insure that the test program executes flawlessly on all DUTs in the test system.

Downloaded by xu yajun (xuyj@beice-sh.com) on Jun 29, 2018, 12:46 am PDT
联系方式：xuyj@beice-sh.com 13917165676

4.3.1.4 Effective neutron flux at the test location

When performing real-time SER testing, it is necessary to either measure the neutron flux directly or make estimates based on the amount of building shielding and the terrestrial neutron flux (see annex A). Measurement of the actual neutron flux is rather involved because several detection schemes are required to obtain counts over a large neutron energy range and there are many interferences. The results should be normalized to NYC flux in the final report for purposes of standardization. A qualitative estimate of sensitivity to thermal neutrons should also be made (see 7).

If the testing is to be done at high altitude, several factors should be taken into consideration when designing the experiment.

1) The cosmic ray dosimetry method and how it is monitored.
2) The electrical power features and stability of the facility. The test setup often requires an independently stabilized uninterruptible power supply to run the test. Note that the overall power consumption for a large sample size can be significant. Make sure that the facility can provide the required power with good stability.
3) The lab should be protected against electrostatic discharge from lightning (i.e., presence of a Faraday cage, a lightning rod, etc.)
4) The environmental conditions that influence cosmic ray flux and how they are monitored (i.e., temperature, hygrometry, average pressure, average accumulation of snow, etc). An assessment of the impact of the variation of these environmental conditions (either important or insignificant) should be noted in the final report. If variation is determined to be insignificant, an average condition can be used in the final report. General guidance on the threshold for significant variation is a 50% impact on measured SER. Annex A details the impact of altitude and barometric pressure. As a quick rule of thumb:

   Example 1 — a 40mmHg drop in atmospheric pressure (which is a significant change in weather conditions), will lead to a 50% increase in neutron flux.

   Example 2 — based on typical values of snow density (~0.4-0.5 gm/cm³), the reduction in neutron flux due to attenuation by snow on a roof is approximately 50% for 5 feet of snow.
5) It is convenient to have real-time monitoring of the experiment remotely through Ethernet access, as well as a remote reset function so that full-time staffing is not required.

4.3.1.5 DRAM and SRAM testing

At the minimum, data patterns must include a logical (external) checkerboard pattern and its complement, alternating by address and by bit. This will average out any asymmetry in SER behavior and represent actual application of the device. Read and write cycles should be selected so that all the elements of the DRAM or SRAM circuit (sense amps, storage capacitor or latches, decoders, multiplexers, etc.) are vulnerable to upset.

If the design supports a broad frequency range and different circuit elements will show different soft error rates as a function of frequency, care must be taken in selecting the core clock. A recommended solution is to run the RTSER test at a nominal frequency defined either by the tester capability or the product specification sheet to get a calibrated overall upset rate. Since the RTSER results can be frequency dependent, the nominal frequency used and how it was selected should be noted on the final RTSER report. Accelerated SER testing can then be used to determine the frequency dependent upset rate of the various circuit elements.

Downloaded by xu yajun (xuyj@beice-sh.com) on Jun 29, 2018, 12:46 am PDT
联系方式：xuyj@beice-sh.com 13917165676

4.3.1.5 DRAM and SRAM testing

For those DRAM and SRAM designs that support a standby or reduced power mode (i.e., read and write operations are not allowed, but the device is expected to maintain its memory), a fraction of the real-time SER testing time should be dedicated to this mode of operation. The final report should include the estimate of SER from this mode vs. normal operating mode.

4.3.1.6 Other device testing

It might not be appropriate to use real-time SER testing procedures on all device types. Memory devices are good candidates because these devices are dominated by the core array and it is possible to capture and log all cell related upsets. Likewise, any FPGA or ASIC technologies using a high SRAM or DRAM content would be good candidates. On the other hand, not all upsets in logic devices will propagate to the output. This will depend on the static and dynamic design elements used. Therefore, an estimate of the expected fail rates should be made initially and the counting statistics discussed in annex B should be use to determine if a real-time SER test is appropriate for a device.

4.4 Differences in real-time SER tests and actual end-user observed fail rates

While the error rates determined from real-time SER testing are representative of device performance under real-life radiation conditions (both alpha particle and atmospheric neutrons), the results are not necessarily directly applicable to end user system applications. In addition to the customer environmental conditions that can be accounted for using Annex A (i.e. geomagnetic location, altitude, building construction, etc.), other factors that need to be taken into consideration in translating real-time SER FITs to actual end user error rates include (but are not limited to):

1) Geometry of end user system (e.g., Are components stacked? Are they above or below the system board? Are the system boards stacked? Are the system boards oriented parallel or perpendicular to the background radiation? etc.)
2) What types of errors are masked by software ECC code of the application (not to be confused with built in hardware ECC in some device designs)?
3) What fraction of errors will be over-written before they are read? (Highly sensitive to application software.)
4) Is the end-system using standard packaging or heat sinks?

4.5 Final report

The following items must be included in the final report for real-time SER tests:

DUT description:

1) Sample size (number of devices tested)
2) Vendor, Part # and Die rev (for commercial components)
3) Process technology (feature size, # and type of metal levels, presence or absence of polyimide or other layers, etc.)
4) Circuit (e.g., SRAM, DRAM, Microprocessor, FF chain, etc.)
5) On-chip error correction (type and coverage of ECC)
6) Dimension of the active device area tested.
7) Package (type, connection to chip, materials and geometries) with description of any modifications made for SER testing (e.g., etch back of encapsulant, etc.).

Downloaded by xu yajun (xuyj@beice-sh.com) on Jun 29, 2018, 12:46 am PDT
联系方式：xuyj@beice-sh.com 13917165676

4.5 Final report (cont'd)

Test Description:

8) Test duration
9) Voltage (external supply, internal regulated, back bias voltages if applicable)
10) Junction & ambient temperature during test
11) Static or Dynamic test (core cycle time or frequency if dynamic) – special note must be made if the DUTs are run at a cycle time different than the intended end use
12) Refresh rate (where applicable)
13) Test patterns and data patterns, including dead-time calculation (see 3.3.3)
14) ATE(commercial model and/or physical description)
15) Description of test board
16) Special shielding from radiation sources (if used)
17) Record any problems or unusual behavior

Fail Information:

18) Time of each failure
19) Failing electrical address or addresses
20) Failing physical location or locations

    Electrical signature of each soft error including a description of the occurrence of SEU, MBU, SEL, and SEFI events. Estimating a failure rate without determining the types of errors occurring (SEU, MBU, MCU, SEL, SEFI, etc.) can lead to erroneously high average failure rates. The effective failure rate of each unique failure signature must be calculated accordingly:

    FIT(total) = [total # of events (SEU, MCU, SEL, etc)/device hours]x10^9

    FIT(single-cell) = [number of single cell events/device hours]x10^9

    FIT(multiple-cell) = [number of multi-cell events/device hours]x10^9

    FIT(SEL) = [number of SEL events/device hours]x10^9

21) Voltage, ECC on/off status, chip power mode and test/data pattern at the time of failure
22) Identification of failures that are multiple-cell errors
23) Electrical signature and source of hard errors (if observed)

<u>**Real-time SER specific items**</u>

Location of devices under test:

24) Latitude and Longitude
25) Altitude
26) Average of atmospheric conditions
27) General building description (e.g., number of floors, building material, windows, etc.) and location of DUTs within building
28) Either a measurement of the neutron flux at the ATE or an estimation showing clear details of the calculation (e.g., direct measurement over a particular energy range, calculations from annex A, etc.)
29) Orientation of DUT to horizon and geometry of boards (i.e., planar or stacked)

Downloaded by xu yajun (xuyj@beice-sh.com) on Jun 29, 2018, 12:46 am PDT
联系方式：xuyj@beice-sh.com 13917165676

4.5 Final report (cont'd)

Additional Test & Fail parameters:

30) Periodicity of test readouts
31) Cumulative duration in hours
32) Range of calendar dates of data collection
33) Calendar date of each failure

SER Calculation:

34) Calculation of real-time SER FIT at test site for each type of event (e.g., cell upset, logic upset, latchup, etc.) The real-time SER should be calculated using the methods outlined in annex C for a specific confidence interval (assumed confidence level must be included in the final report). This will be customer driven depending on the application and level of ECC used.

    NOTE The omission of a specific failure rate requirement is intentional, and the failure measurement technique, data analysis and reporting must follow the well-established procedure defined in this document.

35) Translation of real-time SER FIT to NYC. (This will require estimation of neutron and alpha particle components. These calculations should be stated clearly in the report.)

5 Accelerated alpha-particle test procedures

5.1 Background

5.1.1 Introduction

Uranium and thorium impurities found in trace amounts in the various production and packaging materials emit alpha particles. Alpha particles are strongly ionizing, so those that impinge on the active device create bursts of free electron-hole pairs in the silicon. This charge disruption can be collected at pn junctions (much like charge created by light), producing a current spike (noise pulse) in the circuit. These current spikes can be large enough to alter the data state on some circuits. This section deals with the method of determining a component's sensitivity to alpha particle radiation from accelerated experiments.

5.1.2 Scope

This section deals strictly with SER induced by alpha particles. The alpha flux is independent of altitude, and is only a function of the type, location, and amount radioactive impurities present in the component or its package.

Alpha particle SER data cannot be used to predict high- or low-energy neutron cosmic-ray-induced failure rates. Conversely, neither can high-energy neutron nor low-energy neutron SER data be used to predict alpha-induced failure rates. An overall assessment of a device's soft error sensitivity is complete ONLY when the alpha AND high- and low-energy neutron induced failure rates have been accounted for.

Downloaded by xu yajun (xuyj@beice-sh.com) on Jun 29, 2018, 12:46 am PDT
联系方式：xuyj@beice-sh.com 13917165676

5.1.3 Safety issues

All of the accelerated test procedures involve the use of ionizing radiation sources that are potentially hazardous. Proper safety and monitoring procedures are essential for tests utilizing these sources.

Test hardware and parts may become contaminated with radioactive material when recoil fragments or larger fragments of the radioisotope escape the alpha source encapsulation. Good ventilation should be provided as some unsealed alpha sources may emit radon as a decay product. When not in use, alpha sources should be stored away from personnel as most alpha sources also produce low-level gamma radiation. Alpha sources should be handled with care even though external alpha emission is not hazardous (alpha particles have insufficient energy to penetrate the dead layers of the skin). Alpha emitting contaminants are extremely hazardous if inhaled or swallowed as alpha particles damage living tissues inside the body. It is the responsibility of the user of this test method in consultation with radiation safety personnel to establish the appropriate safety and health practices and the applicability of regulatory limitations.

5.1.4 Guideline

The test method described below defines the requirements and procedures for accelerated SER testing with alpha particle radiation. Generalized real-time (unaccelerated), or field testing has been dealt with in 4, while accelerated testing for SER induced by cosmic radiation is dealt with in 6 (high-energy) and 7 (low-energy).

5.1.5 Limits of test method

The accelerated test method in this section applies ONLY to alpha-particle-induced events. It does NOT apply to terrestrial-cosmic-radiation-induced events or events induced by the reaction of thermal neutrons with ^{10}B. This test method can be applied to the testing of memory, sequential logic, combinational logic, or components combining these circuit types.

5.1.6 Goal of test method

The end product of this accelerated testing is a well-defined estimate of the alpha-particle-induced failure rate for components. The soft failure rate can be characterized as a function of voltage, timing, and possibly other operating variables.

5.2 Alpha particle environment

See detailed description in annex D.

5.3 Packaging for alpha particle testing

Unlike accelerated neutron and proton test methods where the package type is not critical, for accelerated alpha particle testing the DUT’s surface must be directly exposed to an isotope source without any intervening solid material and with a minimal air gap.

Recommended DUT package types are the ceramic dual-in-line (CERDIP) or pin-grid array (CERPGA) package, as illustrated in Figure 5.1a and Figure 5.1b respectively. Certainly, other package types that offer access to the top surface of the chip can also be used but these types in particular are mechanically robust, particularly when used with zero-insertion force (ZIF) sockets allowing reliable loading and unloading over many cycles.

Downloaded by xu yajun (xuyj@beice-sh.com) on Jun 29, 2018, 12:46 am PDT
联系方式：xuyj@beice-sh.com 13917165676

5.3 Packaging for alpha particle testing (cont'd)

The die should be mounted and wirebonded within the well or cavity such that the surface of the die is as close as possible to the top surface of the package without anything, such as the bond wires, projecting above this plane. This configuration is required to minimize the alpha source-to-die spacing, while providing a convenient indexing surface for the isotope source. The metal lid for the package should be installed with tape to protect the DUT between tests.

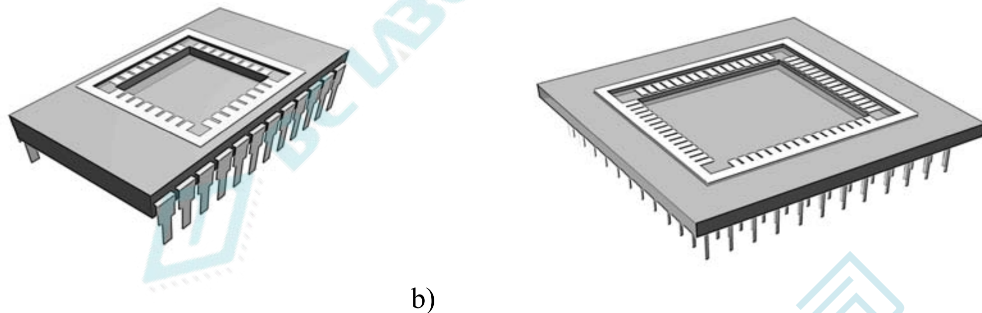

Figure 5.1 — Recommended packages for alpha particle testing, a) ceramic dual-in-line package (CERDIP), and b) ceramic pin-grid array (CPGA).

If the product to be tested is already encapsulated in a plastic package, the material over the die must be etched back to fully expose the active area. If the manufacturer's packaging includes a die coating, typically polyimide, over the surface of the die, this coating must be left in place at full thickness for accurate testing. In this case it is best to have unpackaged, but coated, samples of the DUT provided by the manufacturer for alpha testing, rather than attempting to etch back the existing packaging material. Lead-over-chip (LOC) packages are not suitable since the lead frame shadows a large portion of the device. Product or test chips with solder bumps distributed over the face of the die (for flip-chip attachment) are also not suitable for the same reason.

Wafer-level testing can also be used to perform alpha-particle testing. The advantage of wafer-level testing is that no packaging issues or costs are incurred. However, the wafer-level test system must have a probecard configured to allow the alpha particle source to be placed accurately and in close proximity to the die without shorting the probe pins.

5.4 Alpha particle sources

5.4.1 Alpha source selection

Different types of alpha sources can be used to simulate the alpha emission from uranium and thorium impurities. Sources that emit alpha particles with energy spectra similar to uranium and thorium impurities simulate the radiation environment of wirebonded components encapsulated in molding compound. Sources that emit alpha particles with similar energy spectra to ^{210}Po are used for simulating components in a flip-chip arrangement with solder bumps. The source should provide an alpha particle spectrum similar to that encountered in the actual component.

Pure radioisotope foils or metallic substrate foils with the radioisotopes deposited or diffusion-bonded may be used. Solid sources that are physically thicker than the range of the highest energy alpha particle emitted are best since the alpha spectrum will be distributed as it would be in the real packaged device.

Downloaded by xu yajun (xuyj@beice-sh.com) on Jun 29, 2018, 12:46 am PDT
联系方式：xuyj@beice-sh.com 13917165676

5.4.1 Alpha source selection (cont'd)

Since the range of alpha particles in dense metals is limited to < 40um at 10MeV, a solid source at least 0.04mm thick should ensure a distributed spectrum is emitted. Thin-film sources produce a mono-energetic spectrum (see Figure D.1) that is typically not representative of the distributed spectrum (see Figure D.2) that would occur in a real packaged device. This can lead to variation in resulting charge deposition profile in the device (see Figure D.3). These effects should be taken into account along with the availability of alpha sources before designing the experiment.

The energy spectrum should be measured and the intensity calibrated on a regular basis (more frequently for sources with short half-lives) to ensure that the source is providing the expected spectrum and flux. The source area should ideally be larger than the device area to ensure that all angles of incidence are allowed.

An alternative is the use of an ion accelerator to provide a monoenergetic and uniaxial beam of alpha particles. The disadvantages of accelerators are the experimental complexity and the fact that many runs will be needed at different energies and angles to obtain the alpha SER. The advantage is that the localized and collimated beam allow identification of sensitive areas and angle dependencies that anisotropic, uncollimated radioisotope sources cannot provide.

5.4.2 Alpha particle source calibration

Alpha sources lose activity by sputtering induced by fragments ejected from the source. Annual calibration is recommended to ensure that the source flux is known, particularly for high activity sources whose intensity can change dramatically over a short period. The type, activity, physical configuration of the radioisotopic source, energy spectrum (if available), and date of last calibration must be included in the final report. Ion accelerator sources must be calibrated and the flux measured from time-to-time to ensure it is at the expected levels.

5.4.3 Alpha particle source fluence

The total number of particles incident during a test must be sufficient to establish with a high statistical confidence that the entire sensitive volume on the DUT has been irradiated. A fluence that will induce a minimum of 100 upsets during the test interval is considered a minimum fluence. See annex B for discussions on statistically based confidence levels.

5.4.4 Alpha particle source flux

If different alpha source intensities are used, usually the tests are started using the source with the highest flux. If the fail rate is too high (> about one per second) the flux should be decreased. It is preferable to also run at a lower flux (e.g., 1/10 normal flux) to check for a nonlinear SER flux dependence. If there is a nonlinear flux dependence, the flux should be dropped until the flux dependence becomes linear. The accelerated flux is many orders of magnitude higher than the flux at use conditions, i.e., nominal package alpha flux; thus the use of lower alpha particle fluxes leads to potentially more accurate SER estimates.

Downloaded by xu yajun (xuyj@beice-sh.com) on Jun 29, 2018, 12:46 am PDT
联系方式：xuyj@beice-sh.com 13917165676

5.4.5 Loading the alpha source

After the component or wafer has been loaded and verified to be functioning as expected, a background test is run with no source as described in 3. When this test is complete, the appropriate alpha source is centered over the DUT. The source-to-DUT spacing should be made as small as physically possible – **a spacing of less than 1mm is recommended**. The actual spacing must be recorded in the final report, especially important if a spacing of ≤ 1mm cannot be used. The active area of the alpha source should be larger than the device area and must also be recorded on the final report. Great care must be used to ensure that the surfaces don't touch, since any contact could short the device and damage the source encapsulation. The recommended configuration is shown in Figure 5.2.

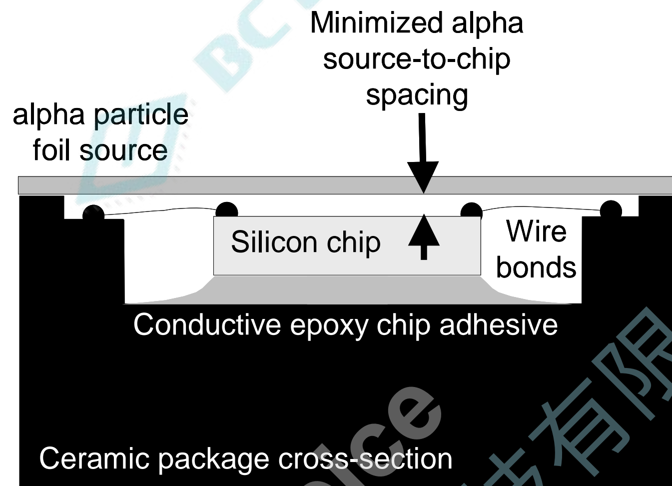

Figure 5.2 — Cross-section through ceramic package illustrating recommended alpha source size and placement – larger than the chip and as close to the chip as possible.

5.5 Basic test methodology

The basic test methodology for memory arrays is storing a known data pattern in the array while the part is exposed to the accelerated alpha particle source and comparing the stored pattern that is present after the device has been irradiated. At some time during and/or after the exposure, the data is evaluated to identify the number of changes in the pattern as errors. Other circuits may have different ATE requirements. Considerably more detail on the testing methodology is found in 3.

The system consists of the input stimulus generator and response recorder that would be designed to accommodate the specified device. Testing requires some sequence of writing data to the DUT, reading the data back, comparing the output data to the written data, and tabulating the number of errors. For simple memory arrays, a bit is failing when the data read from that bit is different from the last data written to that bit. It is also useful to identify failing addresses and time of failure for dynamic tests.

Downloaded by xu yajun (xuyj@beice-sh.com) on Jun 29, 2018, 12:46 am PDT
联系方式：xuyj@beice-sh.com 13917165676

5.6 Test procedure and results

5.6.1 General test specification

The test method utilizes an alpha particle source (either a solid source emitting alpha particles from nuclear decay or a helium ion beam source) with alpha particles having a similar energy spectrum to the alpha particles emitted in the nominal use environment but providing a flux at the DUT that is significantly higher than the actual use environment. See annex D for a detailed description of the typical packaging environment.

At least one run should be performed without the source for the maximum test duration to be used. For the background test(s), the DUT must exhibit no soft errors. After the background run is performed the actual testing under radiation exposure is performed.

Typically multiple tests are run under irradiation using various test patterns, voltages, cycle times, and different DUTs. The number and type of errors observed and the duration of each test are recorded as well as any evidence of MBU, SEL, or SEFI.

5.6.2 Basic alpha particle flux acceleration factor

The intensity of alpha particle sources is often reported in the International System of units (SI), the becquerel (Bq), representing a radioactivity of 1 disintegration/sec into 4 pi steradians (a spherical volume). To obtain a surface emission of alpha particles in $cm^{-2}h^{-1}$ (a hemispherical volume), the source can be placed in a detector capable of measuring the alpha particle flux. Since the high rate of alpha events from typical alpha sources can overwhelm the response of many standard detectors, care must be taken to ensure that the source activity is not underestimated.

A basic alpha particle source acceleration factor is simply the ratio of the number of alpha particles per unit time emitted by the source and the those emitted by the packaging materials in contact with the die surface in the final component (the standard unit is cm^2-hr) as shown in Equation 5.1.

$$\text{Acceleration Factor} = \frac{\text{Alpha Particle Source Flux}}{\text{Packaged Component Alpha Flux}} \sim 10^5 \text{ to } 10^{14} \quad (5.1)$$

Note the large range of acceleration factors available. Ultimately the acceleration factor used should be determined by the desired test time and total dose and sensitivity considerations.

This simple acceleration factor cannot directly be used to extrapolate the alpha particle SER because of geometry and absorption effects that must be accounted for.

5.6.3 Geometry factor and shielding

If the accelerated alpha SER test is performed in a vacuum with a source that is very much larger than the component being tested, with a known and calibrated source flux and with a small DUT-to-alpha source spacing (< 1 mm), the need for an accurate geometry calculation is minimized, since the acceleration factor will be close to the ratio shown in Equation 5.1.

Downloaded by xu yajun (xuyj@beice-sh.com) on Jun 29, 2018, 12:46 am PDT
联系方式：xuyj@beice-sh.com 13917165676

5.6.3 Geometry factor and shielding (cont'd)

In most test situations however, a more elaborate model is needed to accurately determine the flux incident on the component. In general, **not accounting for, or miscalculating geometry and shielding factors leads to significant errors in the extrapolated alpha SER of the actual component**. Using a simple analytic model for a circular DUT and alpha source centered about a central axis [7], the effect of source size and source spacing on the alpha flux incident on the DUT area were calculated (Figure 5.3). The dotted line represents the point source approximation. When both the source and device are the same size (solid squares) with a spacing of 1mm, the incident flux is reduced by more than 30%! For a larger source area (solid triangles) at the 1mm spacing the reduction in flux is nearly 10%. Clearly, minimizing the source-device spacing and using a source that is larger than the device being tested ensures that errors are minimized.

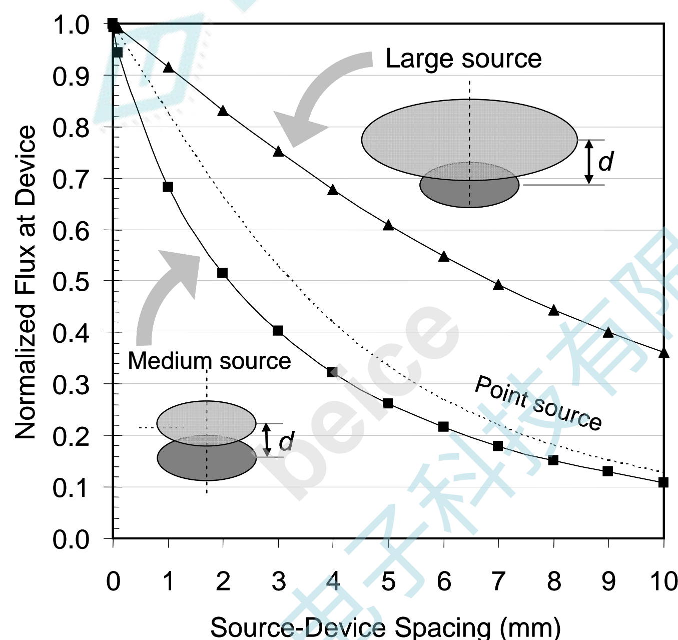

Figure 5.3 — Normalized alpha flux, averaged over the entire device area, incident on a device as a function of the source-device spacing and the source size.

The calculation shown here is given only as an example. For rectangular component areas these curves fall-off even more rapidly with increased spacing. Actual device and source geometries can be calculated more accurately with computer modeling accounting for typical test situations such as rectangular die and non-axial alignments. The final alpha flux incident on the active device area must be recorded in the final report.

NOTE If a thin-film source with mono-energetic spectra is used, see annex D, the air gap will introduce some energy dispersion effects along with a reduction of the flux. This effect might actually maximize the measured SER by fine-tuning the alpha particle energy to stopping range in the device. While this technique can be used to characterize the sensitive volume of the device, the intent of this specification is to allow extrapolation of accelerated alpha SER to real use conditions. In most cases, the package is either in intimate contact, for plastic mold compound or underfill, or very close proximity, for ceramic packages.

Downloaded by xu yajun (xuyj@beice-sh.com) on Jun 29, 2018, 12:46 am PDT
联系方式：xuyj@beice-sh.com 13917165676

5.6.3 Geometry factor and shielding (cont'd)

A further complication results if a test chip is being used to extrapolate the SER of a different component. The extrapolation will only be accurate for a component that has the same number, type, and thicknesses of metal, dielectric, passivation, and polyimide layers. Often test chips have fewer metal layers, while production components have significantly more layers, providing a higher level of alpha particle shielding. Not accounting for, or miscalculating the loss of alpha flux from shielding during testing and in the actual production component can lead to significant errors in the final extrapolated SER.

To properly account for shielding it is strongly recommended that simulations to determine the differences in shielding due to differences in the number of different layers, or controlled ASER experiments with components utilizing different numbers of metal layers be performed.

5.6.4 Extrapolating the failure rate to use conditions

To determine the actual field product failure rate from soft errors requires extrapolating the accelerated test results to use conditions. The product SER under normal use conditions can be obtained by multiplying the observed SER (rate of soft errors) during the accelerated testing by the ratio of the alpha particle flux reaching the DUT active device area under normal use conditions and the alpha flux reaching the DUT active device areas during the accelerated test according to Equation 5.2.

$$Unaccelerated\ Alpha\ Particle\ SER = \frac{(\dot{\Phi}_{pkg})\cdot(F_{geopkg})\cdot(F_{shieldpkg})}{(\dot{\Phi}_{dut})\cdot(F_{geodut})\cdot(F_{shielddut})}\cdot ASER \qquad (5.2)$$

Where ASER is the soft error rate obtained from the DUT during accelerated testing (number of errors for a given number of alpha particle events), and in the numerator of the ratio, $\dot{\Phi}_{pkg}$ is the alpha particle flux reaching the actual production component ($cm^{-2}h^{-1}$), F_{geopkg} is the geometry factor associated with the production component (usually this is 1 unless there is some distance between the chip surface and the final packaging materials see Figure 5.3), and $F_{shieldpkg}$ is the amount of shielding, respectively, in the final production package (this accounts for energy lost by alpha particles traversing metal layers and polyimide layers). In the denominator, $\dot{\Phi}_{dut}$ is the alpha particle flux reaching the DUT during the experiment (normalized to $cm^{-2}h^{-1}$), F_{geodut} is the geometry factor during the experiment (defined by the source-to-die spacing and source and die size, offset, etc.), and $F_{shielddut}$ is the amount of absorption loss (due to polyimide and metal layers), respectively, in the DUT under the accelerated experimental conditions. As mentioned earlier, since the accelerated source uses an alpha particle source with a flux that is significantly higher than the nominal package environment, this ratio will always be much less than 1 and consequently the unaccelerated SER will be significantly lower than the SER observed during accelerated testing. This equation and method are not part of the actual requirement, however, all alpha particle SER data must include a description of the assumptions made for geometry factor and shielding along with all experimental parameters (e.g., source size, DUT active area, source-to-DUT spacing, etc.) that would enable an outside observer to verify that the assumptions used were valid.

Downloaded by xu yajun (xuyj@beice-sh.com) on Jun 29, 2018, 12:46 am PDT
联系方式：xuyj@beice-sh.com 13917165676

5.6.4 Extrapolating the failure rate to use conditions (cont'd)

If the same metal-dielectric stack is used both for the test component and the final product, then $F_{shieldpkg} = F_{shielddut}$ thus simplifying the extrapolation. If the alpha source used for the accelerated testing is placed in direct contact with the active layers and is sufficiently large enough to mitigate edge effects, assuming that packaging materials were in direct contact with the final product die, then $F_{geopkg} = F_{geodut}$. In reality, due to practical and safety concerns, the alpha source will generally not be placed in direct contact with the die so the geometry factor will probably need to be calculated.

Finally, it is not uncommon to use dedicated test structures instead of the final product during accelerated testing. This is particularly true in cases where a technology's alpha-particle SER sensitivity is being determined prior to actual qualified production. It is recommended that alpha testing of at least a few actual production components be done following test chip data to ensure that the test chip used is representative of the SER sensitivity in actual products.

5.7 Interferences

5.7.1 Rate of errors in accelerated tests

It is possible for the high flux associated with accelerated testing to produce abnormal fail rates. It is recommended that parts be evaluated at several different fluxes. If the normalized fail rate (i.e., fails per incident particle) is the same under the different fluxes, there is no issue. If the normalized fail rate changes with the lower flux (ie there appears to be a non-linear relationship between the number of fails and the number of incident particles), then the flux should be lowered until the normalized fail rate becomes independent of flux. If the normalized fail rate increases at a lower flux, the ATE should be evaluated to assure it can record fails fast enough under the higher flux conditions – in other words the ATE speed must be adequate to handle the flux arriving at the DUT, or the flux must be reduced accordingly.

If no SEE events are measured after a device receives a high (with respect to the final use environment) fluence of particles, the test can be regarded as having ended with no errors. The detection limit of the test must be recorded (e.g. < 0.01 FIT/Mbit) and confidence intervals can be used for the detection limit according to annex C.

5.7.2 Generalized noise issues

To reduce the possible effects of an electrically noisy environment, ground and shielding techniques must be optimized. A background test should be run for the maximum planned radiation exposures. In the absence of the radiation source, the DUT must register no errors after this maximum test time. This confirmation must be done with the DUT and ATE in position for testing. Running tests with the DUT in the test location will assure that the DUT and ATE are not suffering from other noise or interference problems.

5.7.3 Total dose

Some parts may suffer total dose damage. This damage may show up as hard failures or as parametric degradation. Parametric degradation may affect the soft error rate and is also an indication that the device is approaching the level where significant damage is occurring. Dose damage may also manifest as timing sensitivity where the DUT may fail at its rated speed but operate adequately at lower speeds.

Downloaded by xu yajun (xuyj@beice-sh.com) on Jun 29, 2018, 12:46 am PDT
联系方式：xuyj@beice-sh.com 13917165676

5.7.3 Total dose (cont'd)

If total dose is a problem, it may be necessary to reduce the targeted number of failures or distribute testing over more DUTs. Total dose effects are evaluated by subjecting a DUT to the same test conditions for the first and last tests of a series. If the results are the same, within experimental error, then total dose is not affecting the results.

5.7.4 Package shadowing

Packaging materials between the top surface of the die and the alpha particle source may attenuate the radiation leading to errors in the calculated error rate. This includes die coats, encapsulants, package lids, and surface contamination such as fingerprints.

Another concern is the use of polymer (polyimide, etc.) layers as mechanical stress relief and for shielding alpha particles. If these layers are used in the final product, the test chip used for alpha particle characterization should have these layer as well. If the test chip does not, then layer absorption simulation methods must be used to determine the effect of these layers in the final product, since depending on the thickness and density of the layers, they may make the final SER better or worse than what is extrapolated from the test chip without the layers.

If the product die is in a flip-chip package, access to the die surface is an issue. Furthermore, even in die form, overlying solder bumps or other materials that mask portions of the active areas from radiation access prevent testing of devices in this configuration. Backside etching to expose the active silicon region may be considered. In this case, the device must be etched to within a few microns of the active silicon region to expose it to an external alpha source. Note that self-heating properties may change with thinner silicon. If this method is used, some testing to demonstrate its equivalence to conventional front side irradiation is required to justify results.

5.7.5 Single event latchup and single event functional interrupt

During accelerated alpha SER testing it may be possible to trigger latchup or other functional error conditions. These are referred to as SEL for Single Event Latchup and, more generically, as Single Event Functional Interrupts (SEFI) for other conditions.

Latchup is the triggering of a parasitic bipolar device in a CMOS IC. The bipolar device acts as a thyristor, shorting a portion of the circuit and remaining on until power is removed. The high current associated with latchup may permanently damage or completely destroy the DUT. In many cases only a portion of the circuit is affected and the increase in current may be difficult to measure. The latchup condition can be removed by cycling power. SEL is dependent on the device designs as well as operating voltage and temperature. As a bare minimum, the device should be tested at nominal operating conditions as defined by the product data sheet. Worst-case SEL occurs at high temperature and high voltage.

A SEFI event often mimics latchup. A complex DUT may enter an internal test mode or lose configuration data established during startup sequencing. The change in state may cause total loss of operation, portions to cease operating, or a significant increase in supply current by entering a new operating mode or reprogramming inputs and outputs. It is possible to damage the DUT from this high current operation. Power cycling will fix the SEFI, assuming that the device is not damaged, but recovery may also be possible by following a sequence of special, device specific operations such as toggling a reset pin.

Downloaded by xu yajun (xuyj@beice-sh.com) on Jun 29, 2018, 12:46 am PDT
联系方式：xuyj@beice-sh.com 13917165676

5.8 Final report

The following items must be included in the final report for alpha particle accelerated SER tests:

DUT description: See description from 4.5

Test Description: See description from 4.5

Fail Information: See description from 4.5

Alpha ASER specific items

Source Description:

1) Source serial number or other means of identification
2) Source isotope(s) (e.g., ^{241}Am, ^{232}Th, etc.)
3) Source activity (in Curies – implies integration over spherical emission volume)
4) The last calibration date
5) Physical configuration of the source (e.g., diffusion bonded with gold over-layer, etc.)
6) Dimension and shape of source active area
7) If available, the source energy spectrum (for thin foil sources with discrete energy peaks a simple list of peak energies will suffice while for sources with distributed spectra a plot is recommended)

Source Setup:

8) Alignment of source with respect to DUT active area tested
9) A description of any shadowing which might affect the final result by obstructing some of the source flux
10) Source-to-die spacing
11) Estimate of the alpha flux reaching the active device surface

Alternatively, if an ion beam is used:

12) The ion energy
13) The ion beam spot size and particle flux
14) The method used to determine the beam flux
15) The date of the last calibration on the detector used to monitor beam flux
16) The beam angle of incidence
17) The distance from a reference point must be noted to account for solid angle effects if appropriate.

SER Calculation:

18) Calculation of unaccelerated alpha SER FIT in product for each type of event (e.g., cell upset, logic upset, latchup, etc.) and for each condition measured (e.g., voltage, ECC state, pattern, frequency, etc.) Record all assumptions, e.g., package material flux. NOTE: The omission of a specific failure rate requirement is intentional, and the failure measurement technique, data analysis and reporting must follow the well-established procedure defined in this document.

Downloaded by xu yajun (xuyj@beice-sh.com) on Jun 29, 2018, 12:46 am PDT
联系方式：xuyj@beice-sh.com 13917165676

6 Accelerated terrestrial cosmic ray test procedures

6.1 Background

6.1.1 Introduction

When cosmic rays enter Earth's atmosphere, they collide with atomic nuclei in air and create cascades of particles of every kind, some of which reach the ground. Among these terrestrial cosmic rays are particles which interact strongly with nuclei: primarily neutrons, plus some protons and a few pions. These particles interact with Si and other nuclei via strong nuclear interactions. These processes produce a variety of secondary particles - protons, neutrons, alpha particles and heavy recoil nuclei. Some of these secondary particles are strongly ionizing, so those that impinge on the active device create bursts of free electron-hole pairs in the silicon. This charge disruption can be collected at pn junctions (much like charge created by light), producing a current spike (noise pulse) in the circuit. These current spikes can be large enough to alter the data state on some circuits. This section deals with the method of determining component sensitivity to high-energy neutron events from accelerated experiments.

6.1.2 Scope

This section deals strictly with SER induced by high-energy neutron events. The high energy neutron flux is dependent on altitude, latitude, longitude, and solar activity (see annex A).

High-energy neutron SER data cannot be used to predict alpha particle or low-energy neutron (i.e., thermal neutron) cosmic-ray induced failure rates. Conversely, neither can alpha particle nor thermal neutron SER data be used to predict high-energy neutron-induced failure rates. An overall assessment of a device's soft error sensitivity is complete ONLY when the alpha, high-energy neutron AND thermal neutron induced failure rates have been accounted for.

6.1.3 Guideline

The test method described below defines the requirements and procedures for accelerated SER testing with high energy proton and/or neutron radiation. Real-time SER testing is dealt with in 4, while accelerated testing for SER induced by alpha particles is dealt with in 5 and SER induced by thermal neutrons is dealt with in 7.

6.1.4 Limits of test method

The accelerated test method in this chapter applies ONLY to terrestrial-cosmic-ray-induced events, which are dominated by high energy (E> 10 MeV) atmospheric neutrons. It does NOT apply to alpha-particle events or events induced by the reaction of thermal neutrons with ^{10}B. This test method can be applied to the testing of memory, sequential and combinational logic, or components combining these circuit types.

6.1.5 Goal of test method

The end product of this accelerated testing is a well-defined estimate of the high-energy neutron induced error rate for components using a uniform methodology. The soft failure rate can be characterized as a function of voltage, timing, and possibly other operating variables.

Downloaded by xu yajun (xuyj@beice-sh.com) on Jun 29, 2018, 12:46 am PDT
联系方式：xuyj@beice-sh.com 13917165676

6.2 Test facilities

To simulate how the atmospheric neutrons induce single event upsets in microelectronic components at a highly accelerated rate, high energy particle beams may be used. Three different types of facilities are discussed in this chapter which provide such high energy particle beams: 1) spallation neutron source, 2) quasi-monoenergetic neutron source and 3) monoenergetic proton source. Neutron and proton facilities available for SEU testing are discussed in annex E.

Spallation neutron sources provide neutrons over a wide range of energies, with the shape of the spectrum being similar to that of the terrestrial neutron environment. Annex A contains the details of the terrestrial neutron spectrum and 6.6 compare the spectra from the spallation neutron sources to that of the terrestrial neutron spectrum.

There is limited access to spallation neutron sources. Therefore monoenergetic neutron and proton sources have been shown to be effective for measuring the SEU response of products and circuits at several energies, which can be used to obtain the SEU rate from the full spectrum of the terrestrial neutron flux. The details for utilizing the monoenergetic SEU data from protons and neutrons is discussed in 6.6

In addition, there is a related source, a quasi-monoenergetic neutron source that may be utilized to measure monoenergetic SEU responses at high energies. This source is discussed more fully in 6.6. At present there is too much uncertainty regarding the use of this type of source for SEU and SER measurements to recommend it, however, in the future this type of source may become a viable alternative.

6.3 Basic test methodology

The basic test methodology for memory arrays is storing a known data pattern in the array while the part is exposed to the accelerated beam and comparing the stored pattern that is present after the device has been irradiated. At some time during and/or after the exposure, the data is evaluated to identify the number of changes in the pattern as errors. Other circuits may have different ATE requirements. Considerably more detail on test methodology is found in 3.

The system consists of the input stimulus generator and response recorder that would be designed to accommodate the specified device. Testing requires some sequence of writing data to the DUT, reading the data back, comparing the output data to the written data, and tabulating the number of errors. For simple memory arrays, a bit is failing when the data read from that bit is different from the last data written to that bit. It is also useful to identify failing addresses and time of failure for dynamic tests.

6.4 Basic test procedure

A test plan shall be developed to support each test. For many additional details pertaining to the test plan and test procedures see 3. The test plan will serve as a guide for the procedures and real-time decisions to be made during the actual irradiation period. In most cases the test plan cannot be followed exclusively, because source/test variables and the results of the earlier runs must be factored into later decisions. Common practice is to perform tests with the beam at normal incidence. In most cases there is no angle dependence, allowing tests to be done at other angles. A cursory check of angle dependence is recommended.

Downloaded by xu yajun (xuyj@beice-sh.com) on Jun 29, 2018, 12:46 am PDT
联系方式：xuyj@beice-sh.com 13917165676

6.4 Basic test procedure (cont'd)

A "reference chip" or "golden chip" with a relatively high soft error rate that is capable of withstanding a relatively high total dose level is recommended as part of the testing approach. Normal practice will be to perform testing on the "reference chip" before each test series in order to provide validation of the test equipment and as a secondary means of calibrating beam dosimetry of the facility. After the "reference chip" is selected, it should be tested multiple times to establish the consistency and variability of the measured SER.

For each part type, the initial test shall be repeated at the end of a sequence of tests. If the second set of tests do not agree with the initial set, then additional testing must be done to determine whether radiation damage (total dose; see 5.7.3) or other testing issues are responsible for the difference in results. Interpretation of these results must take the normal variation expected for such testing into account.

A minimal test plan would include:

1) Setup and check-out of the ATE;
2) Initial beam and setup check using 'golden' part;
3) Initial test for part;
4) Data collection;
5) Final test for part using the same conditions as step 3) to verify consistency of results (this is also an indirect total dose check);
6) Repeat steps 3) through 5) for additional parts;
7) Final beam and setup check ('golden' part).

6.5 Beam parameters

6.5.1 Beam check

Most facilities provide beam calibration. In most cases users will rely on calibration and beam uniformity at the facility. In cases where facility calibration is not well established, then it will be necessary to measure the flux, energy and spatial uniformity (area) of the beam. Details vary with facility and are beyond the scope of this document.

6.5.2 Beam fluence

The total number of particles must be sufficient to establish with a high statistical confidence that the entire sensitive volume on the DUT has been irradiated. A fluence that will induce a minimum of 100 upsets during the test interval is considered a minimum fluence. See annex B for discussions on statistically based confidence levels.

6.5.3 Beam flux

Typically, start with the highest flux. If the fail rate is too high (> about one per second), the flux should be decreased. It is preferable to also run at a lower flux (e.g., 1/10 normal flux) to check for a nonlinear SER flux dependence. If there is a nonlinear flux dependence, the flux should be dropped until the flux dependence becomes linear. The beam flux is many orders of magnitude higher than the flux at use conditions, i.e., at ground level; thus the lower flux measurements would be the most useful.

Downloaded by xu yajun (xuyj@beice-sh.com) on Jun 29, 2018, 12:46 am PDT
联系方式：xuyj@beice-sh.com 13917165676

6.5.3 Beam flux (cont'd)

If high-energy protons and monoenergetic neutrons are used, then testing should be carried out at a minimum of four different energies, 14 MeV (neutrons) and approximately 50, 100 and 200 MeV (protons, the exact energy depending on the test facility). For energies < 50 MeV, only monoenergetic neutrons should be used, as discussed in 6.6.

6.6 Fundamental quantities: SEU cross-section and SEU rate

There are two complementary quantities to characterize the SEU sensitivity of a chip/circuit: (1) the SEU cross section, and (2) the SEU rate, also known as soft error rate (SER), or soft fail rate.

The SEU cross section is an *intrinsic parameter* of a chip/circuit that specifies its *response to a particle species* (e.g. neutron, proton, pion, heavy ion, etc.). It is measured using a beam of particles produced at an accelerator. The SEU cross-section depends on the particle type and particle energy. In general it is also a function of the operating conditions of the irradiated chip (e.g., applied voltage, temperature, etc.). The units commonly used for SEU cross section are cm^2/bit, cm^2/Mb or cm^2/device.

The SEU rate is a measure of a chip's *response to a particular type of radiation environment*. Its value varies from one location to another, depending on the radiation environment that is present. For example, due to the variations of the terrestrial neutron flux (altitude and geomagnetic effects), the neutron-induced SEU rate of a chip is larger at high altitudes than at sea level. Also the SEU rate is lower at locations close to the geomagnetic equator, compared with locations close to the geomagnetic pole. The computation of terrestrial neutron flux is essential for the evaluation of fail rates, and it is discussed in annex A.

For terrestrial applications, based on the knowledge of SEU cross section (as a function of particle energy) and the particle energy spectrum at a given location, the SEU rate at any given location can be computed. It is important to note that from the SEU rate measurements alone one cannot extract any information on the energy dependence of SEU cross section. In general the equation that relates SEU rate with SEU cross section cannot be inverted to solve for the SEU cross section from a given SEU rate, as is obvious from the structure of Equation 6.10 formulated in 6.6.4.1.

Proton-induced and neutron-induced SEU cross sections are often used interchangeably as the basic parameters to characterize SEU sensitivity. Protons and neutrons interact with semiconductor materials via nuclear reactions. Over a wide energy range, e.g., MeV to GeV, these reactions produce charged, ionizing fragments like alpha particles, recoil nuclei and other secondary particles mainly from reactions that have energy thresholds > ~5 MeV; these secondary particles induce upsets in circuits. In general the nuclear interactions of protons and neutrons with most semiconductor materials (especially light elements like Si and O) are very similar for incident particle energies above 50 MeV [8]. For the purposes of this standard, the user should be aware that for new technologies the proton- and neutron- induced SEU cross sections at energies *below* 30 MeV can show some noticeable differences because of device scaling and the consequent decrease in circuit critical charge and also because of significant resonance behavior of neutron-nucleus reactions.

6.6.1 SEU cross-section dependence on type of facility

The basic features of the major SEU test facilities are discussed in [9] and the list of facilities available is found in annex E. Here we summarize the basic measurements made in these facilities during SEU testing.

Downloaded by xu yajun (xuyj@beice-sh.com) on Jun 29, 2018, 12:46 am PDT
联系方式：xuyj@beice-sh.com 13917165676

6.6.2 Measured quantities using particle beams

6.6.2.1 Monoenergetic proton beam: proton-induced SEU cross-sections at E_p

Proton-induced SEU cross sections are measured using a monoenergetic proton beam. They can be defined in two ways:

$$\sigma_{SEU\text{-}dev}(E_p) = N_{SEU} / (\Phi_{proton}) \quad (6.1)$$

and

$$\sigma_{SEU\text{-}bit}(E_p) = N_{SEU} / (\Phi_{proton} \times N_{bit}) \quad (6.2)$$

In Equations 6.1 and 6.2, E_p is the proton energy; N_{SEU} is the number of SEU measured in the irradiated sample during each test; Φ_{proton} is the fluence of the protons to which the device was exposed in units of protons/cm^2; N_{bit} is the number of bits in the sample under test; $\sigma_{SEU\text{-}dev}(E_p)$ is in units of cm^2/device and $\sigma_{SEU\text{-}bit}(E_p)$ is in units of cm^2/bit. In applying Equations 6.1 and 6.2, the surface of the sample should be normal to the incident proton beam. If the beam is not normal, the angle of incidence should be specified.

6.6.2.2 Monoenergetic neutron beam: neutron-induced SEU cross-sections at E_n

Neutron-induced SEU cross sections can be measured using a monoenergetic neutron beam. Monoenergetic neutron beams are to be distinguished from quasi-monoenergetic neutron beams discussed in 6.6.2.3. There are three main types of truly monoenergetic neutron beams > 1 MeV in which almost all of the neutrons are within ±1 MeV of the peak energy. All are produced by accelerating a charged particle into a tritium (T) or deuterium (D) target. D-T reactions produce neutrons of 14 MeV, and this is the most common type of neutron generator. D-D reactions produce neutrons of 3-5 MeV, depending on the energy of the deuteron, and p-T reactions produce neutrons with energies depending on the energy of the proton. For more detail on neutron production, the user can refer to [9]. Similar to the proton case, neutron SEU cross sections can be defined in two ways:

$$\sigma_{SEU\text{-}dev}(E_n) = N_{SEU} / (\Phi_{neutron}) \quad (6.3)$$

and

$$\sigma_{SEU\text{-}bit}(E_n) = N_{SEU} / (\Phi_{neutron} \times N_{bit}) \quad (6.4)$$

In Equations 6.3 and 6.4, E_n is the neutron energy, $\Phi_{neutron}$ is the fluence of neutrons to which a device is exposed, in units of neutrons/cm^2; $\sigma_{SEU\text{-}dev}(E_n)$ is in units of cm^2/device and $\sigma_{SEU\text{-}bit}(E_n)$ is in units of cm^2/bit and all other parameters are as in 6.6.2.1. The incident neutron beam should be normal to the surface of the sample.

Downloaded by xu yajun (xuyj@beice-sh.com) on Jun 29, 2018, 12:46 am PDT
联系方式：xuyj@beice-sh.com 13917165676

6.6.2.3 Quasi-monoenergetic neutron beam: neutron-induced SEU cross-sections at E_n

Neutron-induced SEU cross sections can also be measured using a quasi-monoenergetic neutron beam [10]. This beam differs from a truly monoenergetic neutron beam in that a significant fraction of the neutrons are at energies less than the peak energy. The standard beam of this kind is obtained by accelerating monoenergetic protons into a lithium target, although other production mechanisms are also possible. The neutrons from this beam comprise a two-part distribution, the neutrons at the peak energy, ~1-2 MeV below the proton energy, and the neutrons within the so-called low energy tail, from E_{peak} ~2 MeV down to ~0 MeV. Thus, the tail may contain neutrons spread out over more than 100 MeV, and the challenge in using this type of source is to separate out the SEU contribution of the neutrons in the low energy tail from those at the energy peak. As in 6.6.2.2, neutron SEU cross sections can be defined in two ways:

$$\sigma_{SEU\text{-}dev}(E_n) = N^*_{SEU} / (\Phi_{neutron}) \tag{6.5}$$

and

$$\sigma_{SEU\text{-}bit}(E_n) = N^*_{SEU} / (\Phi_{neutron} \times N_{bit}) \tag{6.6}$$

In Equations 6.5 and 6.6, E_n is the energy at the neutron peak, $\Phi_{neutron}$ is the fluence of neutrons in the peak, in units of neutrons/cm^2; N^*_{SEU} is the number of error events measured in the irradiated sample adjusted to account for upsets only from the neutrons at peak energy and all other parameters are as in 6.6.2.2. The incident neutron beam should be normal to the sample.

Methods for extracting the SEU cross section at the peak energies are available in the literature. However, at the present time the unfolding techniques are not well enough understood, and there is notable uncertainty in the published SEU results using this kind of neutron source. When robust unfolding methods are firmly established, the quasi-monoenergetic neutron beam can become an alternative option in the near future.

6.6.2.4 Spallation neutron beam: averaged neutron SEU cross-section over neutron spectrum

A spallation neutron source, such as the ICE House (formerly known as the Weapons Neutron Research, WNR) facility at the Los Alamos Neutron Science Center (LANSCE) or the TRIUMF Neutron Facility (see annex E for other facilities) allows one to measure the SEU rate and derive an *averaged* SEU cross section. Because the neutrons produced from a spallation source cover a wide energy spectrum, the user cannot extract a SEU cross section at a specific energy from such measurements, but rather obtains the contribution of SEU events from neutrons of all energies within the spectrum. The major reason that a spallation neutron source is widely used is that the shape of the energy spectrum from this beam is similar to the spectrum of the terrestrial neutrons on the ground and in the atmosphere [11]. In Figure 6.1, we compare the neutron spectra from the beams at Los Alamos and TRIUMF with the scaled neutron spectrum at ground level from annex A.

The ICE House spectrum in Figure 6.1 is at the location of the LANL fission detector, which was at a point 19.97 meters down the flight path from the tungsten target. DUTs are located further down the flight path, so that the neutron flux will be reduced by the following ratio $r^2/(r+d)^2$, where r is the distance to the detector (19.97 m in this case) and d is the distance between the detector and the DUT. At TRIUMF the spectrum in Figure 6.1 also applies at the location of the DUT so no correction needs to be made.

Downloaded by xu yajun (xuyj@beice-sh.com) on Jun 29, 2018, 12:46 am PDT
联系方式：xuyj@beice-sh.com 13917165676

6.6.2.4 Spallation neutron beam: averaged neutron SEU cross-section over neutron spectrum (cont'd)

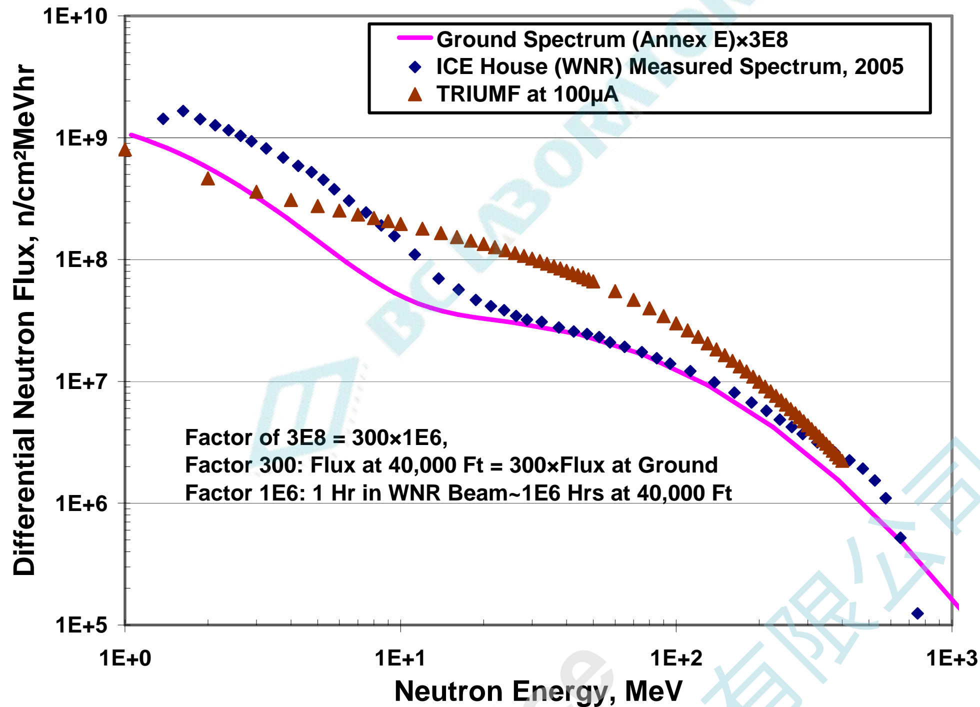

Figure 6.1 — Comparison of Los Alamos and TRIUMF neutron beam spectra with terrestrial neutron spectrum from annex A.

When testing with a spallation neutron source, the SEUs recorded will be due primarily to the high energy (e.g. > 10 MeV) neutrons. The SEU contribution of the neutrons in the 1<*E*<10 MeV range is small, < 10%, but these neutrons comprise ~40% of all neutrons > 1 MeV in the terrestrial spectrum (as can be seen in Figure 6.1). Further, if a spallation neutron source is used that contains thermal neutrons, which is not true at Los Alamos, care must be taken to subtract out the SEUs that are caused by the thermal neutrons (see 7).

With measurements using spallation neutrons, one can derive an *averaged* neutron SEU cross which can be defined in two ways:

$$\overline{\sigma_{SEU-dev}} = \mathrm{N}_{\mathrm{SEU}} / \Phi_{spec} \tag{6.7}$$

and

$$\overline{\sigma_{SEU-bit}} = \mathrm{N}_{\mathrm{SEU}} / \left(\Phi_{spec} \times \mathrm{N}_{\mathrm{bit}}\right) \tag{6.8}$$

In Equations 6.7 and 6.8, the averaged cross sections depend on the entire spallation neutron spectrum; Φ_{spec} is the fluence of neutrons over the spectrum from *E*>10 MeV, in units of cm^{-2}; $\overline{\sigma_{SEU-dev}}$ is the spallation SEU cross section in units of cm^2/device and $\overline{\sigma_{SEU-bit}}$ is in units of cm^2/bit and all other parameters are as in 6.6.2.2. The incident neutron beam should be normal to the sample. It is important to emphasize that the *averaged* neutron SEU cross sections defined in this section *not be confused* with the neutron SEU cross sections discussed in 6.6.2.2 and 6.6.2.3.

Downloaded by xu yajun (xuyj@beice-sh.com) on Jun 29, 2018, 12:46 am PDT
联系方式：xuyj@beice-sh.com 13917165676

6.6.3 Energy variation of SEU cross section

Figure 6.2 shows the variation of the SEU cross section per bit with neutron or proton energy. It contains the three recommended types of measured SEU cross sections discussed in 6.6.2, using monoenergetic protons, monoenergetic neutrons and spallation neutrons, and these were measured in two different SRAMs. The data for these devices should be regarded as typical for many other SRAMs, although not too many have been tested with both spallation neutrons and monoenergetic particles, and only a few recent devices have been tested with protons at energies as high as 500 MeV.

Above a threshold energy the SEU cross section curve rises rapidly with increasing energy and tends to reach a plateau. For recent technologies this energy threshold is in the range of ~ 1–10 MeV. As seen in Figure 6.2 for SRAMs A and D using monoenergetic proton measurements, there appears to be a slight dip in the curve around 150 MeV, which has also been seen in other devices.

It is often convenient to fit the SEU cross-section data points by a smooth curve. The preferred method is the four-parameter Weibull distribution [12], which has the form of:

$$\sigma_{Weib\text{-}SEU}(E) = \sigma_{P/N\text{-}L}\,(1\text{-}exp\{\text{-}[(E - E_0)/W]^S\}) \qquad (6.9)$$

where $\sigma_{P/N\text{-}L}$ is the limiting or asymptotic proton/neutron cross-section (high energy); E_0 is the cutoff energy below which SEU cross section is zero; W is the “width” parameter; S is the shape factor.

Another alternative is to use a piece-wise linear fit between the data points, an approach which has occasionally been used. However, the Weibull fit is the preferred method for obtaining the smoothed function fit, since it provides a “best” fit in a least squares sense to all of the SEU cross section data, and allows for averaging “dips” at one or more energies. An effective way to implement the Weibull fit is to use the SOLVER routine within the EXCEL spreadsheet application since this allows the user to obtain a set of the four parameters that minimizes a function such as the square of the difference between the smooth curve and the actual data.

Figure 6.2 illustrates how the accuracy of the SEU cross-section fit depends on the quality of the data taken. A minimum of four data points, at four different energies should be used to obtain the Weibull fit. Suggested energies are: a) 14 MeV (monoenergetic neutron), b) 50-60 MeV (proton), c) 90-100 MeV (proton) and d) > 200 MeV (proton). However, more data points are always helpful, each based on a large enough number of upsets to be statistically valid, in order to improve the internal consistency of the data, as well as of the fit to the data. Using a low energy (E < 10 MeV) monoenergetic neutron beam would allow a value of E_0 < 10 to be accurately obtained.

Figure 6.2 contains the Weibull fits to the SEU cross section data for SRAMs A and D, and both sets of data include a 14 MeV monoenergetic neutron point and several monoenergetic proton energy points. The good consistency with the proton SEU cross section is also seen with other data in the literature.

Downloaded by xu yajun (xuyj@beice-sh.com) on Jun 29, 2018, 12:46 am PDT
联系方式：xuyj@beice-sh.com 13917165676

6.6.3 Energy variation of SEU cross section

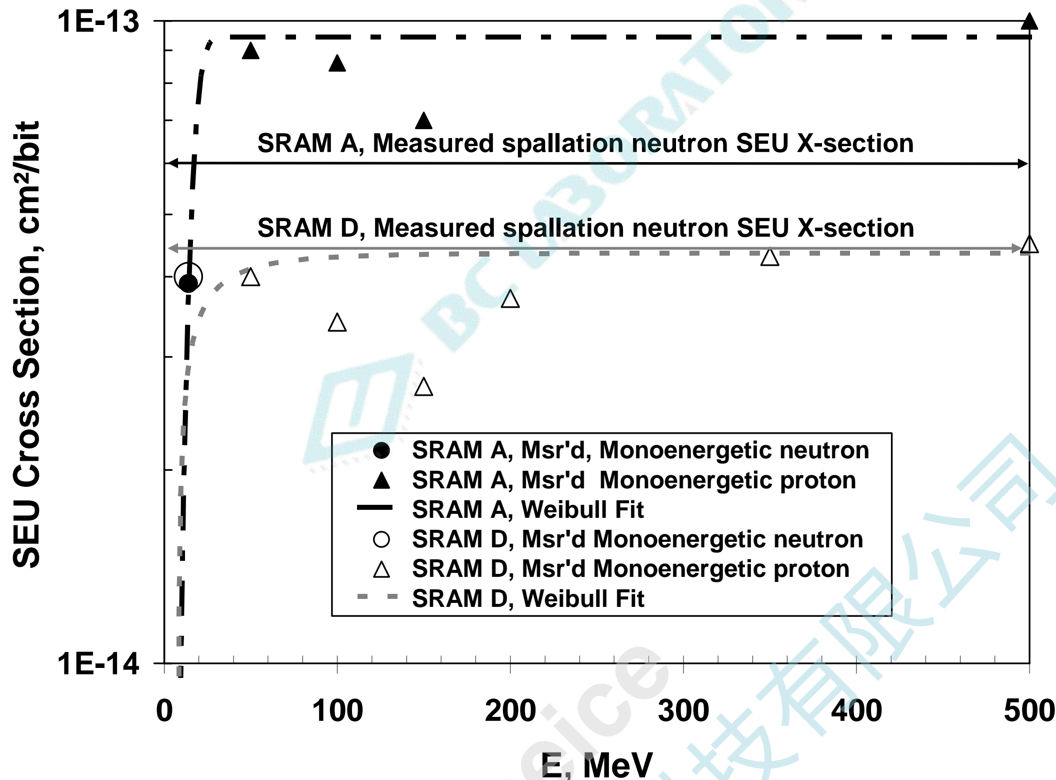

Figure 6.2 — Comparison of measured SEU cross sections from monoenergetic and spallation neutron sources and Weibull fits in two different SRAMs

6.6.4 Analysis Methods Available

6.6.4.1 Computation of Fail Rate from Proton- or Neutron-Induced SEU Cross Section

The SEU rate can be computed from the SEU cross-section and particle spectrum as follows:

$$SEU\ rate = \int_{E_{\min}}^{E_{\max}} dE \left(d\dot{\Phi}(E) / dE \right) \sigma_{SEU}(E) \qquad (6.10)$$

In Equation 6.10, $d\dot{\Phi}(E)/dE$ is the differential flux of the particle, given in units of particle number $cm^{-2}MeV^{-1}s^{-1}$; $\sigma_{SEU}(E)$ is the SEU cross section at proton or neutron energy E, given in units of $cm^2 \times device^{-1}$ or $cm^2 \times bit^{-1}$; E_{min} and E_{max} are the lower and upper limits of the energy spectrum over which $\sigma_{SEU}(E)$ is defined. Note that $\sigma_{SEU}(E)$ in Equation 6.10 is a generic term: if $\sigma_{SEU\text{-}dev}$ (defined in Equations 6.1 and 6.5) is used, the SEU rate will be in units of $fails \times device^{-1}s^{-1}$; if $\sigma_{SEU\text{-}bit}$ (defined in Equations 6.2 and 6.6) is used, the SEU rate will be in units of ($fails \times bit^{-1}s^{-1}$). For most commercial IC devices terrestrial neutrons are the most important source of SEUs. Recent measurements of the terrestrial neutron flux and an effective parameterization of the differential flux $d\dot{\Phi}(E)/dE$ is given in annex A, which should be used to calculate the fail rate. The $\sigma_{SEU}(E)$ term in Equation 6.10 should be the Weibull fit to the SEU cross section data taken at various neutron and/or proton energies.

Downloaded by xu yajun (xuyj@beice-sh.com) on Jun 29, 2018, 12:46 am PDT
联系方式：xuyj@beice-sh.com 13917165676

6.6.4.1 Computation of Fail Rate from Proton- or Neutron-Induced SEU Cross Section (cont'd)

Since the neutron flux is given in annex A as either values in 36 different energy bins (1-1000 MeV) or in analytical form, and the Weibull fit to the SEU cross section is in analytical form, the integration in Equation 6.10 can be calculated very easily in spreadsheet format (using averaged values across the energy bins or Simpson's rule).

Another approach for implementing Equation 6.10 is to use a linear-log algorithm. This can be useful because $d\dot{\Phi}(E)/dE$ changes by several orders of magnitude. The fail rate of Equation 6.10 would now be computed as:

$$SEU\ rate = \sum_{j=1}^{N-1} (F_{j+1} - F_j)\ (E_{j+1} - E_j)\ /\ ln(F_{j+1}/F_j) \qquad (6.11)$$

In Equation 6.11, $F_j = \left(d\dot{\Phi}(E_j)/dE\right)\ \sigma_{SEU}(E_j)$, E_j is the *j-th* energy point; $j=1$ corresponds to the lowest energy point E_{min}, and $j=N$ corresponds to the highest energy point E_{max}.

6.6.4.2 Computation of fail rate from spallation SEU cross section

From the spallation (averaged) SEU cross section discussed in 6.6.2.4, the SEU rate (fails×bit^{-1}s^{-1}) can be calculated as follows:

$$SEU\ rate = 3.\ 6\times 10^{-3} \times \overline{\sigma_{SEU-bit}} \qquad (6.12)$$

Here, the nominal integral neutron flux on the ground above 10 MeV is 3. 6×10^{-3} cm^{-2}s^{-1} (13 cm^{-2}h^{-1}); it is obtained by integrating the differential flux $d\dot{\Phi}(E)/dE$ in E (see A.2). This upset rate can be adjusted for specific locations and conditions using the scaling factors given in annex A. The flux > 10 MeV is used because the neutron flux in the range of 1-10 MeV, constitutes ~ 35% of the entire neutron spectrum > 1 MeV, but these lower energy neutrons contribute only a few percent of all of the SEU events over the entire spectrum.

6.7 Interferences

6.7.1 Rate of errors in accelerated tests

See description in 5.7.1.

6.7.2 Generalized noise issues

See description in 5.7.2.

6.7.3 Total dose

See description in 5.7.3.

Downloaded by xu yajun (xuyj@beice-sh.com) on Jun 29, 2018, 12:46 am PDT
联系方式：xuyj@beice-sh.com 13917165676

6.7.4 Scattering and secondary ion effects at the DUT

Particle scattering can be a problem in any beam experiment, particularly when dense high Z materials are placed in the beam in close proximity to the DUT. Thermal neutrons are more easily scattered due to their low energy and thus any shielding that is done must enclose the device. It should also be noted that the higher the Z of the shield or scattering material, the larger the likelihood that high-energy protons will be emitted as a reaction product (this is mainly a concern in neutron beams containing high energy neutrons). These higher energy protons can penetrate the DUT and cause additional soft errors. Spurious results might be obtained if a high Z metal shield were to be used to enclose a DUT if a large fraction of the observed SER was related to the resulting secondary protons. If this is thought to be a problem, using Boron as a shielding material instead of Cd or Gd should reduce this effect considerably.

The scattering effects can also be seen if large metallic heat sinks are used in the DUT. Any type of scattering material in the neutron beam during the experiments needs to be described in detail in the final report. If a large metallic heat sink is part of the DUT in the neutron beam, it is advisable to repeat the neutron testing at several different beam incidence angles to ensure that scattering effects and secondary proton fluxes do not significantly alter the test results (this presumes that the actual neutron flux under nominal conditions will be roughly isotropic with only a weak angular dependence).

6.7.5 Proton range in thick packaging

When testing with proton beams the energy and range of the protons needs to be considered if the DUT packaging that covers the die is not delidded, and the thickness of the packaging cover must be known. The energy of a proton may be degraded significantly as it passes through the packaging before reaching the die. Using 3 mm as a typical thickness of epoxy plastic covering the die, per the TRIM/SRIM code, a 30 MeV proton will have a range of 4.8 mm. Thus the energy of a proton exiting the 3 mm of plastic would be reduced to 17.5 MeV, making interpreting the test data uncertain. At higher energies, e.g., 90 MeV, the energy loss is much smaller, the residual energy being 85.5 MeV. The use of other packaging materials and designs (e.g., flip-chip) also need to be accounted for in this assessment.

6.7.6 Single event latchup and single event functional interrupt

See description in 5.7.5.

6.8 Final report

The following items shall be included in the final report for accelerated neutron/proton tests:

DUT description:

1) See description from 4.5

Test Description:

2) See description from 4.5

Fail Information:

3) See description from 4.5

Downloaded by xu yajun (xuyj@beice-sh.com) on Jun 29, 2018, 12:46 am PDT
联系方式：xuyj@beice-sh.com 13917165676

6.8 Final report (CONT'D)

Cosmic ASER specific items

Source Description:

4) Name, location, type and overall description of accelerator facility and facility contact person
5) Particles in beam and their energy
6) If it is not a monoenergetic beam, a description of the source energy spectrum (graph preferred)
7) Estimate of the beam flux at each DUT location and how it was obtained, along with beam spot size
8) Beam angle of incidence with respect to the DUT
9) Beam flux or fluence monitor that is used and calibration factor if applicable
10) Alignment of beam with respect to DUT (e.g., use of stacked test cards, moving test card to allow beam to expose various DUTs on same card during successive runs, etc.)
11) Use of any filters with the beam (e.g., cadmium strip or borated shield for thermal neutrons)
12) Any shadowing which might affect the final result by obstructing some of the beam flux reaching each DUT
13) The distance from a reference point must be noted to account for solid angle effects if appropriate.

SER Calculation:

14) Calculation of unaccelerated cosmic SER FIT in product at NYC for each type of event (e.g., cell upset, logic upset, latchup, etc.) and for each condition measured (e.g., voltage, ECC state, pattern, frequency, etc.) Record all assumptions.

NOTE The omission of a specific failure rate requirement is intentional, and the failure measurement technique, data analysis and reporting must follow the well-established procedure defined in this document.

7 Accelerated thermal neutron test procedures

7.1 Background

7.1.1 Introduction

Boron has two isotopes, ^{10}B (20% in natural abundance) and ^{11}B (80% in natural abundance). Like most other nuclides when ^{11}B captures a neutron it emits a photon which cannot cause a single event upset. In stark contrast, ^{10}B not only has a very high neutron capture cross-section but upon capturing a neutron the ^{10}B nucleus has a high probability of fissioning into two highly ionizing particles each of which can cause a soft error [13, 14]. The dominant nuclear reaction is:

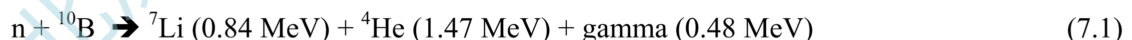

$$n + {}^{10}B \rightarrow {}^{7}Li\ (0.84\ MeV) + {}^{4}He\ (1.47\ MeV) + gamma\ (0.48\ MeV) \quad (7.1)$$

Downloaded by xu yajun (xuyj@beice-sh.com) on Jun 29, 2018, 12:46 am PDT
联系方式：xuyj@beice-sh.com 13917165676

7.1.1 Introduction (cont'd)

^{10}B can be present in large quantities in the device in the form of polysilicon doping, substrate doping or boro-phospho-silicate glass (BPSG). Using high concentrations of boron in its natural isotopic abundance in any of these layers is the primary concern [15] for this reaction because it contains high amounts of ^{10}B (for example BPSG typically contains 4 - 9% boron by weight) and covers a large portion of the chip area. It should be noted that in more recent technologies, very highly doped substrates, polysilicon layers and implants are being used that could place high concentrations of ^{10}B in proximity to the active devices. Even if the device does not use BPSG, this is not sufficient grounds to rule out the need to do thermal neutron SER testing. The range of a 1.47MeV alpha particle is ~5um (see Fig. D.3), so all sources of ^{10}B within this region are potential sources for thermal neutron upset. Unlike many of the high-energy neutron reactions discussed in 6 that have reaction thresholds of > 5 MeV, the ^{10}B neutron capture reaction actually increases as the neutron energy is reduced. This reaction is dominated by neutron energies below 0.4 eV.

The resultant alpha and lithium particles from the ^{10}B neutron reaction are both strongly ionizing, so if either impinges on the active device it creates bursts of free electron-hole pairs in the silicon. This charge disruption can be collected at pn junctions (much like charge created by light), producing a current spike (noise pulse) in the circuit. These current spikes can be large enough to alter the data state of some circuits. The circuit does not suffer a meaningful level of physical damage, so the circuit still works properly, but the data or instructions within the circuitry may have been corrupted.

7.1.2 Scope

This chapter deals with the method to determine the relative sensitivity of a component to soft errors from thermal neutrons from accelerated experiments. SER from reactions by low energy neutrons, i.e., thermal and epithermal neutrons, with ^{10}B depends on altitude, latitude, solar activity, the local shielding environment, and most importantly, to the amount of ^{10}B present in IC overlayers.

In cases where the composition of materials and structures used in the manufacture of the product is not known (e.g., presence of BPSG, polysilicon doping level and type, substrate doping, etc), then a test should be done to assess the impact of thermal neutron on the overall SER of the product. In cases where the details of the manufacturing process are known (e.g., merchant vendors), it is possible to do a pre-assessment on importance of thermal neutron SER due to the presence of ^{10}B. The following are examples of mitigating techniques:

1) BPSG is not used and the concentrations of boron implants and substrate doping are low.

2) BPSG using an enhanced ratio of ^{11}B to ^{10}B will reduce the impact of thermal neutron-induced SER.

^{10}B SER data cannot be used to predict high-energy neutron OR alpha particle induced failure rates. Similarly, neither high-energy neutron nor alpha particle data can be used to predict ^{10}B failure rates. An overall assessment of a device's soft error sensitivity is complete ONLY when the alpha AND both low-energy and high-energy cosmic-ray components have been accounted for.

Downloaded by xu yajun (xuyj@beice-sh.com) on Jun 29, 2018, 12:46 am PDT
联系方式：xuyj@beice-sh.com 13917165676

7.1.3 Safety issues

Test hardware and parts may become radioactive when exposed to thermal and high-energy neutron radiation. It is advisable to visit the test facility during the planning stage to determine the necessary cable length and shielding for the power supplies and control circuits that will be near the test fixture. The expected radiation level of the DUT exposure position should also be determined and sufficient shielding for these components provided. Experiments should be designed to minimize the amount of material, particularly heavy metals, or materials with large neutron nuclear cross-sections, that are exposed to the thermal neutrons. The length of cable necessary to reach the operator area should also be determined. It is the responsibility of the user of this test method in consultation with radiation safety personnel of the facility to establish the appropriate safety and health practices and the applicability of regulatory limitations prior to use.

7.1.4 Guideline

The test method described below defines the requirements and procedures for accelerated SER testing with low-energy or thermal-energy neutron beams (mean neutron energy ~ 0.025 eV). Generalized real-time (unaccelerated), or field testing has been dealt with in 4, while accelerated testing for SER induced by alpha particles is dealt with in 5, and accelerated testing for SER induced by high-energy cosmic radiation is dealt with in 6.

7.1.5 Limits of test method

The accelerated test method in this section applies ONLY to events caused by low energy (E< 20 eV) neutron reactions with ^{10}B. It does NOT apply to high-energy neutron-induced events nor does it encompass errors due to alpha particles. This test method can be applied to the testing of memory, sequential logic, combinational logic, or components combining these types of circuits.

7.1.6 Goal of test method

The end product of this accelerated testing is a determination of whether-or-not a particular component has a ^{10}B SER problem and the relative magnitude of the thermal neutron SER as compared with the high-energy neutron SER. It is beyond the scope of this method to derive an absolute measure of the SER from low energy neutrons.

7.2 The terrestrial thermal neutron environment

See description in A.4.

7.3 Packaging for thermal neutron testing

The DUT package has little effect on thermal neutron testing and on the test results since neutrons are uncharged and interact only by nuclear reaction with matter. Components encapsulated in plastic, lead-over-chip (LOC), and most chip-scale packages are suitable for thermal neutron testing. The only limitations related to packages are those with large metal heatsinks that might scatter the thermal neutron beam (see 7.7.5).

Downloaded by xu yajun (xuyj@beice-sh.com) on Jun 29, 2018, 12:46 am PDT
联系方式：xuyj@beice-sh.com 13917165676

7.4 Thermal neutron sources

7.4.1 Thermal neutron source selection

Testing for chip SER due to thermal neutrons can be done using a wide variety of sources (see annex E). Thermal neutrons are available from both nuclear reactors and particle accelerators. Particle accelerator facilities use nuclear reactions such as energetic protons on Li targets to produce neutrons. These neutrons are then moderated (lowered in energy) by passing the neutrons through low-Z materials like polyethylene; a few such facilities are indicated in annex E. 14 MeV neutron generators may also be used to produce thermal neutrons, again by using a moderating material to slow down the higher energy neutrons. Calibration is a critical issue for thermal neutron testing because the SER cross-section varies significantly with small changes in neutron energy – thus the measurement is very sensitive to the energy distribution of the low energy neutrons. Thermal neutrons are also available at nuclear reactors, where the flux calibration may already exist, but the associated gamma ray field in the reactor volume and its effect on the DUT must be accounted for.

Since low-energy neutrons are easily scattered, the concept of a well-defined beam is not necessarily applicable as there may be significant dispersion such that a neutron field exists within a large volume of the test area. This has ramification for shielding personnel, equipment, and DUTs. Thus the term “beam” is used loosely in this chapter and can in fact refer to a neutron field with little directional dependence.

7.4.2 Source calibration

Most facilities provide beam calibration. In most cases users will rely on calibration and beam uniformity at the facility. In cases where facility calibration is not well established, then it will be necessary to measure the flux, energy, and spatial uniformity (area) of the beam following standard procedures such as ASTM E262-03 (Standard Method for Determining Thermal Neutron Reaction and Fluence Rates by Radioactivation Techniques). This is generally done with activation foils, such as with ^{197}Au or ^{23}Na, but the details vary with facility and are beyond the scope of this document.

7.4.3 Thermal neutron source fluence

The total number of neutrons incident on the DUT must be sufficient to establish with a high statistical confidence that the entire sensitive volume has been irradiated uniformly. See annex B for discussion on statistically based confidence levels. SER experiments using thermal neutrons are similar to those using particle accelerators (discussed in 6), however the beam almost always activates any chips or sockets placed in the beam (activate means to make temporarily radioactive).

7.4.4 Beam flux

Typically, start with the highest flux. If the fail rate is too high (> about one per second), the flux should be dropped. It is preferable to also run at a lower flux (e.g., 1/10 normal flux) to check for a nonlinear SER flux dependence. If there is a nonlinear flux dependence, the flux should be dropped until the flux dependence becomes linear. The beam flux is many orders of magnitude higher than the flux at use conditions; thus lower flux measurements would be the most useful.

Downloaded by xu yajun (xuyj@beice-sh.com) on Jun 29, 2018, 12:46 am PDT
联系方式：xuyj@beice-sh.com 13917165676

7.4.5 Thermal neutron shielding

A variety of materials containing high concentrations of isotopes with high thermal neutron cross-sections can be used as a thermal neutron shield. An estimation of the degree of shielding is important to ensure that the shielded results are as low as possible.

Three materials that have been commonly used for shielding thermal neutrons are boron (20% ^{10}B), cadmium (Cd) metal and gadolinium (Gd) metal. The very dramatic increase in the thermal neutron cross-section for these three materials is shown in Figure 7.1. The neutron cross section is commonly expressed in units of barns (10^{-24} cm²). The ^{10}B cross-section is seen to decrease with energy at an almost constant slope, its cross section varying as *1/v* or as $1/E^{½}$. In contrast, the cross sections for both ^{113}Cd and ^{157}Gd are seen to have a very sharp increase for low energies, E < 0.4 eV. As the energy decreases from 0.4 eV to 0.1 eV, the cross section for these two metals increases by about two orders of magnitude, thus these metals are very effective in shielding out low energy neutrons with E < 0.4 eV, while allowing higher energy neutrons and gamma photons to pass through.

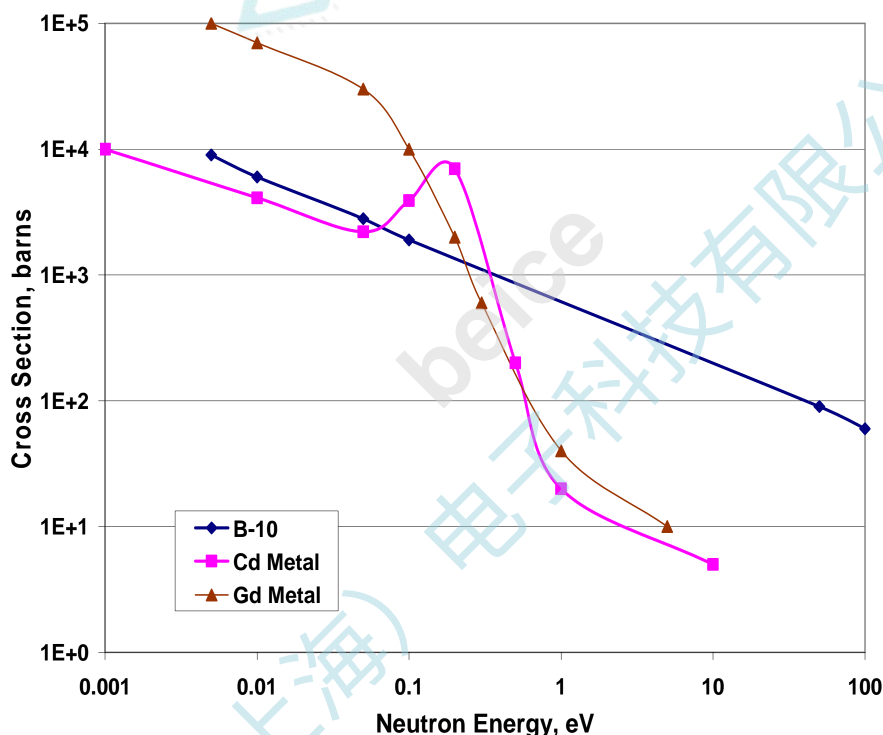

Figure 7.1 — Variation of the thermal neutron cross section with energy for B, Cd and Gd

Table 7.1 — Neutron attenuation as a function of thickness for various materials

Shield Thickness, mm	Boron (^{10}B)	Cadmium (^{113}Cd)	Gadolinium (^{157}Gd)
.01	9.1E-1	8.9E-1	3E-1
.1	3.7E-1	3.1E-1	5.8E-6
1	4.7E-5	8.8E-6	4.3E-53

Downloaded by xu yajun (xuyj@beice-sh.com) on Jun 29, 2018, 12:46 am PDT
联系方式：xuyj@beice-sh.com 13917165676

7.4.5 Thermal neutron shielding (cont'd)

Cd and Gd may be used to shield DUTs in a neutron beam comprised of both thermal and higher energy neutrons with the advantage that higher energy neutrons (E_n > 0.4 eV) pass unaffected [16]. Because the thermal neutron cross sections are so high, only a minimal thickness is required, <1mm, to virtually shield out all neutrons with E < 0.4 eV as shown in Table 7.1.

Another standard approach to shielding thermal neutrons has been to use products that contain large quantities of boron, such as boric acid and borated polymer sheets (sold commercially) but several millimeters of these materials will be needed since the shield is not composed entirely of boron.

Whatever the material, it must be conformal or at least placed in such a way that the entire device is surrounded by shielding material. This is necessary to preclude any stray scattered thermal neutrons from reaching the device and causing errors during the shielded test. In some facilities it may be possible to place the shielding material in the beam upstream from the DUT such that the number of scattered thermal neutrons is reduced – but the efficiency of such a shield should be confirmed with neutron detectors prior to running any component tests.

7.5 Basic test methodology

The basic test methodology for memory arrays is storing a known data pattern in the array while the part is exposed to the accelerated beam and comparing the stored pattern that is present after the device has been irradiated. At some time during and/or after the exposure, the data is evaluated to identify the number of changes in the pattern as errors. Other circuits may have different ATE requirements. Considerable more detail on test methodology is found in 3.

The system consists of the input stimulus generator and response recorder that would be designed to accommodate the specified device. Testing requires some sequence of writing data to the DUT, reading the data back, comparing the output data to the written data, and tabulating the number of errors. For simple memory arrays, a bit is failing when the data read from that bit is different from the last data written to that bit. It is also useful to identify failing addresses and time of failure for dynamic tests.

7.6 Test procedure and results

7.6.1 General test specification

The test method utilizes a beam of neutrons with most neutrons being at thermal energies or below. The flux of thermal neutrons should be well defined and validated either with activation foils and/or a calibrated neutron detector. The purpose of this test method is first to determine whether or not a component has a thermal neutron sensitivity, and then, if a sensitivity is observed, to give a relative quantification of the SER from thermal neutrons (as compared with the SER from high-energy neutrons). Two approaches are recommended here for determining the impact of thermal neutron SER.

The first approach involves doing dedicated SER testing at a facility that provides a calibrated thermal neutron beam and the absence of high-energy neutrons, like NIST (see annex E for other facilities). After the background runs are completed the DUT is irradiated with the thermal neutron beam and the number of soft errors are recorded.

Downloaded by xu yajun (xuyj@beice-sh.com) on Jun 29, 2018, 12:46 am PDT
联系方式：xuyj@beice-sh.com 13917165676

7.6.1 General test specification (cont'd)

The DUT is then surrounded with shielding material (see 7.4.5) and the thermal neutron irradiation repeated with the same fluence as the first experiment. It is expected that a very large fraction if not all the neutrons will be shielded. If a large decrease in the error rate is observed with the shield in place, then the DUT has a high concentration of ^{10}B near active device layers. For components with BPSG (but without ^{11}B enhancement), the thermal neutron test without a shield is expected to be higher than the shielded condition.

The second approach assumes that both the thermal and high-energy neutron SER testing will be done at a single high-energy neutron spallation source. This requires that the spallation source contain a well-quantified thermal neutron component whose flux level is similar to that of the high-energy neutron component, like TRIUMF. In spallation facilities that do not have an appreciable thermal neutron flux, the use of a moderator could adequately increase the thermal neutron component, but it would have to be calibrated; see annex E for other facilities. The primary difference in this approach is that the shielding will remove only the thermal and epi-thermal neutrons while leaving virtually all of the high-energy neutrons unchanged. As before, after the background tests have established that the DUT and ATE give error-free results, the DUT is irradiated by the spallation beam and the resultant errors are recorded after the DUT has been exposed to known neutron fluences (thermal and high energy). The test is then repeated with the DUT surrounded by the thermal neutron shielding material.

For components with BPSG (but without ^{11}B enhancement), the spallation neutron test without a shield are expected to yield higher error rates which represent the SER due to both high-energy and thermal neutron reactions. In the shielded condition the DUT will also exhibit failures but this time they will be only due to high energy neutron reactions, since the thermal neutrons will be removed from the beam. For DUTs without any high concentrations of ^{10}B in their construction, this test will show a non-zero error rate which should be similar for both the shielded and non-shielded irradiations. For these types of components thermal neutron reactions should not play an important role in the observed SER that is dominated by high-energy neutron reactions.

For both approaches, for each run, record the exposure time, neutron fluences, fail counts, fail locations, test patterns, voltages, core operating cycles, and the DUT identification. An estimate of the thermal neutron flux within the unshielded beam must also be included. The final error rates from the shielded and unshielded experiments must be summarized in the final report.

At least one run should be performed without the source for the maximum test duration to be used. For the background test(s), the DUT must exhibit no soft errors. After the background run is performed the actual testing under radiation exposure is performed.

Typically, multiple tests are run under irradiation using various test patterns, voltages, cycle times, and different DUTs. The number and type of errors observed and the duration of each test are recorded as well as any evidence of MCU, SEL, or SEFI.

Both of these test methods determine if the DUT has any SER sensitivity to thermal neutrons. Thus a go-no-go determination can be made as to a component's sensitivity to thermal neutrons. If a large difference in SER response is seen between the shielded and unshielded experiments, the device contains a significant amount of ^{10}B (probably as borophosphosilicate glass, BPSG). At this point, further work is justified to determine the magnitude of failures induced by the thermal neutron flux.

Downloaded by xu yajun (xuyj@beice-sh.com) on Jun 29, 2018, 12:46 am PDT
联系方式：xuyj@beice-sh.com 13917165676

7.6.2 Computation of fail rate from thermal neutron SEU cross section

If a calibrated thermal neutron beam is used, in an analogous way to the (averaged) SEU cross section discussed in 6.6.2.4, the "average" thermal neutron cross-section (this presumes that the thermal neutron energy distributions of the beam and the environment are similar – large differences in cross-section can result if the neutron energy distributions are not the same) can be extracted from a thermal neutron beam experiment and can be defined in two ways:

$$\overline{\sigma_{SEU-dev}} = \mathrm{N}_{\mathrm{SEU}} / \Phi_{spec} \tag{7.2}$$

and

$$\overline{\sigma_{SEU-bit}} = \mathrm{N}_{\mathrm{SEU}} / \left(\Phi_{spec} \times \mathrm{N}_{\mathrm{bit}}\right) \tag{7.3}$$

The averaged cross sections depend on the shape of the thermal neutron spectrum; Φ_{spec} is the fluence of neutrons over the spectrum from $E = 0$ to 20 eV, in units of neutrons/cm^2; $\overline{\sigma_{SEU-dev}}$ is the thermal SEU cross section in units of cm$^2\times$device^{-1} and $\overline{\sigma_{SEU-bit}}$ is in units of cm$^2\times$bit^{-1}. The SEU rate (fails$\times$bit^{-1}s^{-1}) due to thermal neutrons can be calculated as follows:

$$\text{SEU rate} = 1.8\times10^{-3} \times \overline{\sigma_{SEU-bit}} \tag{7.4}$$

Here, the nominal integral thermal neutron flux on the ground, centered around $E \sim 0.025$ eV, is 1.8×10^{-3} cm^{-2}s^{-1} (6.5 cm^{-2} h^{-1}); see A.3. This upset rate can be adjusted for specific locations and conditions using the methods described in A.3.

Note: The accuracy of this method hinges on the thermal neutron beam spectrum being similar to the cosmic thermal neutron background AND assumes that the calibration of the neutron source has been done correctly and is accurate. In addition, since there is a ~2x difference in reported measured thermal neutron fluxes and a dependence on scattering/shielding environment, the confidence in the absolute thermal neutron SER is lower than for the other accelerated tests (see A.4).

7.6.3 Computation of the relative thermal neutron SER

Using a spallation source one cannot directly extract the "average" thermal neutron cross-section particularly since the neutron spectrum changes drastically for the shielded and unshielded experiment. In this case we presume that the spallation source provides a thermal and high-energy neutron spectral distribution that is similar to the actual terrestrial environment and that the ratio of neutrons in the thermal distribution is of the same order as those in the high-energy distribution. In the terrestrial environment it has been shown that at sea-level the integral of the thermal neutron distribution yields between 4 - 8 cm^{-2}h^{-1} [17, 18] while the integral of the high-energy (> 10 MeV) distribution gives ~ 13 cm^{-2}h^{-1}. (see A.3 and A.4)

In order to avoid uncertainties in trying to extrapolate the thermal neutron flux it is helpful to define the relative thermal neutron SER according to:

Downloaded by xu yajun (xuyj@beice-sh.com) on Jun 29, 2018, 12:46 am PDT
联系方式：xuyj@beice-sh.com 13917165676

7.6.3 Computation of the relative thermal neutron SER (cont'd)

$$\text{Relative Thermal SER} = \frac{ASER_{thermal}}{ASER_{high}} = \frac{ASER_{total} - ASER_{high}}{ASER_{high}} \tag{7.5}$$

Where $ASER_{thermal}$ is measured directly and is calculated by subtracting the accelerated SER obtained with shielding, $ASER_{high}$, from the accelerated SER obtained without shielding, $ASER_{total}$. Further, $ASER_{thermal}$ is used to define the thermal neutron SEU cross section, $\overline{\sigma_{SEU-dev}}$ in Equation 7.2, since $ASER_{thermal}$ is proportional to $\overline{\sigma_{SEU-dev}} \times \Phi_{spec}$, where Φ_{spec} is the fluence of thermal neutrons (defined as having energies < 0.4 eV) within the neutron spectrum of the test facility. In components without high concentrations of ^{10}B and no strong thermal neutron sensitivity $ASER_{total} \sim ASER_{high}$ and thus the relative thermal neutron SER << 1. If the component has a large concentration of ^{10}B and a strong thermal neutron sensitivity $ASER_{total} >> ASER_{high}$ and the relative thermal neutron SER > 1. The higher the ratio, the greater the thermal neutron SER sensitivity.

7.7 Interferences

7.7.1 Rate of errors in accelerated tests

See description in 5.7.1.

7.7.2 Generalized noise issues

See description in 5.7.2.

7.7.3 Total dose

See description in 5.7.3.

7.7.5 Scattering and secondary ion effects at the DUT

Particle scattering can be a problem in any beam experiment, particularly when dense high Z materials are placed in the beam in close proximity to the DUT. Thermal neutrons are more easily scattered due to their low energy and thus any shielding that is done must enclose the device. It should also be noted that the higher the Z of the shield or scattering material, the larger the likelihood that high-energy protons will be emitted as a reaction product (this is mainly a concern in neutron beams containing high energy neutrons). These higher energy protons can penetrate the DUT and cause addition SER. This implies that spurious results might be obtained if a high Z metal shield were used to enclose a DUT if a large fraction of the observed SER were related to secondary proton induced events. If this is thought to be a problem, using Boron as a shielding material instead of Cd or Gd should reduce this effect considerably.

The scattering effects can also be seen if large metallic heat sinks are used in the DUT. Any type of scattering material in the neutron beam during the experiments needs to be described in detail in the final report. If a large metallic heat sink is part of the DUT in the neutron beam, it is advisable to repeat the neutron testing at several different beam incidence angles to ensure that scattering effects and secondary proton fluxes do not significantly alter the test results (this presumes that the actual neutron flux under nominal conditions will be roughly isotropic with only a weak angular dependence).

Downloaded by xu yajun (xuyj@beice-sh.com) on Jun 29, 2018, 12:46 am PDT
联系方式：xuyj@beice-sh.com 13917165676

7.7.6 Gamma flux from nuclear reactor neutron beams

If performing neutron experiments at a nuclear reactor facility, the effect of the large gamma photon flux mixed with the neutron flux must be determined. While many advanced components do not have a high sensitivity to gamma irradiation, a test should be performed using a neutron shield that ensures that no neutrons are getting to the DUT even when it is in the beam. In this case only gamma photons will be reaching the DUT. The DUT should be exposed for the longest planned duration. If the gamma photons do not contribute to the SER it is expected that no errors will be observed. If errors are observed in the shielded case then the component is sensitive to the gamma flux and this must be included in the final report.

It is important to note that for long exposures or in intense neutron beams that contain gamma photons, total dose effects may also manifest themselves.

7.7.7 Single event latchup and single event functional interrupt

See description in 5.7.5.

7.8 Final report

The following items must be included in the final report for accelerated thermal neutron testing:

DUT description:

1) See description from 4.5

Test Description:

2) See description from 4.5

Fail Information:

3) See description from 4.5

Downloaded by xu yajun (xuyj@beice-sh.com) on Jun 29, 2018, 12:46 am PDT
联系方式：xuyj@beice-sh.com 13917165676

7.8 Final report (cont'd)

<u>Thermal neutron ASER specific items</u>

Source Description:

4) Name, location, type and overall description of accelerator facility and facility contact person

5) Type of reaction producing the neutron flux.

6) Thermal neutron flux (integrated flux < 0.4 eV in $cm^{-2}h^{-1}$ or $cm^{-2}s^{-1}$)

7) Neutron energy spectrum.

8) Method of neutron flux determination (foils, neutron detectors, etc.).

9) Date of last calibration on detector used to monitor beam flux.

10) Special configurations used (e.g., moderators, neutron guides, etc.).

11) Dimension and shape of beam spot.

12) Beam angle of incidence with respect to the DUT.

13) Description of beam flux uniformity over spot (e.g. uniform, Gaussian, etc.)

14) Alignment of beam with respect to DUT active area tested (centered).

15) Any shadowing which might affect the final result by obstructing some of the source flux (e.g., large metallic heat sink on DUT, etc.).

16) Any type of scattering material in the neutron beam during the experiments needs to be described in detail (see 7.7.5)

17) The distance from a reference point must be noted to account for solid angle effects if appropriate. (see 3.7)

18) An estimate of the thermal neutron flux within the unshielded beam. Include the final error rates from any shielded and unshielded experiments. (see 7.6.1)

19) For nuclear reactor facility: gamma check results (see 7.7.6)

SER Calculation:

20) Estimation of Relative thermal neutron SER (see 7.6.3) for each condition measured (e.g., voltage, ECC state, pattern, frequency, etc.) Record all assumptions.

NOTE The omission of a specific failure rate requirement is intentional, and the failure measurement technique, data analysis and reporting must follow the well-established procedure defined in this document.

Downloaded by xu yajun (xuyj@beice-sh.com) on Jun 29, 2018, 12:46 am PDT
联系方式：xuyj@beice-sh.com 13917165676

Annex A - Determination of terrestrial neutron flux (normative)

A.1 Introduction

This annex provides the cosmic-ray-induced neutron differential flux above 1 MeV for a reference location and conditions and also provides formulas and tables that allow the reference spectrum to be scaled to other locations and conditions. This annex describes the use of a Web-page calculator that is available to simplify determination of the flux scaling factor. The neutron spectrum below 1 MeV, especially thermal-energy neutrons, and the effects of shielding by buildings are also discussed.

The intensity of cosmic-ray-induced neutrons (and other secondary cosmic radiation, including protons) in the atmosphere varies with altitude, location in the geomagnetic field, and solar magnetic activity. Atmospheric shielding at a given altitude is determined by the mass thickness per unit area of the air above, called areal density or atmospheric depth. The geomagnetic field deflects low-momentum primary cosmic particles back into space, lowering the neutron flux produced in the atmosphere. The minimum momentum per unit charge (magnetic rigidity) that an incident (often, vertically incident) particle can have and still reach a given location above the Earth is called the geomagnetic cut-off rigidity (cutoff) for that point. The varying magnetic field carried outward from the Sun by the solar wind plasma that permeates the solar system also reduces the cosmic-ray intensity at Earth. This solar modulation has been measured for decades by a number of neutron monitors on the ground at various locations. The cosmic-ray-induced terrestrial neutron flux is highest when sunspots and other solar activity are at a minimum (quiet sun), and lowest when the sun is most active. The effects on the terrestrial neutron flux of atmospheric depth, geomagnetic cutoff, and solar activity are not independent. For example, the change in flux with cutoff depends on solar activity and to some extent on atmospheric depth.

The most important parameter determining the terrestrial neutron flux is atmospheric depth, which is proportional to barometric pressure and changes with altitude. The neutron flux is roughly 10 times higher at an altitude of 3,000 m (9,843 ft) than it is at sea level. The global variation with cutoff is about a factor of 2 from equator to pole at sea level, and 3 at the highest inhabited altitudes. Solar modulation is smaller still, about a 25% decrease from maximum to minimum recorded monthly-averaged rates at polar locations near sea level and ~7% at the equator, and 30% to 12% for polar and equatorial sites at high elevations.

Fortunately, the *shape* of the outdoor ground-level neutron spectrum above a few MeV does not change significantly with altitude, cutoff, or solar modulation. This makes it possible to describe the neutron differential flux at one location under reference conditions and then scale the reference spectrum to obtain the neutron differential flux anywhere on Earth at any time.

A.2 Reference neutron spectrum

The location and conditions for the reference cosmic-ray-induced terrestrial neutron differential flux have been chosen to be New York City outdoors at sea level at a time of average solar activity. Values of the neutron flux in units of neutrons/(cm^2 MeV s) at 46 energies above 1 MeV are given in Table A.2-A. The reference spectrum was determined primarily by measurements, and is taken from Gordon et al. [17], where those interested can find details of the measurements and the scaling functions described below in A.3.

Downloaded by xu yajun (xuyj@beice-sh.com) on Jun 29, 2018, 12:46 am PDT
联系方式：xuyj@beice-sh.com 13917165676

A.2 Reference neutron spectrum (cont'd)

Table A.2-A — Cosmic ray induced neutron differential flux for reference conditions (sea level, New York City, mid-level solar activity, outdoors)

Neutron Energy (MeV)	Differential Flux (cm^{-2} s^{-1} MeV^{-1})	Neutron Energy (MeV)	Differential Flux (cm^{-2} s^{-1} MeV^{-1})	Neutron Energy (MeV)	Differential Flux (cm^{-2} s^{-1} MeV^{-1})
1.054	6.83×10^{-4}	5.220	1.53×10^{-4}	130.7	9.64×10^{-6}
1.165	8.19×10^{-4}	5.769	1.25×10^{-4}	224.6	4.30×10^{-6}
1.287	7.61×10^{-4}	6.376	1.16×10^{-4}	386.3	1.33×10^{-6}
1.423	7.02×10^{-4}	7.047	8.90×10^{-5}	664.2	3.99×10^{-7}
1.572	6.00×10^{-4}	7.788	7.16×10^{-5}	1.142×10^{3}	1.02×10^{-7}
1.738	5.72×10^{-4}	8.607	6.73×10^{-5}	1.964×10^{3}	2.24×10^{-8}
1.920	5.06×10^{-4}	9.512	5.53×10^{-5}	3.376×10^{3}	3.36×10^{-9}
2.122	5.02×10^{-4}	10.51	4.58×10^{-5}	5.805×10^{3}	4.71×10^{-10}
2.346	5.44×10^{-4}	11.62	4.09×10^{-5}	9.982×10^{3}	9.87×10^{-11}
2.592	4.30×10^{-4}	12.84	3.80×10^{-5}	1.716×10^{4}	3.83×10^{-11}
2.865	3.34×10^{-4}	14.19	3.44×10^{-5}	2.951×10^{4}	8.60×10^{-12}
3.166	2.65×10^{-4}	16.16	3.02×10^{-5}	5.074×10^{4}	2.17×10^{-12}
3.499	1.86×10^{-4}	18.52	3.22×10^{-5}	8.725×10^{4}	6.97×10^{-13}
3.867	1.64×10^{-4}	25.70	2.59×10^{-5}	1.500×10^{5}	1.88×10^{-13}
4.274	1.73×10^{-4}	44.19	2.09×10^{-5}		
4.724	1.88×10^{-4}	75.98	1.53×10^{-5}		

To provide values at energies between those given in Table A.2-A, an analytic expression has been fit to the reference spectrum:

$$\frac{d\dot{\Phi}_0(E)}{dE} = 1.006\times10^{-6}\exp\left[-0.35(\ln(E))^2 + 2.1451\ln(E)\right] + 1.011\times10^{-3}\exp\left[-0.4106(\ln(E))^2 - 0.667\ln(E)\right], \quad \text{(A.1)}$$

where E is neutron energy and $d\dot{\Phi}_0(E)/dE$ is the reference neutron differential flux.

The total flux of the measured reference spectrum above 10 MeV is 3.596×10^{-3} cm^{-2} s^{-1} (12.9 cm^{-2} h^{-1}). The total flux of the analytic fit above 10 MeV is 3.585×10^{-3} cm^{-2} s^{-1} — within 0.3% of the measurement. The estimated uncertainty in the measured value of the neutron flux above 10 MeV is over 10%. An appropriately rounded value of the total neutron flux of the reference spectrum above 10 MeV is 3.6×10^{-3} $cm^{-2}s^{-1}$ or equivalently 13 $cm^{-2}h^{-1}$.

Figure A.2.1 is a graph of the reference spectrum, the differential flux of cosmic-ray-induced neutrons as a function of neutron energy. The points are the values in Table A.2-A. The solid curve is the analytic fit. The dashed curve is a model of the spectrum from the previous version of this standard, JESD89 (August 2001).

Downloaded by xu yajun (xuyj@beice-sh.com) on Jun 29, 2018, 12:46 am PDT
联系方式：xuyj@beice-sh.com 13917165676

A.2 Reference neutron spectrum (cont'd)

Figure A.2.2 presents the same information as Figure A.2.1, but using a different representation of the neutron spectrum, plotting energy times differential flux as a function of energy. This representation is standard in the field of radiation protection, but it is not yet routine in the literature on SER or cosmic-ray physics. It is conceptually simpler to plot the differential flux, $d\dot{\Phi}/dE$, but for neutrons, that typically requires a log–log plot covering many orders of magnitude on both axes, making details difficult to see. The large range of neutron $d\dot{\Phi}/dE$ stems from its characteristic $1/E$ dependence when neutrons slow down in a scattering medium. $E(d\dot{\Phi}/dE)$ is relatively flat and can be plotted on a linear scale. $E(d\dot{\Phi}/dE)$ is mathematically identical to $d\dot{\Phi}/d(\ln(E))$. In a plot of $E(d\dot{\Phi}/dE)$ against $\log(E)$, equal areas under the spectrum in different energy regions represent equal integral fluxes.

In Figure A.2.2, the histogram is the measurement-based reference spectrum, and, as in Figure A.2.1, the solid and dashed curves are the analytic fit to the reference spectrum and the model of the spectrum from the previous version of this standard, JESD89 (August 2001). Note that Figure A.2.2 begins at 0.1 MeV.

The old model underestimates the reference measured flux integrated from 50 MeV to 1 GeV (old/measured = 0.75) and overestimates it from 5 to 50 MeV and again from 1 to 10 GeV by factors of 1.7 and 1.3, respectively. For the flux integrated from 10 MeV to 10 GeV, the old model and the new reference spectrum agree within 3.3%.

The reference spectrum applies only to locations on the ground. It is not accurate for airplanes.

High-energy secondary protons are also present in the cosmic-ray-induced particle showers that produce neutrons, and such protons can also cause single-event effects in electronics. The reference neutron spectrum does not include protons. Calculations indicate that the terrestrial cosmic-ray proton flux is roughly 5% to 20% of the neutron flux above 10 MeV, depending on altitude and cutoff, with the higher fraction of protons at high altitude and high cutoff. The proton spectrum peaks at higher energy than the upper peak of the neutron spectrum does, so the ratio of proton flux to neutron flux increases with increasing energy. If the response of a device or component is higher at, say, 50 MeV than it is at 10 MeV, the SER at high mountain elevations may be as much as 25% higher than it would be from the neutrons alone.

The angular distribution of high-energy cosmic-ray-induced neutrons is not isotropic. As the energy increases above 100 MeV, the neutrons tend to be directed more and more downward. However, the anisotropy of the cosmic-ray neutron angular distribution is generally not of much importance to SER studies and does not need to be factored into SER calculations except when making detailed calculations of shielding by buildings with thick walls (see A.5).

Downloaded by xu yajun (xuyj@beice-sh.com) on Jun 29, 2018, 12:46 am PDT
联系方式：xuyj@beice-sh.com 13917165676

A.2 Reference neutron spectrum (cont'd)

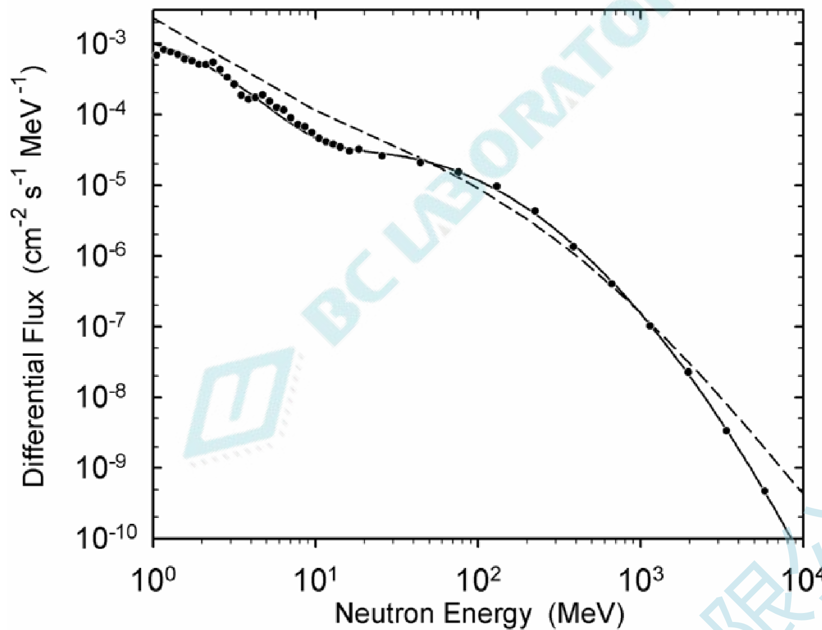

Figure A.2.1 — The differential flux of cosmic-ray-induced neutrons as a function of neutron energy under reference conditions (sea level, New York City, mid-level solar activity, outdoors). The data points are the reference spectrum, the solid curve is the analytic fit to the reference spectrum, and the dashed curve is the model from the previous version of this standard, JESD89 (2001).

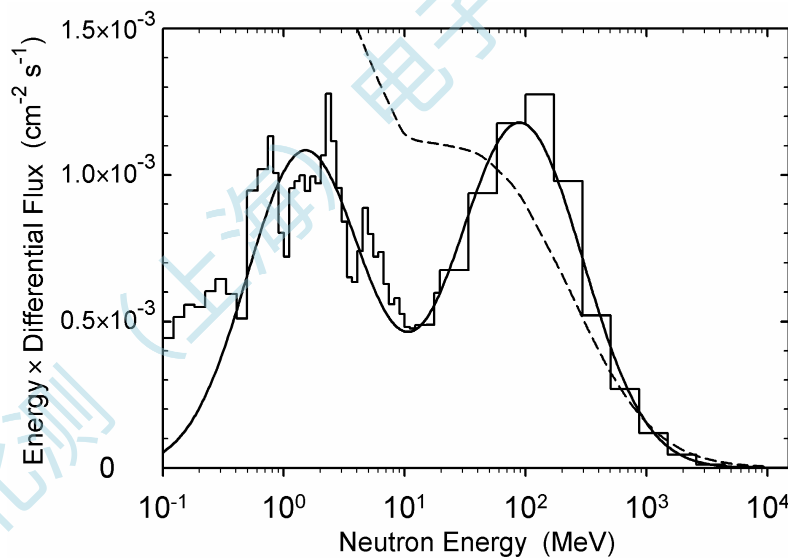

Figure A.2.2 — Reference spectrum of cosmic-ray-induced neutrons plotted as energy times differential flux as a function of neutron energy. The histogram is the reference spectrum, the solid curve is the analytic fit to the reference spectrum, and the dashed curve is the model from the previous version of this standard, JESD89 (2001).

Downloaded by xu yajun (xuyj@beice-sh.com) on Jun 29, 2018, 12:46 am PDT
联系方式：xuyj@beice-sh.com 13917165676

A.3 Scaling the reference neutron spectrum to other locations/conditions

To account for the effects of altitude, cutoff, and solar modulation, the neutron spectrum outdoors at any location can be expressed as follows:

$$\frac{d\dot{\Phi}(E)}{dE} = \frac{d\dot{\Phi}_0(E)}{dE} \cdot F_A(d) \cdot F_B(R_c, I, d), \tag{A.2}$$

where $d\dot{\Phi}_0(E)/dE$ is the reference spectrum, d is the atmospheric depth, R_c is the vertical geomagnetic cutoff rigidity, I is the relative count rate of a neutron monitor measuring solar modulation, $F_A(d)$ is a function describing the principal dependence on altitude (i.e., on atmospheric depth) and $F_B(R_c, I, d)$ is a function describing the dependence on geomagnetic location and solar modulation which also has a dependence on depth. Atmospheric depth is given by $d = p/g$, where p is the barometric pressure and g is the acceleration of gravity. Vertical cutoff depends primarily on the horizontal component of the Earth's magnetic field. It is near zero at the poles and has a maximum of 15 to 17 GV at the equator. (GV is a unit of rigidity; GeV is a unit of energy.) Consequently, the cosmic-ray induced neutron flux is higher at the poles and lower at the equator. Values of R_c for cosmic rays reaching the atmosphere have been calculated several times for a grid of locations covering the globe [19]. Values of F_B given in this standard have been calculated using values of R_c calculated by Shea and Smart from the International Geomagnetic Reference Field for 1995.

The neutron differential flux at any location is the product of the reference spectrum and the scaling factor $F_A \cdot F_B$. Formulas for F_A and F_B, a table of F_B at sample values of cutoff rigidity, and a table of $F_A \cdot F_B$ for several cities and other locations are given below. A Web-page calculator has been developed to calculate the scaling factor $F_A \cdot F_B$ for an arbitrary location on Earth given the latitude, longitude, and barometric pressure or elevation at the location. In Equation A.2, the main altitude dependence is exponential attenuation:

$$F_A(d) = \exp[(1033.2 - d)/131.3], \tag{A.3}$$

where 1033.2 g/cm^2 is the mean atmospheric depth at sea level, and 131.3 g/cm^2 is the effective mass attenuation length in the atmosphere for neutrons above 10 MeV. Barometric pressure is often given in millibar (hectoPascal, hPa) or in mmHg. Standard sea level pressure is 1013.25 millibar or hPa, which is equal to 760 mmHg. Using barometric pressure p in hPa, atmospheric depth d in g/cm^2 is given by

$$d(\text{g/cm}^2) = p(\text{hPa})/0.980665, \tag{A.4}$$

where 0.980665 is the average acceleration of gravity at sea level, 9.80665 m/s^2, divided by 10. Atmospheric depth is best determined from actual barometer readings, but when the barometric pressure is not available, its average value at a given elevation, z, in meters can be determined using

$$p(\text{hPa}) = ((44331.514 - z)/11880.516)^{5.255877}. \tag{A.5}$$

Although F_A describes the main dependence of the neutron flux on atmospheric depth (altitude), for best accuracy it should not be used alone, even when the cutoff is held constant (for example, comparing the flux at the bottom and top of the same mountain) because F_B also contains some depth dependence. Without the depth dependence of F_B, the attenuation length in air would be about 135 g/cm^2.

Downloaded by xu yajun (xuyj@beice-sh.com) on Jun 29, 2018, 12:46 am PDT
联系方式：xuyj@beice-sh.com 13917165676

A.3 Scaling the reference neutron spectrum to other locations/conditions (cont'd)

The expression for F_B comes from theoretical calculations [20, 21] that were done only for the extreme conditions of solar modulation: quiet sun, when the terrestrial cosmic ray flux is at its peak, and active sun, when the terrestrial cosmic ray flux is at its minimum. For these two conditions,

$$F_{B,quiet}(R_c, h) = 1.098\left[1-\exp\left(-\alpha_1/R_c^{k_1}\right)\right] \quad (A.6)$$

and

$$F_{B,active}(R_c, h) = 1.098\left[1-\exp\left(-\alpha_2/R_c^{k_2}\right)\right] \times \left[1-\exp\left(-\alpha_1/50^{k_1}\right)\right] / \left[1-\exp\left(-\alpha_2/50^{k_2}\right)\right], \quad (A.7)$$

where the parameters α and k are given by

$$\alpha_1 = \exp\left[1.84 + 0.094h - 0.09\exp(-11h)\right], \quad (A.8)$$

$$k_1 = 1.4 - 0.56h + 0.24\exp(-8.8h), \quad (A.9)$$

$$\alpha_2 = \exp\left[1.93 + 0.15h - 0.18\exp(-10h)\right], \quad (A.10)$$

and

$$k_2 = 1.32 - 0.49h + 0.18\exp(-9.5h). \quad (A.11)$$

Unlike Equations A.2 – A.5, Equations A.6 – A.11 use barometric pressure, h, in bar (1 bar = 10^5 Pa) instead of depth or pressure in millibar: $h = p/1000$.

Since the terrestrial neutron flux changes by less than 30% between these extremes (less than 20% for most locations), in many cases, especially at low altitudes and latitudes, it is practical to set F_B equal to the average of the results from Equations E.5 and E.6 and ignore solar modulation. This should not be done for determinations of the neutron flux at high-altitude facilities used for accelerated testing with natural radiation. In such cases, where an especially accurate knowledge of the neutron flux is desired, readings from a neutron monitor during the test period should be used to determine the state of solar activity, and an interpolation made between the values from Equations E.5 and E.6. The neutron monitor must be one with available data over several solar activity cycles
(see, for example, http://neutronm.bartol.udel.edu/, http://cosmicrays.oulu.fi/, http://ulysses.sr.unh.edu/NeutronMonitor/neutron_mon.html, and http://helios.izmiran.troitsk.ru/cosray/main.htm).

For example, if monthly average neutron monitor readings are 20% of the way from their typical minimum values at active sun to their maximum values at quiet sun, interpolate 20% of the way from $F_{B,active}$ to $F_{B,quiet}$. ("Typical minimum values" means exclude the very low values seen in some months of 1989 - 1991.)

Table A.3-A gives values of $F_{B,active}$, $F_{B,quiet}$, and their mean at sea level for integer values of geomagnetic vertical cutoff rigidity from 0 (magnetic poles) to 17 GV (the maximum value, found in southeastern Asia). Multiplying the reference neutron spectrum by these values gives the terrestrial cosmic-ray neutron differential flux at sea level locations with the indicated cutoff rigidity. The cutoff rigidity at New York City is 2.08 GV. Since this is the reference location, the value in Table A.3-A at 2 GV for average solar modulation is very close to 1. The values in Table A.3-A (and Table A.3-B) are given to 3 significant figures so that trends may be understood more easily, but the overall uncertainty of the values for F_B is as large as 10%, especially for low latitudes (high cutoffs), where F_B tends to predict fluxes that are too low.

Downloaded by xu yajun (xuyj@beice-sh.com) on Jun 29, 2018, 12:46 am PDT
联系方式：xuyj@beice-sh.com 13917165676

A.3 Scaling the reference neutron spectrum to other locations/conditions (cont'd)

Table A.3-A — Relative neutron flux at sea level vs. geomagnetic vertical cutoff rigidity

Cutoff Rigidity (GV)	Relative Neutron Flux			Cutoff Rigidity (GV)	Relative Neutron Flux		
	Active Sun Minimum	Quiet Sun Peak	Average		Active Sun Minimum	Quiet Sun Peak	Average
0	0.939	1.098	1.019	9	0.686	0.737	0.712
1	0.938	1.097	1.018	10	0.657	0.702	0.679
2	0.929	1.076	1.002	11	0.630	0.670	0.650
3	0.902	1.030	0.966	12	0.606	0.640	0.623
4	0.866	0.975	0.920	13	0.583	0.614	0.598
5	0.827	0.919	0.873	14	0.562	0.589	0.576
6	0.789	0.867	0.828	15	0.542	0.567	0.555
7	0.752	0.819	0.786	16	0.524	0.547	0.535
8	0.718	0.776	0.747	17	0.508	0.528	0.518

Table A.3-B gives a brief list of cities and some high-elevation research locations with the latitude, longitude, and elevation (altitude) of each, and the corresponding geomagnetic vertical cutoff rigidity, typical atmospheric depth, and $F_A \cdot F_B$ for active sun, quiet sun, and average solar modulation. To determine the long-term average cosmic-ray induced neutron differential flux for one of the listed locations, multiply the reference spectrum by the number in the last column of the table for the location of interest. The elevations given in Table A.3-B may not be correct for a particular point in the city or research site, but they are the elevations assumed for the flux factor calculations. The calculated flux factors have an uncertainty of about 10%.

A Web-page calculator has been developed to calculate the scaling factor $F_A \cdot F_B$ for an arbitrary location on Earth given the latitude, longitude, and barometric pressure or elevation at the location. The URL for the calculator is http://www.seutest.com/FluxCalculation.htm. Below is a procedure to determine the neutron flux for an arbitrary city or location at a given time using the Web-page flux-factor calculator and two examples. It is assumed that the user has Internet access and is familiar with Web browser software.

1. Obtain the latitude and longitude of the city or location and an average or typical barometric pressure for the time of interest. If the barometric pressure cannot be found, the elevation of the location may be used instead.
2. Type http://www.seutest.com into the address window of your Web browser. Click/select "Flux calculation". Read the instructions on the Web page for the use of the calculator. They may differ from the instructions given here.
3. Enter the latitude and longitude in the boxes provided. Choose North or South for latitude and East or West for longitude. Latitude and longitude should be in decimal degrees, and 0.1 degree accuracy is more than sufficient.

Downloaded by xu yajun (xuyj@beice-sh.com) on Jun 29, 2018, 12:46 am PDT
联系方式：xuyj@beice-sh.com 13917165676

A.3 Scaling the reference neutron spectrum to other locations/conditions (cont'd)

4. Enter a value for *one* of the following: barometric pressure, elevation (altitude), or atmospheric depth. Caution: use the station (actual) barometric pressure, not the pressure corrected to sea level. The pressure may be entered in millibar (hPa), mmHg, or inches Hg. Be sure to select the unit you use. If you do not know the barometric pressure, enter the elevation of the location in the box for elevation and select the unit (meters or feet).
5. Under "Solar Modulation", generally choose the default value, 50%. For high-altitude locations where the most accurate value is desired for a particular time period, obtain count rate data from one or more neutron monitors (for example, http://neutronm.bartol.udel.edu/, http://cosmicrays.oulu.fi/, http://ulysses.sr.unh.edu/NeutronMonitor/neutron_mon.html) for that time period and for several solar cycles. (A solar cycle with both polarities of the solar magnetic field is ~22 years.) Compare the average rate for the time of interest with the historical maximum and minimum monthly average rates and interpolate between the quiet and active sun values of F_B accordingly.
6. Click/select "Submit" to start the calculation. The calculator will return a value for the flux scaling factor, for the two pressure-related quantities that were not entered, F_A and F_B from Equations E.3 and E.6 – E.11, and the geomagnetic cutoff (truncated to the nearest integer) used in the calculation.
7. Read the flux scaling factor. Also, check that the values returned by the calculator for the two pressure-related quantities that were not entered seem reasonable. To assure that correct values of the latitude and longitude were entered, including N-S and E-W, check that the value returned for the geomagnetic rigidity cutoff is reasonable by comparing it with Table A.3-C or A.3-D or with the cutoff contour map displayed when you click on the "Rigidity cutoff" link next to the value displayed.
8. Multiply the reference differential flux from Table A.2-A or Equation A.1 by the flux scaling factor to obtain the differential flux at the location.

Example 1: City location — Albuquerque, New Mexico, USA.

Latitude = 35° 40' N ≅ 35.7° N; Longitude = 106° 39' W = 106.65° W.

Barometric pressure hard to find; use elevation. Elevation = 4945 feet = 1507 m.

Type http://www.seutest.com/ into Web browser address window. Click/select "Flux calculation". In the "Latitude" box, enter 35.7 and select "North"; in the "Longitude" box, enter 106.65 and select "West". In the "Elevation" box, enter 1507 and choose "meters". Leave the "Station pressure" and "Depth" boxes blank. In the box labeled "Solar cycle" leave the default value, 50%.

Downloaded by xu yajun (xuyj@beice-sh.com) on Jun 29, 2018, 12:46 am PDT
联系方式：xuyj@beice-sh.com 13917165676

A.3 Scaling the reference neutron spectrum to other locations/conditions (cont'd)

Table A.3-B — Cosmic-ray neutron flux at selected places relative to reference flux

City or location	Latitude (°)	Longit. (° E)	Elevat. (m)	Atm. Depth (g/cm^2)	Cutoff Rigidity (GV)	Relative Neutron Flux		
						Active Sun Low	Quiet Sun Peak	**Avg.**
Cities								
Bangkok, Thailand	13.4 N	100.3	20	1031	17.4	0.51	0.53	0.52
Beijing, China	39.9 N	116.4	55	1027	9.4	0.71	0.76	0.73
Berlin, Germany	52.5 N	13.4	40	1028	2.8	0.94	1.08	1.01
Bogotá, Columbia	4.6 N	285.9	2586	753	12.3	3.70	4.00	3.85
Chicago, IL, USA	41.9 N	272.4	180	1011	1.8	1.09	1.28	1.19
Denver, CO, USA	39.7 N	255.0	1609	851	2.8	3.43	4.08	3.76
Hong Kong, China	22.3 N	114.2	30	1030	16.1	0.53	0.56	0.55
Houston, TX, USA	30.0 N	264.6	15	1031	4.6	0.88	0.98	0.93
Johannesburg, S. Africa	26.2 S	28.0	1770	834	7.1	2.95	3.30	3.13
La Paz, Bolivia	16.5 S	291.9	4070	623	12.2	8.59	9.39	8.99
London, UK	51.5 N	359.9	10	1032	2.9	0.91	1.05	0.98
Los Angeles, CA, USA	34.0 N	241.7	100	1021	5.3	0.89	0.99	0.94
Mexico City, Mexico	19.4 N	260.9	2240	787	8.4	3.75	4.16	3.96
Moscow, Russia	55.8 N	37.6	150	1015	2.2	1.06	1.22	1.14
New Delhi, India	28.6 N	77.2	220	1007	14.1	0.66	0.70	0.68
New York, NY, USA (ref)	40.7 N	286.0	0	1033	2.08	0.927	1.073	1.000
Paris, France	48.9 N	2.3	50	1027	3.6	0.92	1.04	0.98
Seattle, WA, USA	47.6 N	237.7	50	1027	2.0	0.97	1.13	1.05
Seoul, South Korea	37.6 N	127.0	50	1027	10.7	0.66	0.71	0.69
Sidney, Australia	33.9 S	151.2	30	1030	4.5	0.87	0.97	0.92
Singapore City, Singapore	1.3 N	103.9	15	1031	17.2	0.51	0.53	0.52
Stockholm, Sweden	59.3 N	18.1	30	1030	1.4	0.96	1.12	1.04
Taipei, Taiwan	25.0 N	121.5	10	1032	15.4	0.54	0.56	0.55
Toronto, Canada	43.7 N	280.6	120	1019	1.5	1.04	1.22	1.13
Tokyo, Japan	35.7 N	139.8	20	1031	11.6	0.62	0.66	0.64
Research Locations								
IAO, Hanle, Ladakh, India	32.8 N	79.0	4500	589	12.35	10.58	11.59	11.08
Jungfraujoch, Switzerland	46.5 N	8.0	3580	664	4.5	11.7	13.89	12.80
Leadville, CO, USA	39.25N	253.7	3100	706	3.0	9.74	11.85	10.79
Los Alamos Natl. Lab., USA	35.9 N	253.7	2250	786	3.9	5.15	6.06	5.60
Mauna Kea (CSO), HI, USA	19.8 N	204.5	4070	623	12.9	8.23	8.97	8.60
Mt. Fuji, Japan	35.4 N	138.7	3776	647	11.8	7.56	8.28	7.92
Plateau de Bure, France	44.6 N	5.9	2550	757	5.2	5.76	6.66	6.21
South Pole Station	90.0 S	-	2820	731	0.1	8.70	10.93	9.81
White Mtn. Res. Sta., USA	37.4 N	241.6	3810	644	4.2	13.72	16.41	15.07

Downloaded by xu yajun (xuyj@beice-sh.com) on Jun 29, 2018, 12:46 am PDT
联系方式：xuyj@beice-sh.com 13917165676

A.3 Scaling the reference neutron spectrum to other locations/conditions (cont'd)

Click/select "Submit" to start the calculation. Calculator returns a flux scaling factor of 3.22. It also returns a value of 633.7 mmHg for pressure and 861.5 g/cm^2 for depth. The returned values of F_A = 3.70 and F_B = 0.87 are appropriate for a location at a high elevation and a cutoff above that of New York City. The returned value of rigidity cutoff, 3.xx, indicates that the cutoff used was between 3 and 4 GV. Table A.3-D gives a value of about 4 GV, as does the map displayed when you click the "Rigidity cutoff" link. The calculator actually used 3.96 GV for the cutoff.

Example 2: High-altitude research location — Mt. Washington, NH, USA, June 2003.
Latitude = 44.27° N; Longitude = 71.30° W.
Mean station barometric pressure during test = 607.7 mmHg (Elevation = 1905 m).
Solar modulation for June 2003: about 20% of the way from typical minimum monthly average rate to maximum monthly average rate.

Type http://www.seutest.com/ into Web browser address window. Click/select "Flux calculation". In the "Latitude" box, enter 44.27 and select "North"; in the "Longitude" box, enter 71.3 and select "West". In the "Station pressure" box, enter 607.7 and select mmHg. Leave the "Elevation" and "Depth" boxes blank. In the box labeled "Solar cycle" enter 20.

Click/select "Submit" to start the calculation. Calculator returns a flux scaling factor of 4.49. It also returns a value of 1847 m for elevation and 607.7 g/cm^2 for depth. Since the calculated elevation is slightly below the actual elevation, the entered pressure value was above average, but reasonable. The returned value of F_A = 4.84 is appropriate for a location at a high elevation. The returned value of F_B = 0.93 seems low for a location with a cutoff below that of New York, but that is because of the solar modulation (and high altitude). The returned value of rigidity cutoff, 1.xx, indicates that the cutoff used was between 1 and 2 GV, consistent with the contours on the map displayed when you click the "Rigidity cutoff" link. Interpolation of Table A.3-D gives a value of about 1.6 GV.

Values of geomagnetic vertical cutoff rigidity used to calculate the relative neutron flux in Table A.3-B and the Web page flux calculator were provided by the Aerospace Medical Research Division of the Federal Aviation Administration's Civil Aerospace Medical Institute. The cutoff data were generated by M.A. Shea and D.F. Smart using the International Geomagnetic Reference Field for 1995. Cutoff values were provided for a worldwide 1° × 1° grid of locations. The Web page flux calculator interpolates between those locations. For reference, an abridged version of the cutoff data, with cutoff values for every 5° latitude and 15° longitude is given below in Tables A.3-C and A.3-D. (They are divided into two tables because of the large amount of data.)

Downloaded by xu yajun (xuyj@beice-sh.com) on Jun 29, 2018, 12:46 am PDT
联系方式：xuyj@beice-sh.com 13917165676

Table A.3-C — Vertical rigidity cutoffs in GV, 0-180° longitude East

Latitude	Longitude East												
	0	**15**	**30**	**45**	**60**	**75**	**90**	**105**	**120**	**135**	**150**	**165**	**180**
90	0.01	0.01	0.01	0.01	0.01	0.01	0.01	0.01	0.01	0.01	0.01	0.01	0.01
85	0.01	0.01	0.02	0.02	0.03	0.03	0.03	0.03	0.03	0.03	0.03	0.02	0.02
80	0.03	0.04	0.06	0.07	0.08	0.09	0.09	0.10	0.10	0.09	0.09	0.07	0.06
75	0.09	0.13	0.15	0.17	0.19	0.18	0.21	0.23	0.21	0.22	0.22	0.20	0.17
70	0.24	0.32	0.38	0.41	0.43	0.43	0.46	0.48	0.51	0.54	0.52	0.51	0.42
65	0.59	0.68	0.74	0.83	0.84	0.87	0.91	0.97	1.01	1.10	1.12	1.07	0.91
60	1.10	1.28	1.40	1.45	1.53	1.61	1.61	1.72	1.82	1.94	1.99	1.91	1.69
55	2.01	2.25	2.35	2.39	2.49	2.59	2.71	2.79	2.98	3.19	3.18	3.06	2.74
50	3.30	3.53	3.69	3.74	3.94	3.98	4.18	4.32	4.53	4.90	4.76	4.53	4.18
45	4.91	5.13	5.23	5.29	5.47	5.71	5.88	6.06	6.41	6.70	6.70	6.28	5.44
40	7.13	7.35	7.36	7.44	7.78	8.23	8.65	8.92	9.36	9.77	9.61	8.80	7.73
35	9.76	9.74	9.95	10.27	10.74	11.28	11.22	11.41	11.74	11.99	11.50	10.50	9.43
30	11.61	11.76	11.93	12.33	12.82	13.53	14.00	14.16	14.12	13.87	13.36	12.63	11.59
25	13.29	13.64	13.94	14.26	14.72	15.22	15.54	15.59	15.40	14.99	14.37	13.64	12.91
20	14.19	14.58	14.91	15.28	15.78	16.31	16.62	16.61	16.32	15.80	15.13	14.43	13.76
15	14.62	15.06	15.45	15.89	16.44	16.99	17.29	17.25	16.90	16.33	15.67	15.03	14.44
10	14.64	15.12	15.58	16.08	16.70	17.26	17.57	17.52	17.16	16.60	16.00	15.45	14.95
5	14.30	14.78	15.29	15.88	16.55	17.13	17.46	17.43	17.10	16.59	16.08	15.66	15.27
0	13.62	14.09	14.64	15.30	16.02	16.62	16.96	16.98	16.70	16.29	15.91	15.63	15.37
-5	12.70	13.10	13.67	14.39	15.15	15.75	16.10	16.17	15.97	15.66	15.44	15.32	15.19
-10	11.56	11.91	12.48	13.23	13.98	14.53	14.86	14.98	14.87	14.67	14.60	14.67	14.72
-15	10.13	10.47	11.03	11.78	12.43	12.96	13.21	13.33	13.25	13.23	13.33	13.60	13.87
-20	8.52	8.75	9.20	9.83	10.33	10.65	10.73	10.80	10.84	10.54	10.66	11.84	12.57
-25	7.07	7.23	7.59	7.99	8.12	7.82	7.42	7.38	7.40	7.65	8.40	9.48	9.99
-30	5.78	5.72	5.83	5.87	5.71	5.37	5.23	5.16	5.09	5.37	5.82	6.54	7.90
-35	4.72	4.33	4.33	4.34	4.18	3.94	3.49	3.36	3.37	3.57	4.11	4.90	5.55
-40	3.85	3.52	3.47	3.27	2.89	2.57	2.18	2.06	2.03	2.22	2.58	3.18	4.11
-45	3.16	2.78	2.54	2.29	1.92	1.56	1.28	1.10	1.10	1.20	1.47	2.07	2.62
-50	2.55	2.16	1.90	1.61	1.31	0.93	0.68	0.53	0.51	0.60	0.75	1.09	1.66
-55	2.00	1.68	1.42	1.10	0.81	0.53	0.33	0.23	0.22	0.24	0.36	0.55	0.90
-60	1.51	1.21	0.96	0.74	0.50	0.28	0.13	0.08	0.06	0.07	0.12	0.25	0.46
-65	1.19	0.90	0.66	0.47	0.27	0.14	0.06	0.02	0.01	0.01	0.03	0.09	0.20
-70	0.79	0.61	0.43	0.29	0.15	0.07	0.02	0.00	0.00	0.00	0.01	0.03	0.08
-75	0.53	0.38	0.25	0.16	0.08	0.04	0.01	0.00	0.00	0.00	0.00	0.01	0.04
-80	0.30	0.24	0.15	0.10	0.06	0.03	0.01	0.00	0.00	0.00	0.00	0.01	0.03
-85	0.16	0.13	0.10	0.08	0.06	0.04	0.03	0.02	0.02	0.02	0.02	0.03	0.04
-90	0.08	0.08	0.08	0.08	0.08	0.08	0.08	0.08	0.08	0.08	0.08	0.08	0.08

Downloaded by xu yajun (xuyj@beice-sh.com) on Jun 29, 2018, 12:46 am PDT
联系方式：xuyj@beice-sh.com 13917165676

Table A.3-D — Vertical rigidity cutoffs in GV, 180-360° longitude East

Latitude	Longitude East												
	180	**195**	**210**	**225**	**240**	**255**	**270**	**285**	**300**	**315**	**330**	**345**	**360**
90	0.01	0.01	0.01	0.01	0.01	0.01	0.01	0.01	0.01	0.01	0.01	0.01	0.01
85	0.02	0.01	0.01	0.00	0.00	0.00	0.00	0.00	0.00	0.00	0.00	0.01	0.01
80	0.06	0.04	0.02	0.01	0.00	0.00	0.00	0.00	0.00	0.00	0.01	0.02	0.03
75	0.17	0.12	0.08	0.04	0.01	0.00	0.00	0.00	0.00	0.01	0.03	0.05	0.09
70	0.42	0.33	0.19	0.11	0.05	0.02	0.01	0.01	0.01	0.04	0.08	0.16	0.24
65	0.91	0.73	0.49	0.30	0.16	0.07	0.04	0.03	0.06	0.18	0.30	0.47	0.59
60	1.69	1.32	0.93	0.64	0.38	0.22	0.17	0.17	0.25	0.44	0.68	0.94	1.10
55	2.74	2.20	1.68	1.21	0.80	0.50	0.38	0.42	0.58	0.91	1.32	1.79	2.01
50	4.18	3.43	2.75	2.07	1.44	1.01	0.78	0.80	1.08	1.62	2.32	2.93	3.30
45	5.44	4.83	4.09	3.13	2.38	1.72	1.38	1.38	1.89	2.65	3.79	4.51	4.91
40	7.73	6.43	5.43	4.64	3.56	2.74	2.20	2.18	2.85	4.14	5.37	6.38	7.13
35	9.43	8.91	7.67	6.03	5.06	4.05	3.21	3.21	4.15	5.68	8.12	9.37	9.76
30	11.59	10.42	9.66	8.66	6.78	5.36	4.33	4.28	5.58	8.57	10.55	11.18	11.61
25	12.91	12.26	11.59	10.71	9.37	7.43	5.93	5.83	7.98	10.73	12.09	12.85	13.29
20	13.76	13.19	12.67	12.00	10.98	8.87	7.41	7.05	9.56	12.06	13.06	13.72	14.19
15	14.44	13.93	13.48	12.96	12.10	10.54	8.99	9.25	11.60	12.79	13.59	14.15	14.62
10	14.95	14.50	14.10	13.65	12.99	12.03	11.10	11.33	12.36	13.18	13.77	14.20	14.64
5	15.27	14.89	14.51	14.11	13.61	12.91	12.26	12.26	12.74	13.30	13.64	13.91	14.30
0	15.37	15.05	14.71	14.34	13.92	13.40	12.87	12.65	12.88	13.17	13.26	13.34	13.62
-5	15.19	14.97	14.69	14.37	14.00	13.57	13.08	12.78	12.80	12.85	12.69	12.55	12.70
-10	14.72	14.62	14.43	14.19	13.89	13.52	13.08	12.71	12.55	12.36	11.92	11.52	11.56
-15	13.87	13.97	13.93	13.81	13.60	13.30	12.89	12.46	12.14	11.73	11.05	10.26	10.13
-20	12.57	12.96	13.16	13.21	13.13	12.91	12.54	12.07	11.59	10.88	9.87	8.93	8.52
-25	9.99	11.02	11.84	12.39	12.49	12.38	12.06	11.55	10.88	9.93	8.68	7.58	7.07
-30	7.90	9.30	9.05	10.75	11.63	11.70	11.46	10.87	9.98	8.90	7.37	6.54	5.78
-35	5.55	6.50	7.87	8.25	9.87	10.85	10.73	10.07	9.11	7.70	6.38	5.45	4.72
-40	4.11	4.66	5.52	6.69	8.15	9.69	9.67	9.14	8.09	6.60	5.73	4.52	3.85
-45	2.62	3.33	4.22	4.89	6.06	7.74	8.64	8.10	7.34	6.23	4.69	3.77	3.16
-50	1.66	2.21	2.91	3.75	4.58	5.47	6.78	6.90	6.08	4.80	3.90	3.11	2.55
-55	0.90	1.36	1.91	2.62	3.35	4.18	4.76	4.81	4.50	3.88	3.16	2.45	2.00
-60	0.46	0.78	1.19	1.73	2.28	2.97	3.58	3.74	3.49	3.07	2.43	1.97	1.51
-65	0.20	0.42	0.65	1.04	1.50	1.94	2.41	2.53	2.39	2.20	1.87	1.47	1.19
-70	0.08	0.21	0.38	0.60	0.91	1.21	1.48	1.61	1.63	1.47	1.24	1.03	0.79
-75	0.04	0.10	0.20	0.34	0.51	0.65	0.81	0.93	0.95	0.87	0.80	0.66	0.53
-80	0.03	0.06	0.11	0.18	0.25	0.34	0.42	0.47	0.48	0.46	0.46	0.36	0.30
-85	0.04	0.06	0.08	0.11	0.12	0.17	0.21	0.19	0.23	0.22	0.19	0.19	0.16
-90	0.08	0.08	0.08	0.08	0.08	0.08	0.08	0.08	0.08	0.08	0.08	0.08	0.08

BC LABORATORY
北测（上海）电子科技有限公司
beice
Downloaded by xu yajun (xuyj@beice-sh.com) on Jun 29, 2018, 12:46 am PDT
联系方式：xuyj@beice-sh.com 13917165676

A.4 The neutron spectrum below 1 MeV, including thermal-energy neutrons

While the shape of the cosmic-ray-induced terrestrial neutron spectrum above a few MeV is nearly constant, that is not the case at lower energies, where the shape of the spectrum depends on how local materials scatter neutrons. Figure A.4.1 shows full energy range cosmic-ray neutron spectra measured outdoors (one was in a thin-roofed building) at five locations [17]. Each spectrum has been scaled to sea level and the cutoff of New York City using the Equations in A.3 and plotted as energy times differential flux as a function of neutron energy. Above a few MeV, the spectra lie practically on top of one another, justifying the use of one reference spectrum. At lower energies, these spectra vary by up to 66%, lowest to highest, and the relative flux at thermal energies (<0.4 eV) does not correlate well with the relative flux at higher energies. For these spectra, scaled to reference conditions, the thermal neutron flux ranged from 1.84×10^{-3} cm^{-2} s^{-1} (6.6 cm^{-2} h^{-1}) to 2.8×10^{-3} cm^{-2} s^{-1} (10 cm^{-2} h^{-1}) and averaged 2.27×10^{-3} cm^{-2} s^{-1} (8.2 cm^{-2} h^{-1}).

Other measurements [18] have found somewhat lower values of the thermal neutron flux. Figure A.4.2 shows a bar chart of the results of measurements of the thermal neutron flux made in 2003 at 52 sites near sea level within 160 km of Annapolis, MD (39.0°N, 76.5°W) on the top floor inside low buildings and outdoors. On land and not during thunderstorms, the measured thermal neutron flux ranged from about 2.6 to 6.3 cm^{-2} h^{-1}, averaging 4 cm^{-2} h^{-1}. Assuming an average elevation of 10 m and an average roof shielding of 5 g/cm^2, scaling the results of these measurements to New York City at sea level with no shielding and average solar modulation multiplies them by 1.087, giving thermal neutron fluxes ranging from 2.8 to 6.8 cm^{-2} h^{-1} with an average of 4.35 cm^{-2} h^{-1}. This set of measurements does not agree with the measurements shown in Figure A.4.1, but the two sets do overlap at 6.6 to 6.8 cm^{-2} h^{-1}.

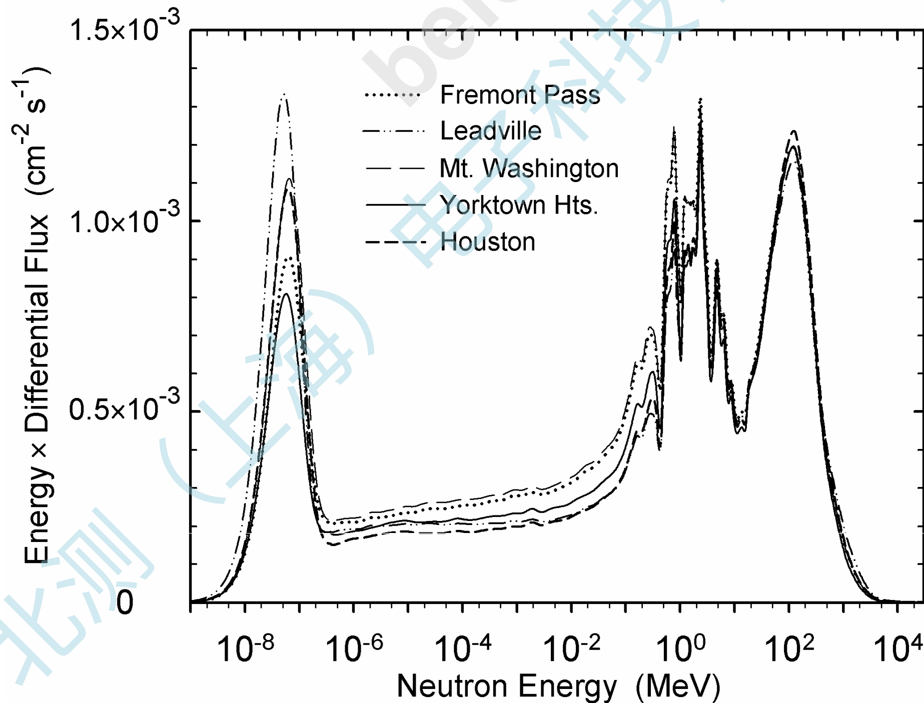

Figure A.4.1 — Spectra of cosmic-ray-induced neutrons measured at five locations. Each spectrum has been scaled to sea level and the cutoff of New York City and plotted as energy times differential flux as a function of neutron energy.

Downloaded by xu yajun (xuyj@beice-sh.com) on Jun 29, 2018, 12:46 am PDT
联系方式：xuyj@beice-sh.com 13917165676

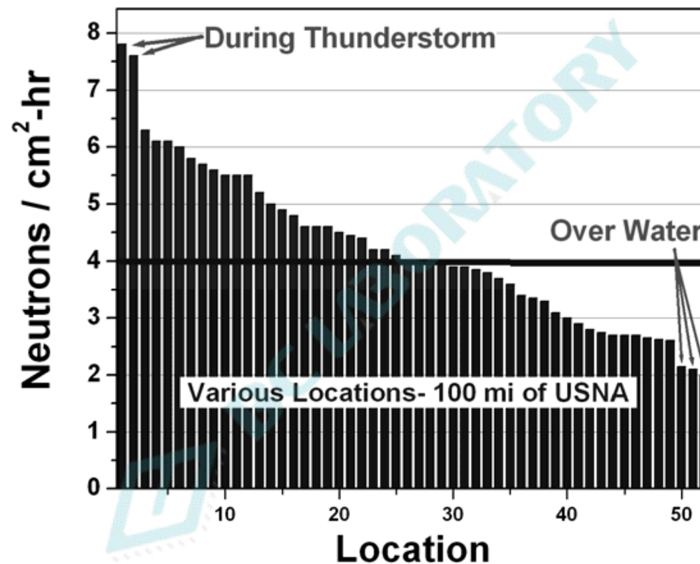

Figure A.4.2 — Thermal neutron flux measured at 52 sites near sea level within 160 km (100 miles) of the U.S Naval Academy in Annapolis, MD (39.0° N, 76.5° W) [18]. The fluxes shown have not been adjusted to the reference conditions.

The reference value for the flux of cosmic-ray-induced terrestrial neutrons at thermal energies (<0.4 eV) at New York City outdoors at sea level at a time of average solar activity is 1.8×10^{-3} cm^{-2} s^{-1} (6.5 cm^{-2} h^{-1}). This value is the average of the means of the two sets of measurements described above [17, 18] after scaling to the reference conditions. Some of the individual measurements differ from the reference value by as much as a factor of 2.3, and this is indicative of the variations that may be encountered in different surroundings. In general, the flux of thermal neutrons may be estimated within about a factor of 2.3 by using the reference value together with the methods described in A.3 to scale the reference thermal flux.

A.5 Effects of shielding by buildings and other material

The procedures in A.3 give the nominal neutron flux to which a device or circuit is exposed at a location without shielding, that is, outdoors with no enclosure. Most applications are indoors, and the materials of the building attenuate the actual flux that impinges on the electronics.

The attenuation by moderate layers of low-atomic-number materials such as wood is roughly similar to that by an equal mass thickness (areal density) of air, so the shape of the spectrum above 10 MeV is not significantly changed, and the attenuation may be treated as similar to increasing the atmospheric depth.

For Concrete, in a large building it was found that two 15-cm (6-inch) slabs (plus associated roofing, ceiling, and flooring material, ductwork, etc. in an industrial building) reduced the high-energy portion (E > 10 MeV) of the neutron spectrum by a factor of 2.3, while the total neutron flux was reduced by a factor of only 1.6. As they penetrate the concrete, low-energy neutrons are scattered, thermalized, and absorbed, but the high-energy neutrons are attenuated by interactions which cause the nuclei in the shielding to emit neutrons with energies in the MeV range, regenerating the low-energy portion of the neutron spectrum.

Downloaded by xu yajun (xuyj@beice-sh.com) on Jun 29, 2018, 12:46 am PDT
联系方式：xuyj@beice-sh.com 13917165676

A.5 Effects of shielding by buildings and other material (cont'd)

For the portion of the spectrum above 10 MeV, the attenuation by horizontal concrete layers above the point of interest may be estimated using exponential attenuation with an attenuation length of 1.2 feet or 0.37 m:

$$\dot{\Phi} = \dot{\Phi}_0 \exp(-x/0.37) \quad \text{(A.12)}$$

where $\dot{\Phi}$ and $\dot{\Phi}_0$ are the attenuated and initial flux and x is concrete thickness in meters. Assuming a density of 2.3 g cm^{-3}, the mass attenuation length of concrete floor slabs is roughly 85 g cm^{-2}. The lower energy portion of the neutron spectrum does not decrease as fast; the attenuation length for the total flux is about 0.65 m or 150 g cm^{-2}. The cosmic ray secondary protons are presumably attenuated more than the neutrons.

If there are thick concrete walls as well as floors and roofs and an accurate differential neutron flux is desired, a high-energy radiation transport code, such as Mcnpx [http://mcnpx.lanl.gov/], Fluka [http://pcfluka.mi.infn.it/], or Geant [http://wwwasd.web.cern.ch/wwwasd/geant/], should be used to model radiation transport through the building. The outdoor reference neutron spectrum scaled as described in A.3 may be used as the incident radiation for such modeling. As an alternative to performing such calculations, if a detection system sensitive only to high-energy nucleons is available, the relative flux of high-energy nucleons inside and outside the building could be measured.

Large amounts of steel (such as aboard ships) or other materials with high atomic number (e.g., lead shields) can significantly distort the neutron spectrum. Each incident high-energy neutron can liberate several neutrons with energies ~1 MeV, sometimes creating an increase of a factor of 2 or more in that region of the spectrum. However, steel shielding above the point of interest attenuates the portion of the spectrum with $E > 10$ MeV. Steel (or iron) also absorbs thermal neutrons, and a room or enclosure with steel walls will have a significantly reduced thermal neutron flux.

Downloaded by xu yajun (xuyj@beice-sh.com) on Jun 29, 2018, 12:46 am PDT
联系方式：xuyj@beice-sh.com 13917165676

Annex B – Counting statistics (normative)

B.1 Confidence Interval

In accelerated SER testing, the total number of particles incident on the DUT must be sufficient to establish with a high statistical confidence that all sensitive volume has been irradiated uniformly. After certain particle fluence, each memory element either passes or fails. The probability of failure for each memory element is calculated as

$$P_E = \frac{F}{N} \quad \text{(B.1)}$$

where P_E is an estimation of probability of failure, N is the total number of memory elements, F is the total failures. If it is desirable that, with (1-α) confidence level, the estimated probability of failure P_E is within a plus and minus ε% bounds of the true probability of failure P, the following condition needs to be satisfied according to the definition of the confidence interval:

$$\Phi^{-1}(\frac{\alpha}{2}) \bullet \frac{1}{\sqrt{F}} \bullet \sqrt{\frac{N-F}{N-1}} \leq \varepsilon\% \quad \text{(B.2)}$$

where $\Phi^{-1}(\alpha/2)$ is the inverse cumulative standard normal distribution function, F is the total observed errors and N is the total number of memory elements.

B.2 Estimating probability for results with low numbers of observed events

In this example, the DUT is an SRAM of 512 K bit, i.e., N=512*1024=524288. After a certain time of radiation exposure, we observed 100 errors, i.e., F=100. Therefore, the estimated error probability p_E is F/N=0.00019, with 95% confidence level, the precision of the estimated probability of failure will be:

$$\Phi^{-1}(\frac{\alpha}{2}) \cdot \frac{1}{\sqrt{F}} \cdot \sqrt{\frac{N-F}{N-1}} \approx 1.96 \cdot \frac{1}{10} = 19.6\% \quad \text{(B.3)}$$

In other words, with 95% confidence level, we can say that estimated probability of failure per bit is within the bounds of minus and plus 19.6% of the true probability of failure. According to Equation B.3, it seems that precision increases with increasing F. In reality, when F approaches N, the effect of the same bit getting hit more than once can no longer be ignored, thus one must be careful to avoid accumulating too many errors or else the soft error rate will be underestimated.

Downloaded by xu yajun (xuyj@beice-sh.com) on Jun 29, 2018, 12:46 am PDT
联系方式：xuyj@beice-sh.com 13917165676

Annex C – Real-Time Testing Statistics (normative)

C.1 Statistics for Real-Time Testing

In the typical real-time test, N devices are placed on test under normal (unaccelerated) operating conditions and the number, location, and time of each soft failure is recorded. Since soft errors are not permanent (eliminated when new data is written) this test can be thought of as a life-test with replacement (in which a failing device is replaced with a new device immediately upon failure detection).

Let us assume the soft failures are random in time and that the probability of an error at any time is constant. Secondly we assume that the number of errors is small relative to the number of units in the test – for soft failures in components this is a good assumption (ignoring big solar events or large changes in barometric pressure that would alter the neutron flux – in any case, these types of events will be averaged out during the test). Thus we apply the exponential or **Poisson distribution** assuming the form:

$$f(t) = N\lambda e^{-N\lambda t} \tag{C.1}$$

Where λ is the mean error rate and N is the number of units on test. Given a real-time experiment, we first want to understand the SER maximum likelihood estimate which is simply the number of errors divided by the time and the number of units on test, according to:

$$component\ SER_{avg} = \frac{r}{NT_r}(10^9)\ \text{FIT} \tag{C.2}$$

Where r is the number of errors observed at T_r. For the purposes of this test we have multiplied the standard formula by 10^9 to convert errors/hour to FIT. The second issue we need to understand is, do we have enough errors to confidently proclaim that the component has an SER below or above certain intervals. The longer a test is run and the more errors accumulated, the greater our confidence in the average failure rate. Since real-time testing can take months, it is crucial to understand when enough errors (enough test time) have been logged to make an acceptable estimation of the component SER. Because Poisson distributed variables have a probability distribution function that is a gamma function, we can use a special case of the gamma function, the chi-squared (χ^2) distribution to answer questions about variance in the mean. Using the χ^2 distribution, the two-sided upper and lower 100 (1-α) percent confidence intervals with k=2(r+1) degrees of freedom for the SER can be expressed as:

$$LowerLimit\ \frac{\chi^2_{1-(\alpha/2);k}}{2NT_r}(10^9), UpperLimit\ \frac{\chi^2_{(\alpha/2);k}}{2NT_r}(10^9)\quad \text{FIT} \tag{C.3}$$

For example, selecting a 90% confidence interval (α=0.1), the average SER of the entire population of devices has a 90% probability of being between the lower and upper limits in C.3. There is a 1-(α/2)=95% probability the average SER is greater than the lower limit and there is only a (α/2)=5% probability that the average SER is greater than the upper limit. As in the previous equation we have multiplied the standard formula by 10^9 to convert errors/hour to FIT.

Downloaded by xu yajun (xuyj@beice-sh.com) on Jun 29, 2018, 12:46 am PDT
联系方式：xuyj@beice-sh.com 13917165676

C.2 Determining Upper and Lower Confidence Intervals

A common aspect of this type of testing is to calculate confidence limits as a function of the number of errors observed so that the experimenter can judge when to terminate the experiment. In other words, when is the SER known to be below a certain failure rate with a certain confidence. Probably the most straightforward way to understand this is to use an actual example of an experiment. The experiment was a real-time test on 3500 identical components. Since this was a soft error rate test and patterns were rewritten after reading, we consider this a test with replacement. The test was continued until nine failures were observed and was terminated on the ninth fail after 1982 hours. The soft failures occurred at 150, 450, 811, 950, 1197, 1327, 1512, 1768, and 2045 hours. The experimental data and the maximum likelihood estimate for the SER are tabulated in Table C.1.

Table C.1

T_r (hr)	Number of Devices	Errors (r)	Component SER FIT,avg
150	3500	1	1905
450	3500	2	1270
811	3500	3	1057
950	3500	4	1203
1197	3500	5	1193
1327	3500	6	1292
1512	3500	7	1323
1768	3500	8	1293
2045	3500	9	1257

Equation C.2 was used to generate the SER maximum likelihood estimate SER column labeled here simply as SER. Applying Equation C.3 we can calculate both the upper and lower confidence bands for this data set. In Table C.2 the chi-squared table is generated for the upper and lower confidence intervals for 90%, 80%, and 60%. Note that k is the degrees-of-freedom (number of errors). In Table C.3 we show the data and in Figure C.1 the plot for SER confidence intervals for 90%, 80%, and 60% based on χ^2 values from Table C.2 and using Equation C.3.

Downloaded by xu yajun (xuyj@beice-sh.com) on Jun 29, 2018, 12:46 am PDT
联系方式：xuyj@beice-sh.com 13917165676

C.2 Determining Upper and Lower Confidence Intervals (cont'd)

Table C.2 — χ^2 values for upper/lower 90, 80, and 60% confidence intervals

		χ^2					
	Confidence Interval (1-α)	90%		80%		60%	
	Lower, Upper Limits 1-(α/2),α/2	95%	5%	90%	10%	80%	20%
Errors (r)	Degrees of Freedom 2(r+1)						
0	2	0.103	5.991	0.211	4.605	0.446	3.219
1	4	0.711	9.488	1.064	7.779	1.649	5.989
2	6	1.635	12.592	2.204	10.645	3.070	8.558
3	8	2.733	15.507	3.490	13.362	4.594	11.030
4	10	3.940	18.307	4.865	15.987	6.179	13.442
5	12	5.226	21.026	6.304	18.549	7.807	15.812
6	14	6.571	23.685	7.790	21.064	9.467	18.151
7	16	7.962	26.296	9.312	23.542	11.152	20.465
8	18	9.390	28.869	10.865	25.989	12.857	22.760
9	20	10.851	31.410	12.443	28.412	14.578	25.038

Table C.3 — Component SER 90, 80, 60% confidence intervals

			Lower and Upper confidence limits for component SER					
		Confidence Interval (1-α)	90%		80%		60%	
		Lower, Upper Limits 1-(α/2),α/2	95%	5%	90%	10%	80%	20%
Time (hr)	Errors (r)	Degrees of Freedom 2(r+1)						
149	0	2	98	5744	202	4415	428	3086
150	1	4	677	9036	1013	7409	1570	5703
450	2	6	519	3997	700	3379	975	2717
811	3	8	481	2732	615	2354	809	1943
950	4	10	593	2753	732	2404	929	2021
1197	5	12	624	2509	752	2214	932	1887
1327	6	14	707	2550	839	2268	1019	1954
1512	7	16	752	2485	880	2224	1054	1934
1768	8	18	759	2333	878	2100	1039	1839
2045	9	20	758	2194	869	1985	1018	1749

Downloaded by xu yajun (xuyj@beice-sh.com) on Jun 29, 2018, 12:46 am PDT
联系方式：xuyj@beice-sh.com 13917165676

C.2 Determining Upper and Lower Confidence Intervals (cont'd)

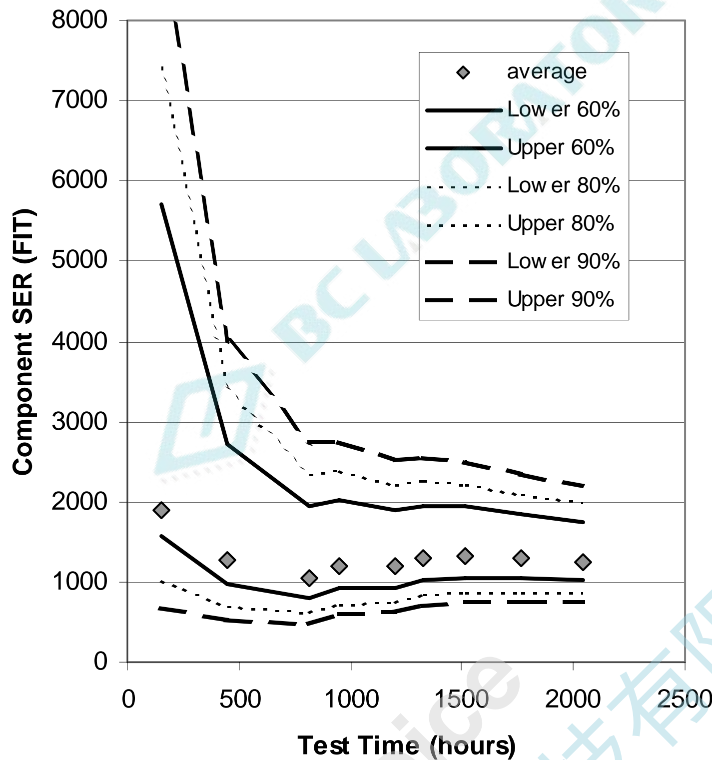

Figure C.1 — Plot showing the max. likelihood SER (average) and the upper and lower confidence intervals at 90, 80, and 60% levels.

Obviously using higher confidence levels means longer test times. If one wanted to be sure that the component tested had an SER < 2000 FIT, at 60% confidence the 3500 units would have to stay on test for about 800 hours while at 80% confidence the same components would need to be tested out to nearly 2000 hours. Conversely, the huge confidence interval shows the risk of using short field tests with no or few errors to test some assumption about average failure rate.

Downloaded by xu yajun (xuyj@beice-sh.com) on Jun 29, 2018, 12:46 am PDT
联系方式：xuyj@beice-sh.com 13917165676

Annex D – The alpha particle environment (informative)

A significant source of ionizing radiation in components is from alpha particles from the naturally occurring radioactive impurities in materials. Alpha particles can be emitted when the nucleus of an unstable isotope decays to a lower energy state. The alpha particle is composed of two neutrons and two protons emitted with specific kinetic energy typically from 4 to 9 MeV.

The activity of a particular isotope is directly proportional to its natural abundance and inversely related to its half-life (the time required for a population of atoms to decay to one-half their original number). ^{238}U, ^{235}U and ^{232}Th (and their associated daughter products) have the highest activities of the naturally occurring radioactive species and are the dominant source of alpha particles in materials. 73.1% of the observed alpha flux would be from ^{238}U decay, 23.5% from ^{232}Th, and 3.4% from ^{235}U respectively if these isotopes were present in equal amounts.

If the half-life of the daughters is less than the half-life of the parent (usually the case for natural isotopes), then these must also be considered since, in equilibrium, the emission of alphas from a daughter product will be equal to the emission from the parent (secular equilibrium). A population of ^{238}U atoms in equilibrium emits eight different alpha particles at discrete energies ranging from 4.15-7.69 MeV, a population of ^{232}Th will emit six alpha particles from 3.96-8.79 MeV, and an equilibrium population of ^{235}U will emit seven alpha particles from 4.15-7.45 MeV. The spectrum emitted from the natural occurring U and Th populations in a thin film are shown in Figure D.1.

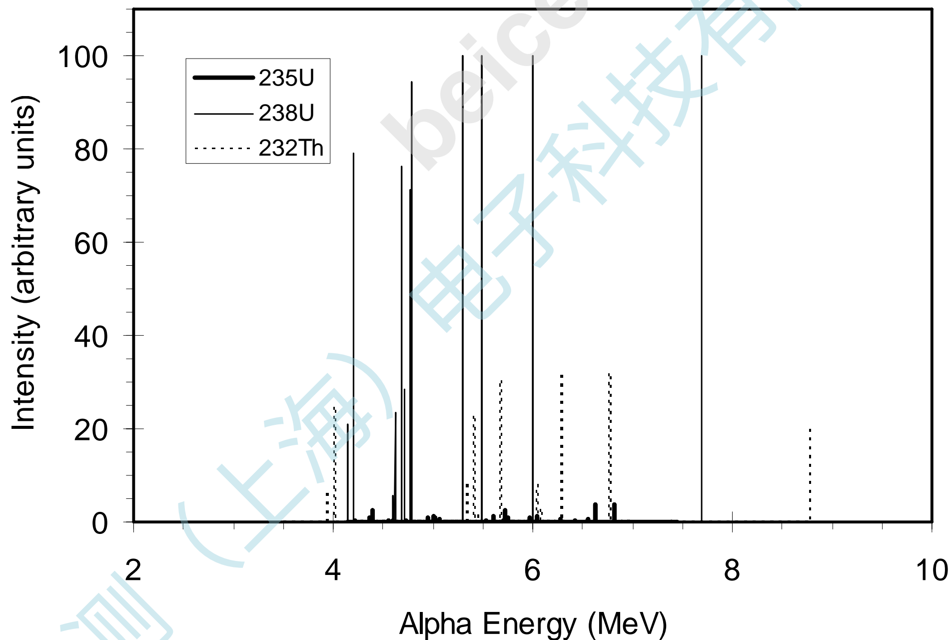

Figure D.1 — Emission Spectra from thin-film ^{238}U, ^{232}Th, and ^{235}U, the predominant natural alpha emitters. Emission is based on activity and natural abundance.

Downloaded by xu yajun (xuyj@beice-sh.com) on Jun 29, 2018, 12:46 am PDT
联系方式：xuyj@beice-sh.com 13917165676

Annex D – The alpha particle environment (informative) (cont'd)

Secular equilibrium is only valid if the material has not undergone any chemical separation or purification. Since virtually all semiconductor materials are highly purified, in general, the alpha emitting impurities will not be in secular equilibrium since various isotope concentrations can become depleted or enriched. Alpha counting investigations are therefore necessary to accurately determine the alpha flux emission.

In actual components the alpha emitters are typically distributed throughout each material. The distinct energy "lines" shown in Figure D.1 are usually not observed since emission can occur anywhere within the material and the fine spectrum is broadened as the alpha particles lose energy traveling to the material surface. The alpha spectrum from a thick source of ^{232}Th is shown in Figure D.2. The spectrum from a distributed source of ^{238,235}U will look very similar.

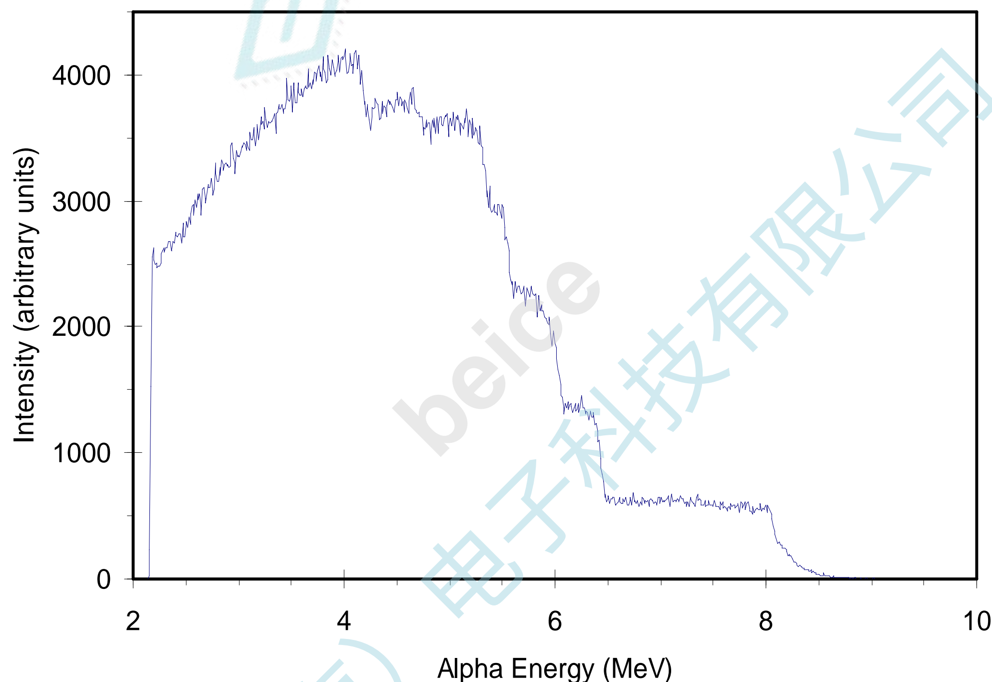

Figure D.2 — Emission Spectrum from thick-film of ^{232}Th. Since alpha particles can be emitted at any depth from the surface, discrete emission lines are broadened into a continuous spectrum of alpha energies.

If the alpha source is confined to a thin layer so that all the alpha particle emission essentially occurs at or very near the surface a discrete spectrum is expected. Two examples of surface distributions are the residue of alpha emitting impurities left after a wet-etch with certain phosphoric acids and the segregation of ^{210}Po to the surface of standard lead-based solders.

Downloaded by xu yajun (xuyj@beice-sh.com) on Jun 29, 2018, 12:46 am PDT
联系方式：xuyj@beice-sh.com 13917165676

Annex D – The alpha particle environment (informative) (cont'd)

The probability that an alpha causes a soft error is based on its energy and on its trajectory. The wrong assumptions about the energy spectrum can lead to errors in estimating the SER from accelerated experiments. Alpha particles interact primarily by elastic coulombic scattering with the electrons surrounding nuclei, effectively freeing electrons from their material nuclei. Significant quantities of electron-hole pairs are generated along the physical trajectory of the ion. For an alpha particle traveling in silicon, an average of 3.6 eV of energy is lost for every electron-hole pair created. The denser the material, the more quickly the alpha particle loses its energy since there is a higher density of charge with which to interact. The charge generation rate (energy loss) increases with the distance the alpha particle travels and reaches a maximum near the end of the alpha particle's path. This non-linear response is due to the increased ionization efficiency as the velocity of the alpha particle is reduced. Knowing the energy spectrum of incident alpha particles is very important to correctly assess device SER. A curve of the stopping power (or linear energy transfer) and range of an alpha particle in silicon as a function of its energy is shown in Figure D.3. The alpha particle generates anywhere from 4 – 16 fC/μm.

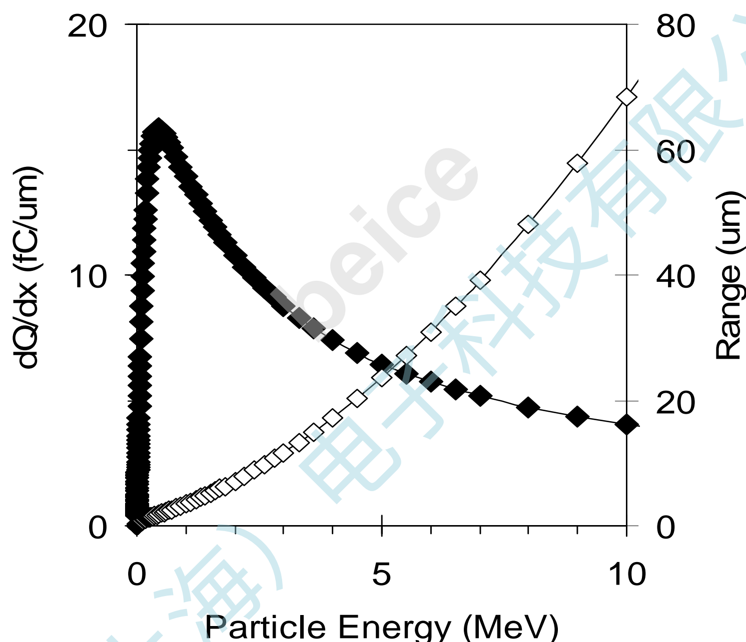

Figure D.3. Stopping power or linear energy transfer (solid triangles) and range (open triangles) of an alpha particle in silicon as a function of its energy.

In a packaged semiconductor product the sources of alpha emitting impurities can be found in the packaging materials, the chip materials, materials used to attach the chip, and in the materials used during the fabrication process. Alpha particle surface emissions from some key production materials determined by alpha counting are summarized in Table D.1. The alpha emissivities are reported at the 90% confidence level. Depending on the grade and type of material, a large range of alpha emissivities was observed.

Downloaded by xu yajun (xuyj@beice-sh.com) on Jun 29, 2018, 12:46 am PDT
联系方式：xuyj@beice-sh.com 13917165676

Annex D – The alpha particle environment (informative) (cont'd)

Table D.1 — Alpha emissivities of various materials

Material	Emissivity ($cm^{-2}h^{-1}$)
Fully Processed Wafers	< 0.0004
30um thick Cu Metal	< 0.0003
20um thick AlCu Metal	< 0.0003
Mold compound	< 0.024 – < 0.0005
Flip Chip Underfill	< 0.004 – < 0.0007
Eutectic Pb-based Solders	< 7.2 – < 0.0009

In a well-controlled manufacturing environment the primary sources of alpha particles are the package materials (mold compound, underfill, solder, etc.) and not the semiconductor manufacturing materials.

There are three ways to reduce alpha particle SER. The first is to use high purity materials and screen for alpha emission. Another is to keep packaging materials with the highest alpha emission separated from sensitive circuit components. Another approach is to shield chips with films of various materials. Knowing the source and energy of the alpha emission is crucial since using a shield that is too thin can raise the SER above unshielded units due to the non-linearity in an alpha particle's charge generation rate.

BC LABORATORY
beice
北测（上海）电子科技有限公司
Downloaded by xu yajun (xuyj@beice-sh.com) on Jun 29, 2018, 12:46 am PDT
联系方式：xuyj@beice-sh.com 13917165676

Annex E – Neutron and Proton Test Facilities (informative)

E.1 Introduction

Most accelerated tests are performed at accelerator facilities which have been built for other applications, e.g., nuclear or high energy physics research at government laboratories or private facilities offering proton cancer treatment. Such facilities usually provide beams for chip testing on a cost recovery basis, which can range from a few percent to a significant fraction of their mission. Normally, the facility provides the beam and the dosimetry, and the user provides the test equipment. Sometimes, facilities collaborate with an outside company which will provide support with the dosimetry and/or test equipment, for a fee.

Radiation effects testing at these facilities covers a wide range of applications, from material damage studies to space effects studies. It is very important that the facility staff is aware of the requirements of the user in beam energy, dose and uniformity and can provide quality assurance that these requirements are met. It is the responsibility of the user to communicate those requirements well in advance of the experiment and to ask for assurance that they can be met. Accelerator facilities are large, complicated systems and on any given day, things can go wrong, so users should maintain flexibility and have some patience.

Sometimes facilities - particularly at government laboratories in the U.S. - require user agreements to be signed and estimated advance payment made before a test run can be scheduled. Ample time should be allowed for this paperwork to be completed, particularly the first time. Typically, university facilities are more flexible in this regard. Users should be aware that most of the time these facilities run 24 hours a day, sometimes 7 days/week. Sometimes the primary mission of the facility takes place during the day, and the availability of beams is limited to nights and weekends, e.g., at some proton therapy centers.

E.2 Online facilities list

The major type of user facilities is described briefly here, along with means of dosimetry and possible issues. A spreadsheet of details (not duplicated here because it will be easier to keep current online) about many available facilities can be obtained at: www.seutest.com.

E.3 Heavy ion facilities

Heavy ion facilities are generally used for testing of parts destined for space orbit, where primary cosmic rays can cause significant damage to microelectronics. Heavy ion testing facilities are well established and could be an option for alpha tests over radioactive sources. These facilities are not included in the database at this time.

Downloaded by xu yajun (xuyj@beice-sh.com) on Jun 29, 2018, 12:46 am PDT
联系方式：xuyj@beice-sh.com 13917165676

E.4 Proton facilities

During the last several years, a number of commercial proton therapy centers have been built to provide treatments for cancer. These facilities include Loma Linda and Massachusetts General Hospital (MGH) in the United States, Tri-University Meson Facility (TRIUMF) in Canada and PSI and Orsay in France. In addition, Indiana University Cyclotron Facility (IUCF) in the U.S. is being converted from a nuclear physics facility to a proton therapy center. Because of their high energies, these facilities are useful as an accepted alternative to monoenergetic neutrons for accelerated testing. Users should recognize that if high-energy proton beams are degraded substantially to lower energies, they are no longer truly monoenergetic. This may have to be taken account in the analysis.

Other proton irradiation facilities are available at universities or government laboratories using accelerators which run or have run in the past for high energy or nuclear physics programs. These include UC Davis and the 88" Cyclotron in the US and TSL and Cyclone in Europe. The energy range of these accelerators vary; some are limited to energies below 100 MeV.

The maximum and minimum flux and size of the beam which is available from any of the proton facilities depends on many factors, e.g., shielding, dosimetry, and radiation training of users (some facilities require additional training courses to run above certain levels). Most facilities are set up so that the part is run in air, which makes it easier to set up and allows the use of shorter cables. However, one should take great care that any radiation sensitive secondary equipment is shielded from the beam.

Proton dosimetry has been well established over the last 30 years by the therapy community and standards exist for calibration of ion chambers, the main means of real-time dosimetry in use. These have been summarized in a report by the International Atomic Energy Agency (IAEA) entitled, 'Absorbed Dose Determination in External Beam Radiotherapy: An International Code of Practice for Dosimetry based on Standards of Absorbed Dose to Water'. Facilities should have calibration dates and data available if requested.

E.5 Neutron facilities

Four types of neutron facilities are available:

1) Thermal neutrons, usually obtained from reactors, used for the studies described in 7
2) (d,d) or (d,t) neutron sources, giving monoenergetic neutrons at 2.5 and 14 MeV, respectively, used for accelerated testing in combination with proton sources, as described in 6,
3) spallation proton sources, which produce a neutron energy spectrum up to the energy of the proton source, also used for accelerated studies as described in 6, and
4) quasi-monoenergetic neutrons of various energies, usually produced using protons on a Be or Li target, an alternative method described in 6

The reactor facilities listed in the database are the Delft Reactor in Europe and the NIST Center in the U.S. Some available (d,t) sources for 14 MeV neutrons are the Boeing Radiation Effects Lab, US Naval Academy and the RARAF facility at Columbia Univ in the US, the ASP in Europe and the Fast Neutron Lab at Tohuku Univ in Japan. These sources are generally well characterized with well-established dosimetry. In combination with proton measurements, a Weibull cross-section plot for SER can be obtained.

Downloaded by xu yajun (xuyj@beice-sh.com) on Jun 29, 2018, 12:46 am PDT
联系方式：xuyj@beice-sh.com 13917165676

E.5 Neutron facilities (cont'd)

Available spallation neutron sources include the ICE House at LANSCE and TRIUMF in No. America and RCNP in Japan. The LANSCE neutron beam has essentially no thermal neutrons whereas the TRIUMF spallation neutron beam has a significant thermal neutron component that should be accounted for. Because the proton energy varies among facilities, the neutron energy spectra is not identical, which could lead to small differences in extracted FIT. The facility should be able to provide an energy spectra, usually measured with time-of-flight. The facility should be asked if there is a thermal component to the neutron beam, as this can have an effect on the results if there is boron present.

Quasi-monoenergetic neutron sources can be used as an alternative to spallation neutron sources, as discussed in 6. Most are produced using the ^{7}Li(p,n) reaction. The analysis will have to include a correction for the lower energy neutrons not in the peak, usually on the order of 40% of the total neutrons, independent of energy. The facility should be able to provide an energy spectra, usually measured with time-of-flight.

Because neutrons have no charge, it is not possible to count the neutrons directly. Instead, secondary reactions which have high probability and are well understood must be used for dosimetry. The most appropriate material for dosimeters for neutrons is dependent on the neutron energy. For thermal neutrons, boron-containing material is efficient for capturing neutrons and can be used for real-time dosimetry. The most accurate method is activation foils, which are very well understood but must be counted offline after the irradiation. For fast neutrons, polyethylene, liquid-scintillator or other hydrogen-containing material is used and the proton recoils are measured. An old technique, which is still used extensively, is fission ion chambers. The fissionable material used, which could be uranium, bismuth or other heavy isotopes, determines the low energy threshold of sensitivity to neutrons. There is no standard for neutron dosimetry as there is for protons, and the dosimetry may not be as well understood as at proton facilities. The user should determine from the facility what the efficiency, accuracy and energy limits are of the dosimetry in use.

Downloaded by xu yajun (xuyj@beice-sh.com) on Jun 29, 2018, 12:46 am PDT
联系方式：xuyj@beice-sh.com 13917165676

Annex F (informative) - Bibliographic References

[1] N. Seifert, N. Tam, "Timing Vulnerability Factors of Sequentials", IEEE Transactions on Device and Materials Reliability, Vol. 4, Nr. 3, pp. 516-522, September 2004.

[2] N. Seifert, P. Shipley, M.D. Pant, V. Ambrose, and B.S. Gill, "Radiation-induced clock jitter and race". IEEE International Reliability Physics Symposium, 2005, pp. 215-222.

[3] Karnik, T.; Hazucha, P, "Characterization of soft errors caused by single event upsets in CMOS processes", Dependable and Secure Computing, IEEE Transactions on, Volume 1, Issue 2, April-June 2004 pp.128–143.

[4] Gadlage, M.J.; Schrimpf, R.D.; Benedetto, J.M.; Eaton, P.H.; Turflinger, T.L.; "Modeling and verification of single event transients in deep submicron technologies", 42nd Annual IEEE International Reliability Physics Symposium Proceedings, April 2004, pp. 673–674.

[5] Balkaran S. Gill, Chris Papachristou, Francis G. Wolff, Norbert Seifert, "Node sensitivity Analysis for Soft Errors in CMOS Logic", IEEE International Test Conference, Nov. 8, 2005, pp. 964-972.

[6] Xiaowei Zhu; Rob Baumann; Charles Pilch; Joe Zhou; Jason Jones; Claude Cirba; Piyush Patel, "Comparison of product failure rate to component soft error rate in a multi-core digital signal processor", 43nd Annual IEEE International Reliability Physics Symposium Proceedings, April 2005, pp. 209-214.

[7] N. Tsoulfanidis, "Measurement and Detection of Radiation", second edition, Taylor & Francis 1995, pp. 273

[8] H.H.K. Tang, "Nuclear physics of cosmic ray interactions with semiconductor materials: Particle-induced soft errors from a physicist's perspective", IBM J. Res. Develop 40(1), pp. 91-108 (1996).

[9] M. Drosg, "Sources of fast monoenergetic neutrons. More recent developments", Proc. of the SPIE – The International Society for Optical Engineering, v. 2339, pp. 145-155 (1995).

[10] T. Grandlund, B. Granbom, and N. Olsson, "A Comparative Study Between Two Neutron Facilities Regarding SEU," IEEE Trans. Nucl. Sci., 51, p. 2922 (2004)

[11] IEC 62396 TS Ed. 1 (June, 2005), "PROCESS MANAGEMENT FOR AVIONICS INDUSTRY - Standard for the Accommodation of Atmospheric Radiation Effects via Single Event Effects within Avionics Electronic Equipment", International Electrotechnical Commission.

[12] E.L.Petersen et al., "Rate Prediction for Single Event Effects", IEEE Trans. Nucl. Sci., TNS-39, p. 1577 (1992).

[13] R. Fleischer, "Cosmic ray interactions with boron: a possible source of soft errors" IEEE Trans. Nucl. Sci., 30(5), p. 4013, Oct. 1983.

[14] T.R. Oldham, S. Murrill, and C.T. Self, "Single Event Upset of VLSI Memory Circuits Induced by Thermal Neutrons", HEART Conf., 1986.

[15] R. C. Baumann and E. B. Smith, "Neutron-induced 10B fission as a major source of soft errors in high density SRAMs," Elsevier Microelec. Reliability, vol. 41, no. 2, p.211, 2001.

[16] IEC62396 TS "PROCESS MANAGEMENT FOR AVIONICS INDUSTRY – Standard for the accommodation of Atmospheric Radiation Effects via Single Event Effects within Avionics Electronic Equipment," International Electrotechnical Commission, 2005.

Downloaded by xu yajun (xuyj@beice-sh.com) on Jun 29, 2018, 12:46 am PDT
联系方式：xuyj@beice-sh.com 13917165676

[17] M. S. Gordon, P. Goldhagen, K. P. Rodbell, T. H. Zabel, H. H. K. Tang, J. M. Clem, and P. Bailey, "Measurement of the Flux and Energy Spectrum of Cosmic-Ray Induced Neutrons on the Ground," IEEE Transactions on Nuclear Science, vol. 51, no. 6, pp. 3427-3434, Dec. 2004.

[18] LT J. D. Dirk, M. E. Nelson, J. F. Ziegler, A. Thompson and T. H. Zabel, "Terrestrial Thermal Neutrons", *IEEE Trans. Nucl. Sci.*, vol. 50, no. 6., pp. 2060-2064, Dec. 2003.

[19] M. E. Shea and D. F. Smart, "Tables of asymptotic directions and vertical cutoff rigidities for a five degree by fifteen degree world grid as calculated using the International Geomagnetic Reference Field for epoch 1975.0," Air Force Geophysics Laboratory, Report AFCRL-TR-75-0185, Hanscom AFB, Massachusetts, 1975. (AD-A012509)

[20] J. Clem and L. Dorman, "Neutron monitor response functions," Space Sci. Rev., vol. 93, no. 1-2, pp. 335-363, 2000, and references therein.

[21] A. Belov, A. Struminsky, and V. Yanke, "Neutron Monitor Response Functions for Galactic and Solar Cosmic Rays", 1999 ISSI Workshop on Cosmic Rays and Earth, poster presentation.

beice 北测（上海）电子科技有限公司

Downloaded by xu yajun (xuyj@beice-sh.com) on Jun 29, 2018, 12:46 am PDT
联系方式：xuyj@beice-sh.com 13917165676

Annex G (informative) Differences between JESD89A and JESD89

This table briefly describes most of the changes made to entries that appear in this standard, JESD89A, compared to its predecessor, JESD89 (August 2001). If the change to a concept involves any words added or deleted (excluding deletion of accidentally repeated words), it is included. Some punctuation changes are not included.

Page	Term and description of change

This information was not provided by the formulating committee upon ballot.

BC LABORATORY
beice
北测（上海）电子科技有限公司
Downloaded by xu yajun (xuyj@beice-sh.com) on Jun 29, 2018, 12:46 am PDT
联系方式：xuyj@beice-sh.com 13917165676

Standard Improvement Form **JEDEC JESD89A**

The purpose of this form is to provide the Technical Committees of JEDEC with input from the industry regarding usage of the subject standard. Individuals or companies are invited to submit comments to JEDEC. All comments will be collected and dispersed to the appropriate committee(s).

If you can provide input, please complete this form and return to:

JEDEC
Attn: Publications Department
2500 Wilson Blvd. Suite 220
Arlington, VA 22201-3834

Fax: 703.907.7583

1. I recommend changes to the following:
   - [ ] Requirement, clause number ____________
   - [ ] Test method number ____________ Clause number ____________

   The referenced clause number has proven to be:
   - [ ] Unclear [ ] Too Rigid [ ] In Error
   - [ ] Other ____________

2. Recommendations for correction:

____
____
____
____

3. Other suggestions for document improvement:

____
____
____
____

Submitted by

Name: ____________ Phone: ____________

Company: ____________ E-mail: ____________

Address: ____________

City/State/Zip: ____________ Date: ____________

Downloaded by xu yajun (xuyj@beice-sh.com) on Jun 29, 2018, 12:46 am PDT
联系方式：xuyj@beice-sh.com 13917165676

BC LABORATORY
beice
北测（上海）电子科技有限公司
Downloaded by xu yajun (xuyj@beice-sh.com) on Jun 29, 2018, 12:46 am PDT
联系方式：xuyj@beice-sh.com 13917165676